PERFORMANCE ANALYSIS OF POWER DISTRIBUTION SYSTEM FOR

HYBRID FIBER/COAX NETWORKS

Mei Qiu

A Thesis

in

The Department

of

Electrical and Computer Engineering

Presented in Partial Fulfillment of the Requirements
for the Degree of Master of Applied Science at
Concordia University
Montréal, Québec, Canada

July 1996

© Mei Qiu, 1996

ABSTRACT

Performance Analysis of Power Distribution System for Hybrid
Fiber/Coax Networks

Mei Qiu

This thesis presents the power distribution system for the hybrid fiber/coax networks. A cost effective and reliable power scheme with 90V 60Hz trapezoidal voltage distribution is selected for powering the network. A simulation based model of the proposed distribution system is developed taking under consideration certain operation constraints. A complete analysis of both the steady state operations and the dynamic performance of the system is given by means of simulations. From the simulation results, the system loading capability under all the possible operating conditions, its performance under the fault conditions and its stability of the operation are presented.

ACKNOWLEDGEMENTS

Table of Contents

CHAPTER 1
Introduction

CHAPTER 2
Selection of Network Power Distribution System

CHAPTER 3
Modeling of Power Distribution Systems for Hybrid Fiber/Coax Networks

CHAPTER 4
Loading Capability of Hybrid Fiber/Coax System

CHAPTER 5
Fault Analysis

CHAPTER 6
Stability of System Operation

CHAPTER 7
Conclusions

List of Figures

List of Tables

List of Abbreviations

HFC   Hybrid Fiber 'Coax (network)

CATV   Community Antenna TeleVision

HTU   Home Termination Unit

UPS   Uninterrupted Power Supply

PCU   Power Conditioning Unit

PI   Power Insert

PN   Power Node

CN   Coax Node

PF   Power Factor

THD   Total Harmonic Distortion

DF   Distortion Factor

List of Symbols

K_a Weight loss factor

S Apparent powe. at the supply terminals

P Average power at the supply terminals

V_{rms} RMS value of the supply voltage

I_{rms} RMS value of the supply current

I_s Maximum value of the supply current

X_{rms} RMS value of the component X

X_{1rms} RMS value of the fundamental component of X

THD_n THD of a certain component

THD_s THD of the supply voltage

$V_{last}(ac)$ RMS value of the voltage at the ac side of the last load

$V_{last}(dc)$ RMS value of the voltage at the dc side of the last load

$V_{i,j}$ Voltage at the load connected to the jth drop box in the ith segment

I_l Average dc current through the load

V_o Average dc voltage across the load

P_l Load power demand

r Resistance of unit length of the coax cable

l Inductance of unit length of the coax cable

c Capacitance of unit length of the coax cable

R Resistance of a cable of 100ft length

L Inductance of a cable of 100ft length

C Capacitance of a cable of 100ft length

Z Impedance of a cable of 100ft length

R_{db} Resistance of distribution cable

L_{db} Inductance of distribution cable

R_{dp} Resistance of drop cable

L_{dp} Inductance of drop cable

C_f Capacitance of the filter at the output of HTU rectifier

I_H Hold current - maximum current device will pass without interruption in 20°C still air environment.

V_{max} Maximum voltage device can withstand without damage at rated current

I_{max} Maximum fault current device can withstand without damage at rated voltage

R_{max} and R_{min}

       Maximum and minimum delivered resistance at 20°C

i_i Instantaneous input current of HTU rectifier

v_i Instantaneous input voltage of HTU rectifier

i_o Instantaneous output current of HTU rectifier

v_o Instantaneous output voltage of HTU rectifier

i_l Instantaneous current through the load

ND_{ON} Numerical Decrement at switch-ON

ND_{OFF} Numerical Decrement at switch-OFF

Chapter 1

Introduction

1.1 Introduction

The existing Community Antenna TeleVision (CATV, introduced in Appendix A) or telephony systems are not able to provide multimedia services to the customer [1]. In the current CATV architecture it is not necessary to distribute power over the drop cable as the home units are locally powered. However, if the basic telephony is provided by using the CATV networks, there is a need to power minimum essential services at the home by network power.

Now the CATV, consumer electronics and telecommunication industries are entering the age of technology and business innovation to achieve new digital infrastructures. These infrastructures, currently known as "Information Superhighway", will be capable of providing a platform for a wide range of broad band, multimedia, entertainment, communication and information services. Power electronics is an integral part of these infrastructures and has been challenged to provide cost effective and reliable end-to-end power solutions.

In recent years, hybrid fiber/coax (HFC) distribution networks have emerged as a preferred approach for distributing multimedia services to the customer [2, 3, 4]. This chapter will introduce the architecture of HFC networks and several powering alternatives for the distribution systems.

1.2 Architecture of HFC networks [5, 6]

Fig. 1.1 shows a simplified diagram of the hybrid fiber/coax distribution network. This network consists of the backbone network and the residential network. In the backbone network, the multimedia signals are received and converted into optical signals at the headend stations. One or more headend typically serves a large area or a city. All the headends and transport nodes are interconnected through fiber optic links. In the residential network video, telephony, audio and broad band signals are brought into a coax node over an optic fiber. The optical signals are converted into electrical signals in the coax node and distributed to the home termination units (HTUs) spread over a wide area using the coax cable.
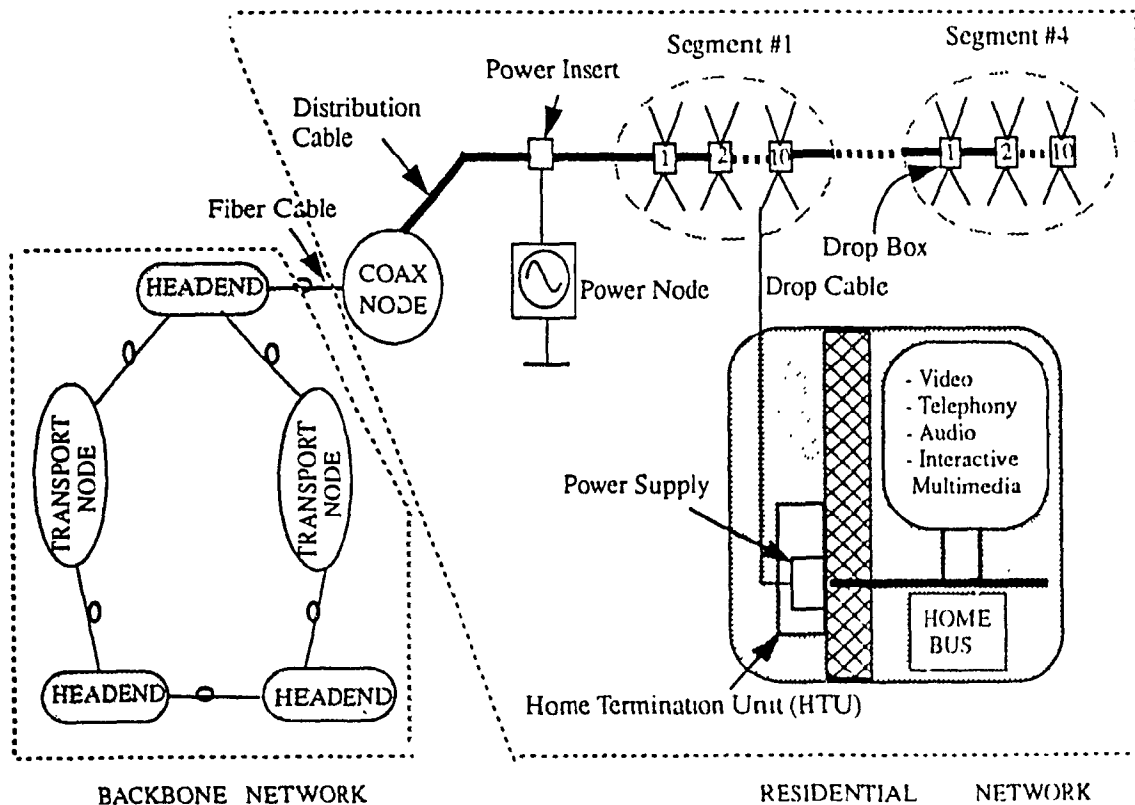
Fig. 1.1: Hybrid fiber/coax network architecture

Bringing the fiber optic line to home to provide broad band services is not economical because of the following reasons:

(i) The optical/electrical conversion in each home unit is very expensive and needs local powering;

(ii) Uninterrupted power supply is required in every home unit to provide basic service during ac mains failures;

(iii) Fiber cable for a long distance is more costly than coax cable.

The home termination unit consists of power supply and loads. The power supply is a rectifier-filter system which converts ac, from the drop cable, to dc to power loads. The loads can be services of video, telephony, audio, interactive multimedia, etc. In this thesis, only telephony loads which need the essential power from the network are considered (the characteristics of telephony loads are introduced in Appendix B [7, 8]).

To serve a typical cluster of up to 160 homes, the coax network is subdivided into four segments. Each segment has a typical length of 1000ft and contains 10 drop boxes over a span of 100ft. Each drop box serves four homes. The typical distance between a drop box and the home is about 100ft.

In this architecture, an attractive feature of these networks is the use of the coax cable for distributing reliable power to the customer. Since the power required for backing up the basic telephony features is relatively low, the resulting powering schemes can offer high distribution efficiency, low voltage drops, high reliability and low cost. The following section will introduce some powering schemes for the HFC distribution networks.

1.3 Powering Options

In the HFC networks (Fig. 1.1), the method of powering the backbone network is straightforward. Each headend requires dc power between 10kW to 100kW, which is obtained locally using AC/DC rectifiers and has battery backups. This method has been used in the telecommunication industry for a long time. However, powering the residential broad band network is very challenging as there are a large numbers of home termination units spread over a wide area requiring uninterrupted power to provide reliable telecommunication services.

Recently several power schemes have been proposed [9, 10, 11]. This section will introduce and compare these options.

1.3.1 Options for powering the networks

Powering the hybrid fiber/coax system imposes the following requirements on the design of a power architecture:

. Uninterrupted power supply to all network elements;

. Safe voltage distribution at the consumer end;

. Low installation and maintenance cost;

. High efficiency for minimum energy cost;

. Compatible with existing CATV network equipments.

There are two possible alternatives to power the system:

(i) local power and,

(ii) network power.

(1) Local powering scheme

The local powering scheme is shown in Fig. 1.2. At each HTU, the equipments are powered locally by an uninterrupted power supply (UPS).
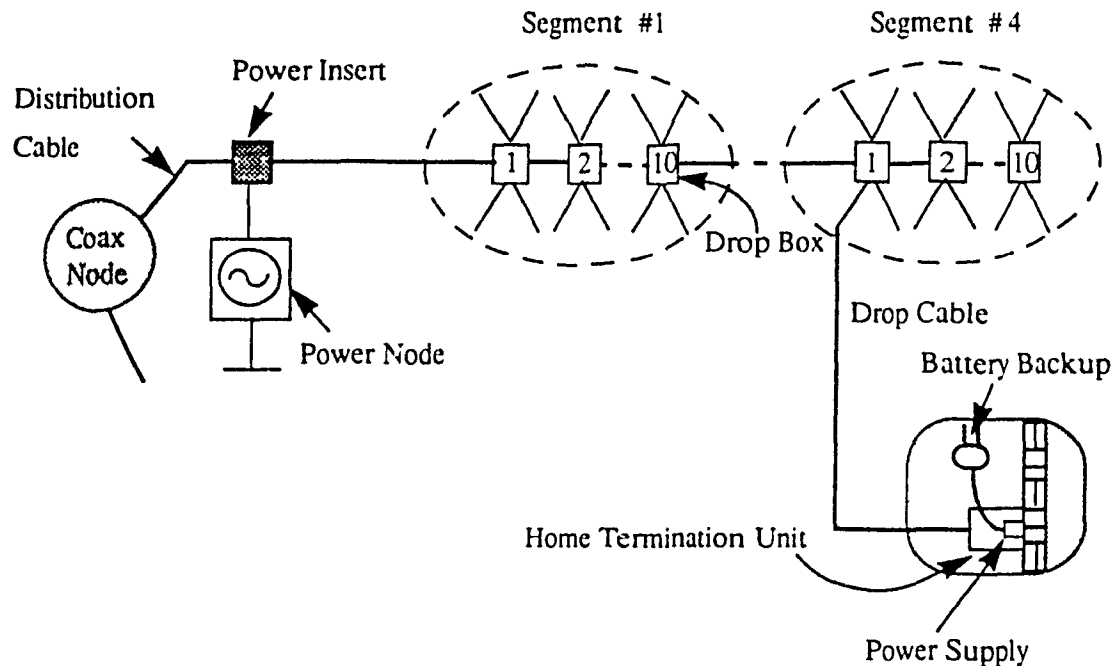
Fig. 1.2: Local powering scheme

It has the advantages that network configuration and growth are independent of power. However, a serious drawback is that it requires a battery backup at each customer site which is very expensive and difficult to maintain.

(2) Network powering scheme

The network powering scheme provides central battery backup, as shown in Fig. 1.3. In this topology, a UPS is inserted near the coax node to power the network. Combined power and communication signals are now distributed on the coax cable and are fed

to the HTU. During ac mains failures, the source powering the HTU is the same battery plant that serves the whole network.
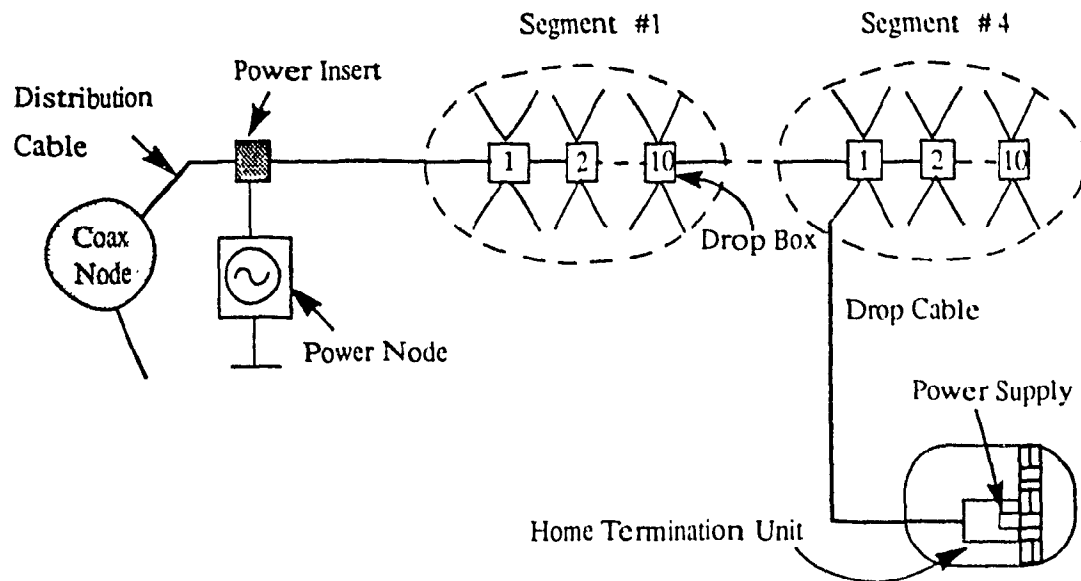
Fig. 1.3: Network powering scheme

This power scheme has the following advantages:

(i) Small size of UPS;

(ii) Low voltage drop across the distribution cable;

(iii) Pay-as-you-play;

(iv) High distribution efficiency.

1.3.2 Options for powering the drop segment

In the HFC network, the distribution cable may be as long as 4000 feet and may deliver up to 1 kW power. The drop cable is, however, only 100 feet long and deliver 5W (average) power to the home. Therefore, it maybe advantageous to distribute different

voltage, frequency and waveform over the drop cable rather than on the distribution cable.

The following alternatives are proposed to supply power to the HTU from the distribution network using a power conditioning unit (PCU) in each drop box:

(i) DC distribution;

(ii) Low frequency ac distribution;

(iii) High frequency ac distribution.

(1) DC distribution

In this type of distribution, the PCU converts the network voltage of 90V, 60Hz to regulated -48V dc. This is then distributed to each HTU over the same coax cable which is carrying the signals to the consumer end. Fig. 1.4 shows the block diagram of the dc voltage distribution.
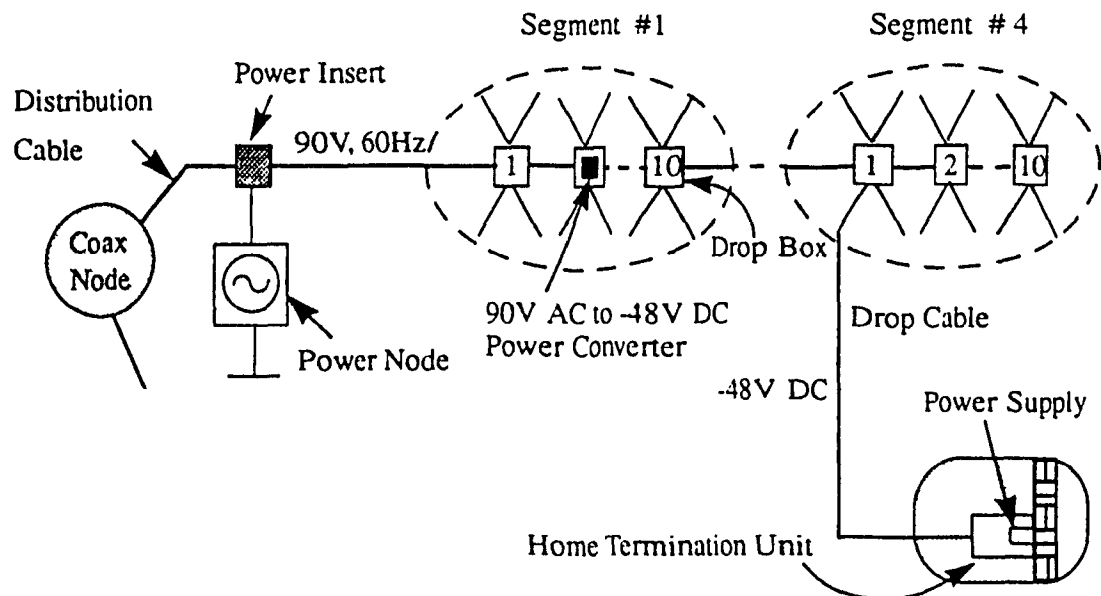
Fig. 1.4: -48V dc distribution

The following are the advantages and disadvantages of this type of distribution:

Advantages:

- Regulated voltage distribution;

- Efficient and small power converter in the HTU;

- Active current limiting;

- Lower power conversion cost;

- Technology readiness.

Disadvantages:

- AC/DC converters are required in the drop box.

(2) Low frequency power distribution

In this type of distribution, a 90V, 60Hz AC power is distributed over both the distribution and drop cables, as shown in Fig. 1.5.
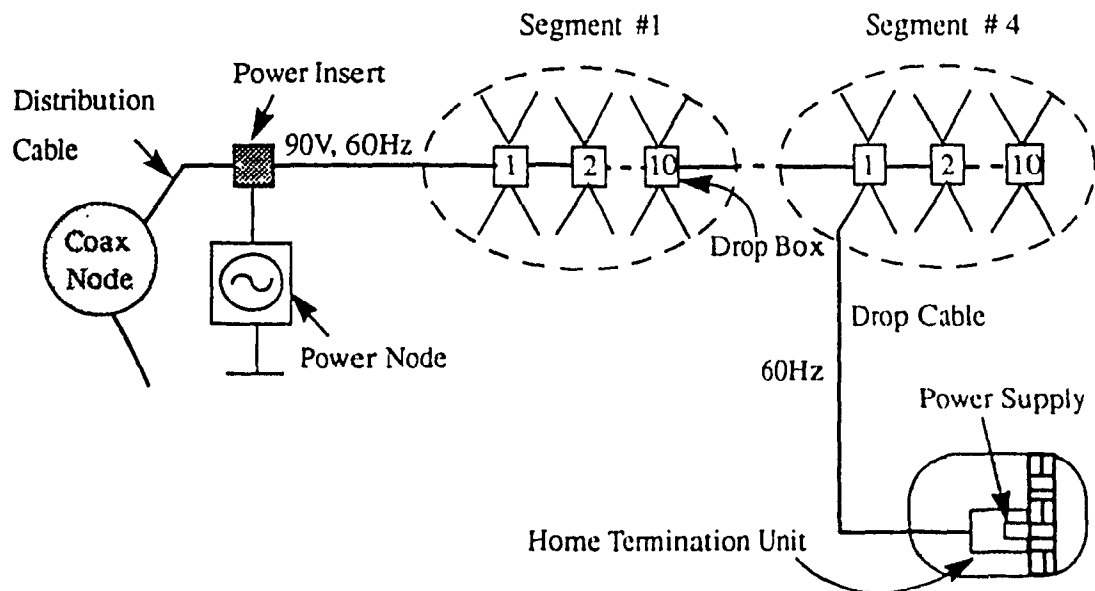
Fig. 1.5: Low frequency power distribution

The main attraction of this type of distribution is its inherent simplicity, simple power distribution and technology readiness. However, the low frequency distribution suffers from the following disadvantages:

- Resistive current limiting in the drop box;

- Bulky and inefficient power converters in the HTU.

- May not satisfy IEC950 safety requirements to distribute 90V to the customer site.

(3) High frequency power distribution

In this type of distribution, the PCU converts the network voltage of 90V, 60Hz to regulated 30V, 128kHz. High frequency ac at 30V is now distributed to each HTU over the coax cable. Fig. 1.6 shows the block diagram of the high frequency ac voltage distribution.
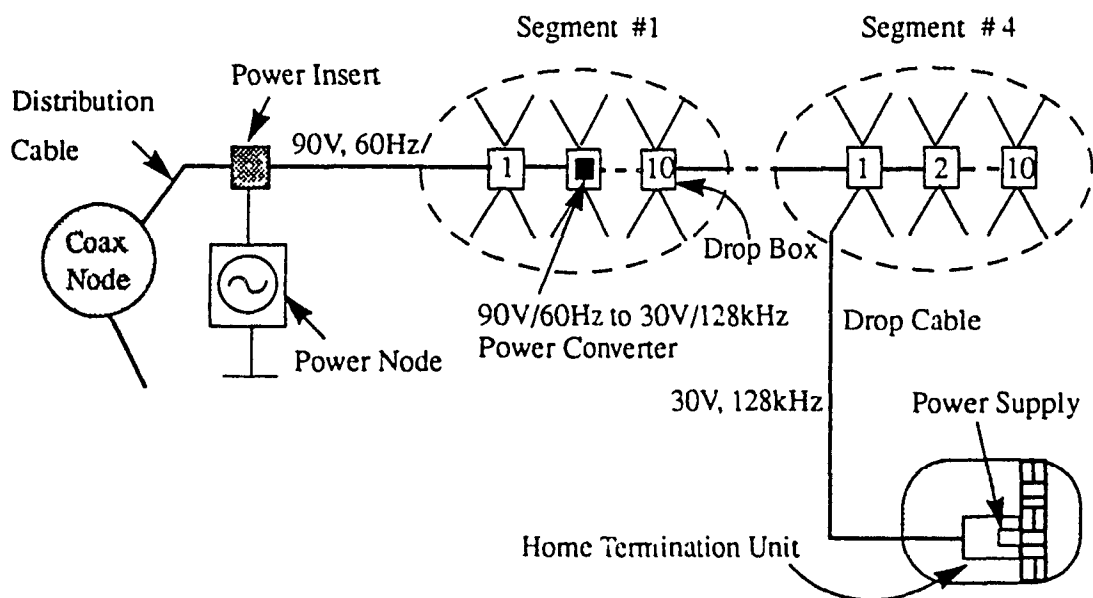
Fig. 1.6: High frequency power distribution

The following are the advantages and disadvantages of this type of distribution:

Advantages:

- Regulated voltage distribution;

- Efficient and small power converter in the HTU;

- Low passive current limiting;

- Lowest power conversion cost;

- Efficient power conversion in the drop box.

Disadvantages:

- Low frequency ac to high frequency ac converters are required in the drop box;

- higher technology risk (untried approach, no past experience);

- More potential for interference with analog TV signals.

(4) Comparison of powering options

A comparison of all the above options is made with respect to:

(i) compatibility with existing CATV network,

(ii) safety regulatory requirements,

(iii) cost of power conversion,

(iv) efficiency,

(v) size, and

(vi) technology readiness.

Table 1.1 shows the performance comparison of various power options. The data presented in this table is approximate and only for the comparison purposes. It is based on the experience gained so far on various power conversion equipment.

Table 1.1: Comparative performance

Parameters	DC Distribution	Low frequency Distribution	High frequency Distribution
Compatibility with Existing CATV Powering	YES	YES	YES
Safety/Regulatory	IEC 950, NEC, CEC	IEC 950, NEC, CEC	IEC 950, NEC, CEC
Total Cost of Power Conversion	0.6	1.0	0.35
Efficiency			
- Drop Box	90%	9?%	92%
- HTU	85%	75%	88%
Size			
- Drop Box	35 IN^3	30 IN^3	35 IN^3
- HTU	1.25 IN^3	10 IN^3	1.0 IN^3
Risk	Lower	Lower	Higher
Technology Readiness	Higher	Higher	Lower

The following points are observed from this Table:

(i) All the three options are compatible with the existing CATV powering scheme.

(ii) All the three options can meet the regulatory safety requirements.

(iii) The high frequency distribution has the highest overall power conversion efficiency while the dc and low frequency ac distribution have lower efficiency.

(iv) The size of the power conversion unit in the drop box is almost the same for either option. However, the size of the HTU power supply is significantly smaller for both the high frequency and dc power distribution, as compared to the low frequency distribution.

(v) The cost of powering the HTU is the lowest for the high frequency distribution.

(vi) The development risk is high for the high frequency distribution as compared to the low frequency and dc distribution.

In the initial development of the network, the passive drop boxes are employed. The low frequency distribution looks more attractive than the dc distribution and high frequency distribution as the former requires no power conditioning unit in the drop box. However, in the future, the active drop boxes will be used in the network and will require a power conditioning unit in the drop box to power its internal circuit. Since the power conditioning unit is required anyway, in the drop box, the high frequency distribution may become more attractive.

1.4 Scope and objectives

Power system is an integral part of the HFC networks. Before these systems can be installed in the field detailed information is required. This thesis focuses on the powering aspects of the HFC networks. The main objectives of this thesis are:

- To select a suitable power scheme for HFC network;
- To get the steady state performance of the system including the system loading capability;
- To simulate the dynamic performance of the system including fault and stability analyses.

1.5 Thesis outline:

- In Chapter 2, the selection of a power system for HFC network including the

power scheme, voltage level, frequency and the waveshape of the supply is discussed.

- In Chapter 3, a simulation model of the power distribution system is developed.

- In Chapter 4, the system loading capability under several operating conditions is found out.

- In Chapter 5, a suitable protective device is selected for overcurrent protection and the system performances under the fault conditions are presented.

- In Chapter 6, the dynamic behavior of the system in the switching transient is studied and the stability criteria is determined.

- Finally in Chapter 7, some conclusions are made for the power scheme, steady state and dynamic performance of the distribution system for the HFC network.

Chapter 2

Selection of Network Power Distribution System

2.1 Introduction

Various alternatives for powering the HFC network have been compared in Chapter 1. It is found that for the initial development of the networks, the network powering scheme with the low frequency distribution for the drop segment is cost-effective and reliable. In this scheme, a power supply with battery backup is inserted at the power node to power the main system over the distribution cable. The distribution cable has a number of drop boxes that provide multiple feeds to the drop cable which distributes the power to the home units.

After defining the power scheme for the HFC systems, the most important thing is to select a suitable power supply. In this chapter the voltage level, frequency and wave-shape of the power supply are defined according to the safety, cables corrosion, power factor, waveform distortions and loading capability.

2.2 Voltage level and frequency

The voltage level and frequency of network power distribution depends primarily on the following three factors [5]:

(i) Loading capability of the system,

(ii) Electrical safety of the people, and

(iii) Corrosion of the distribution cables and connectors.

The voltage level of the power supply should be low for the safety requirement.

However, from the point of view of the loading capability, the distribution voltage should be as high as possible. A good compromise is made at 90V (see the comparison of the loading capability between the 90V system and 60V system in Section 4.2).

Figs. 2.1 and 2.2 show the safe voltage and weight loss factor K_a of the cables and connectors as a function of frequency. Higher frequencies minimize the weight loss of the connectors and cables. However, the safe voltage level reduces with the increasing frequencies, up to 1kHz, and then increases slowly above this value. A good compromise is made at 60Hz from Figs. 2.3 and 2.4, which allows high enough safe voltage and frequency for low distribution power loss and corrosion.
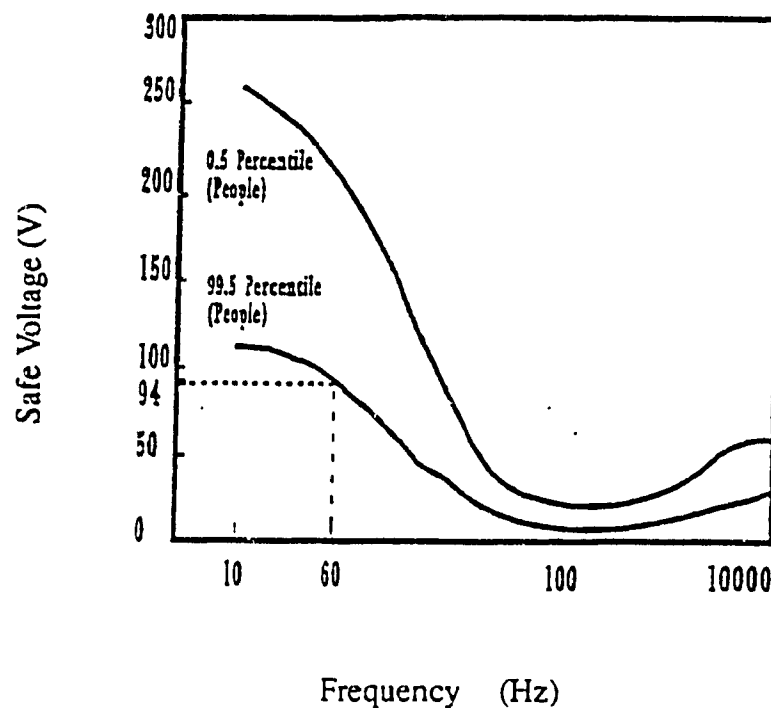
Fig. 2.1: The safe voltage as a function of the frequency
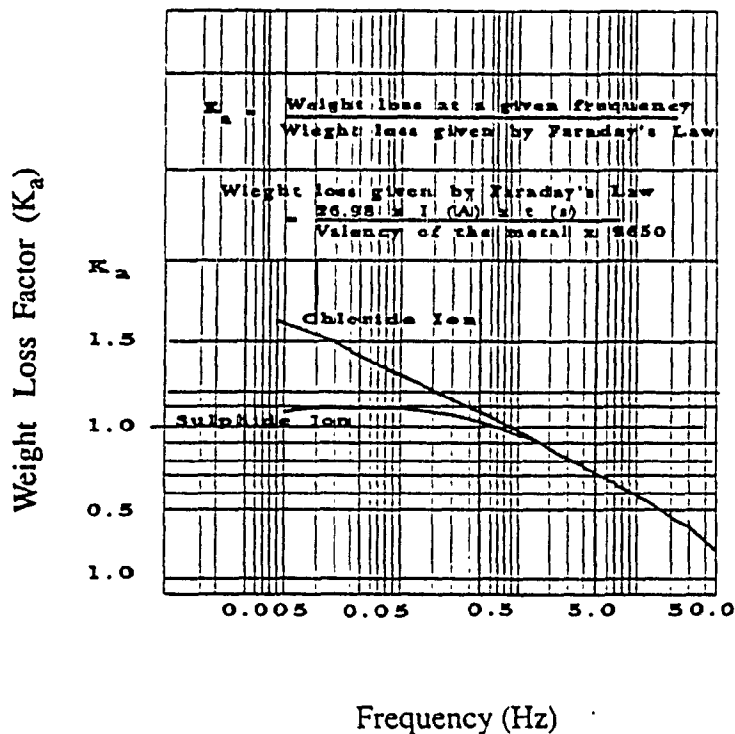
Fig. 2.2: The weight loss factor K_a as a function of the frequency

2.3 Waveshape of voltage supply

AC power can be in the form of a sine wave, quasi-sine wave or trapezoidal. The sine wave is common to AC power distribution systems. However, in a coax plant, the equipment has low cost power converters which have a non-linear nature and draw power near the peak of the AC waveform only. In the following subsections by the aid of simulations, the comparison between the system with sinusoidal, ideal trapezoidal and non-ideal trapezoidal source is made in terms of power factor, waveform distortion and loading capability.

The simulation circuit is shown in Fig. 2.3. It is a 3-segment system and there are 10 subcircuits, as shown in Fig. 2.3(b), in each segment. The detailed considerations and procedures of modeling system are described in section 3.4.

(a) 3-segment System

(b) Basic element in the segment
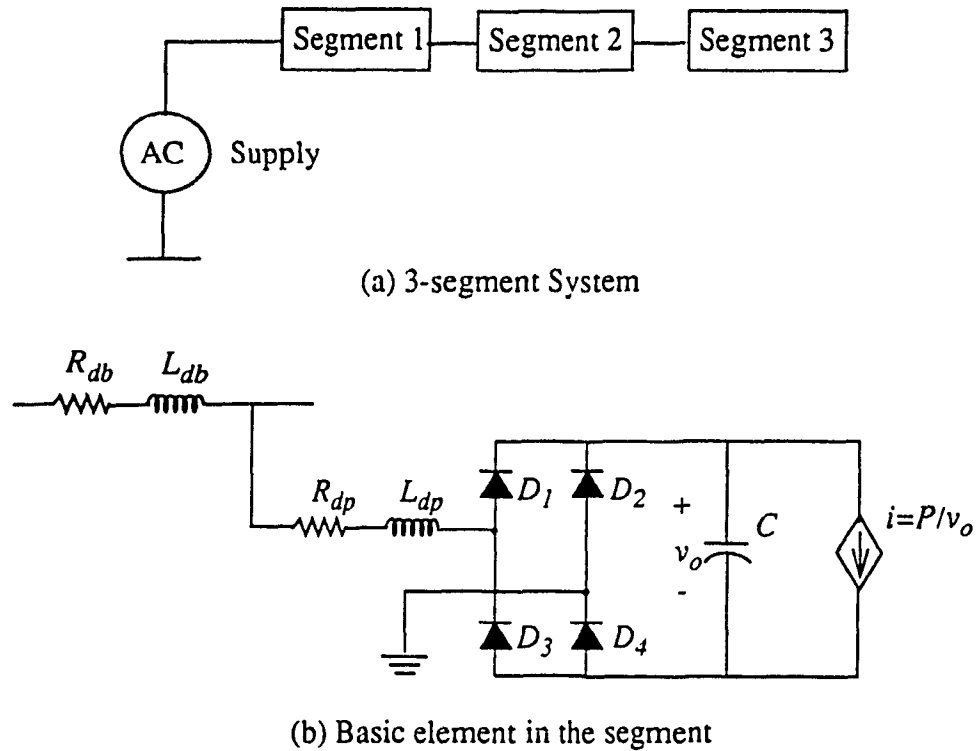
Fig. 2.3: Simulation Circuit

Following assumptions are made for the simulations:

- The rms value of the source output voltage, the load power demand and the system operating condition are the same for all types of sources.
- No current limitation (15A).

2.3.1 Effects of the supply waveshape on the power factor

The source capability can be expressed in terms of rms voltage and current:

$$S = V_{rms}I_{rms} \qquad\qquad (2\text{-}1)$$

This is known as the apparent power. The source generally supplies an average power less than the apparent power $V_{rms}I_{rms}$ at its terminals. It is not operating at its full capability at this voltage and current.

To reflect how effectively the available power of the source is being used, a measure called power factor (PF) is defined as the ratio of the average power P to the apparent power S at the supply terminals [12]:

$$PF = \frac{P}{S} = \frac{P}{V_{rms}I_{rms}} \qquad\qquad (2\text{-}2)$$

The source voltage and current waveforms are shown in Fig. 2.4 (a), (b) & (c) for sinusoidal, ideal and non-ideal trapezoidal sources respectively, and the instantaneous power at source terminals in Fig. 2.5.
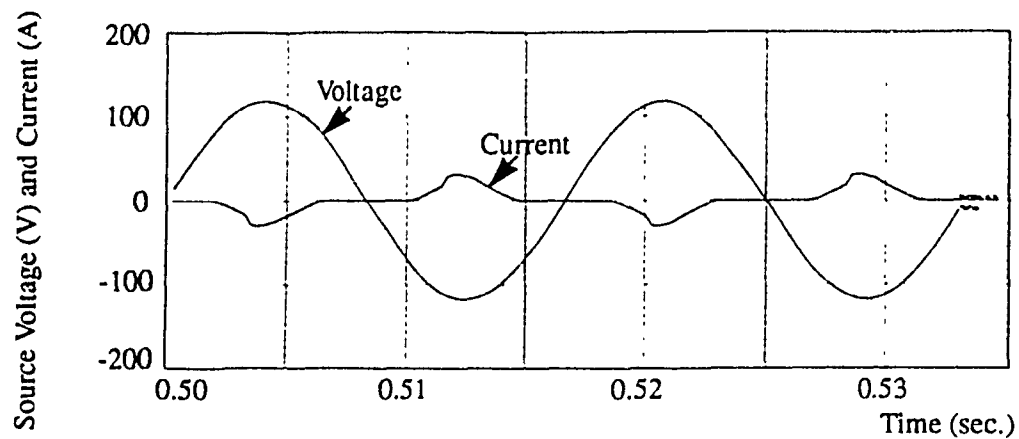
(a) Generated by the sinusoidal source
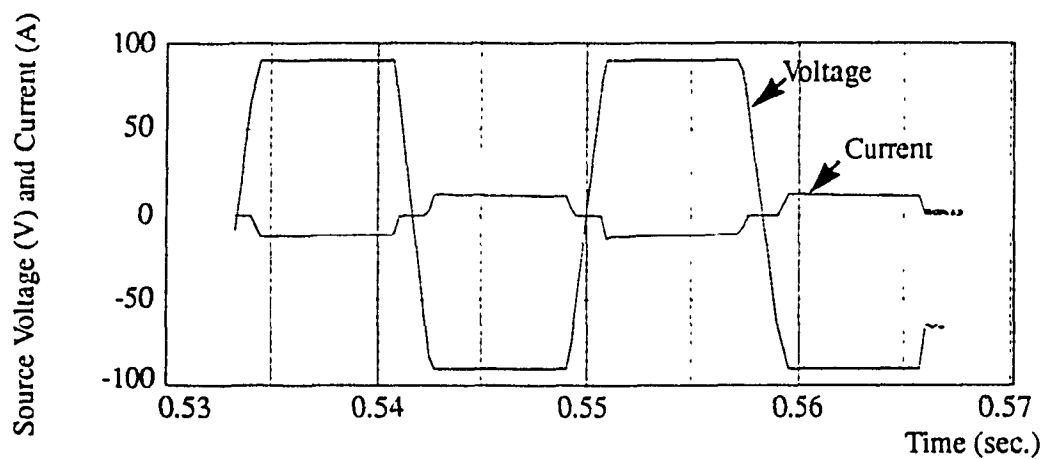
(b) Generated by the ideal trapezoidal source
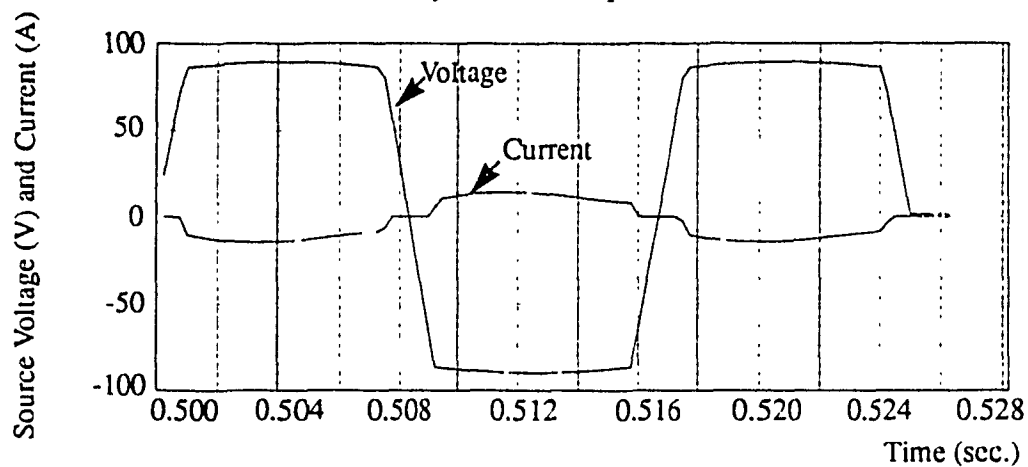
(c) Generated by the non-ideal trapezoidal source

Fig. 2.4: Voltage and current supplied by the voltage source
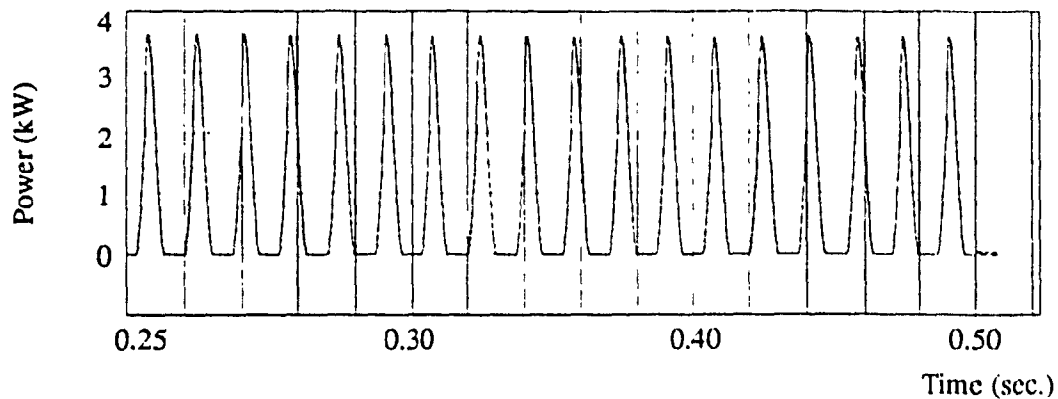
(a) Generated by the sinusoidal source
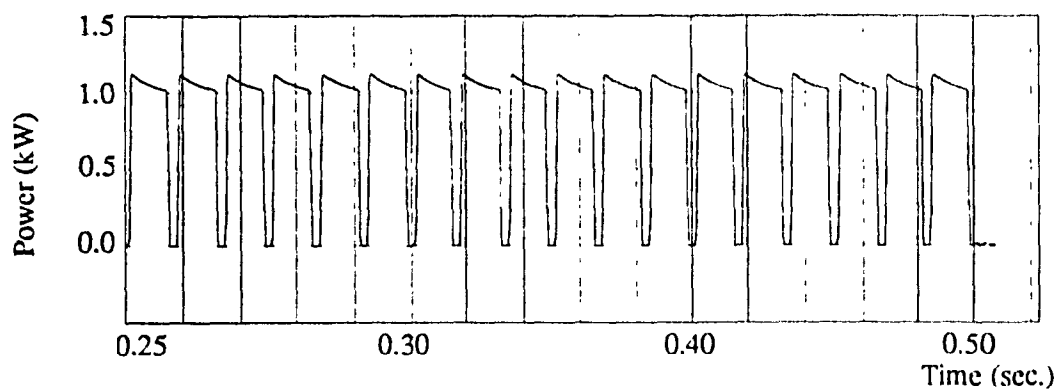
(b) Generated by the ideal trapezoidal source
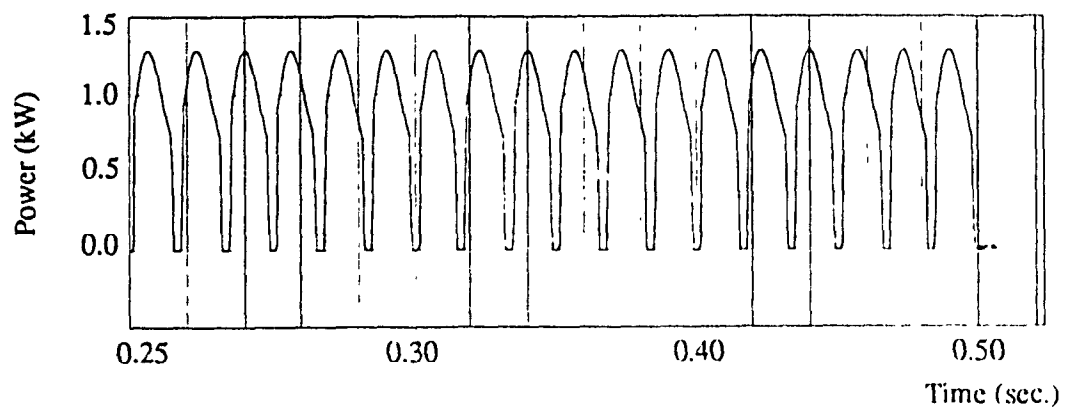
(c) Generated by the non-ideal trapezoidal source

Fig. 2.5: Instantaneous power supplied by the voltage source

From these figures, the rms values of source voltage and current, the average power and apparent power of the source can be obtained to calculate the PF, as shown in Table 2.1.

Table 2.1: Comparison of power factor

	Sinusoidal	Ideal-Trapezoidal	Non-Ideal Trapezoidal
V_{rms}	83.9 V	83.5 V	82.3 V
I_{rms}	14.7 A	10.5 A	11.0A
S	1233.3 VA	876.7 VA	905.3 VA
P	925.47 W	846.64 W	859.68 W
PF	0.75	0.97	0.95

As seen from Table 2.1, the trapezoidal source can supply 97% of its power capability as compared to 75% for the sinusoidal source. The non-ideal trapezoidal source has a small effect on the power factor.

2.3.2 Effects of the supply waveshape on the waveform distortion

The waveform distortion at the supply point and ac sides of the first load and last load generated by the sinusoidal, ideal and non-ideal trapezoidal sources respectively are presented in Fig. 2.6 (a), (b) and (c).
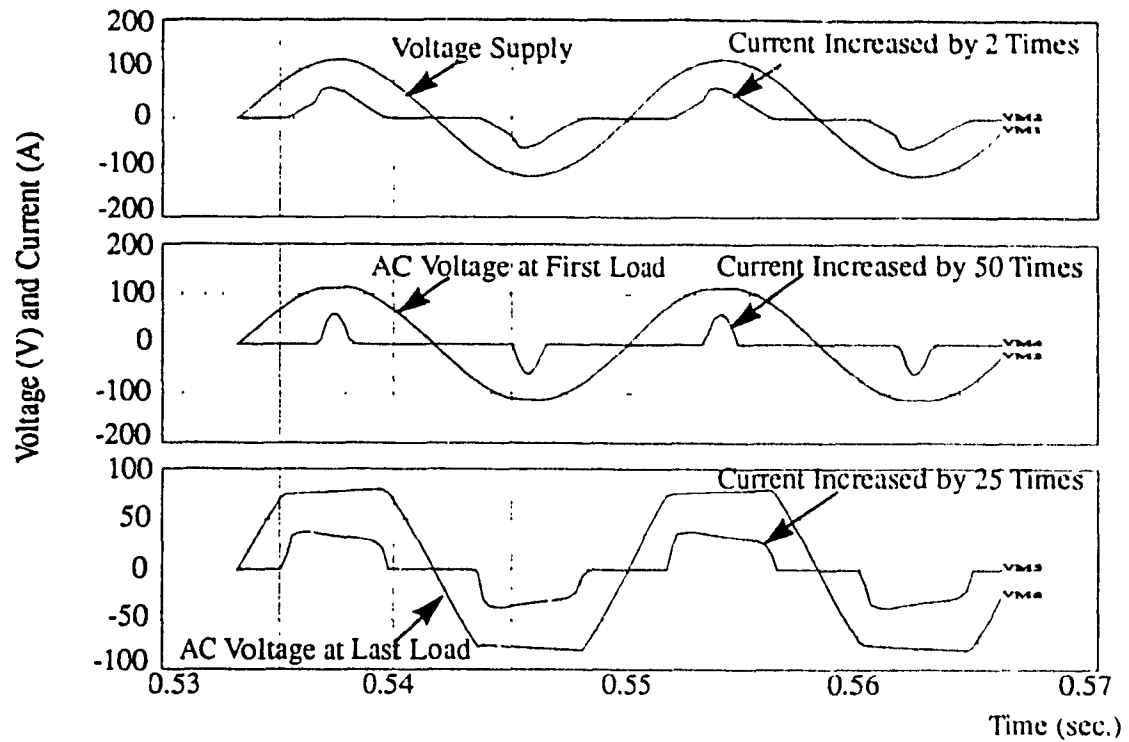
Fig. 2.6 (a): Generated by the sinusoidal source
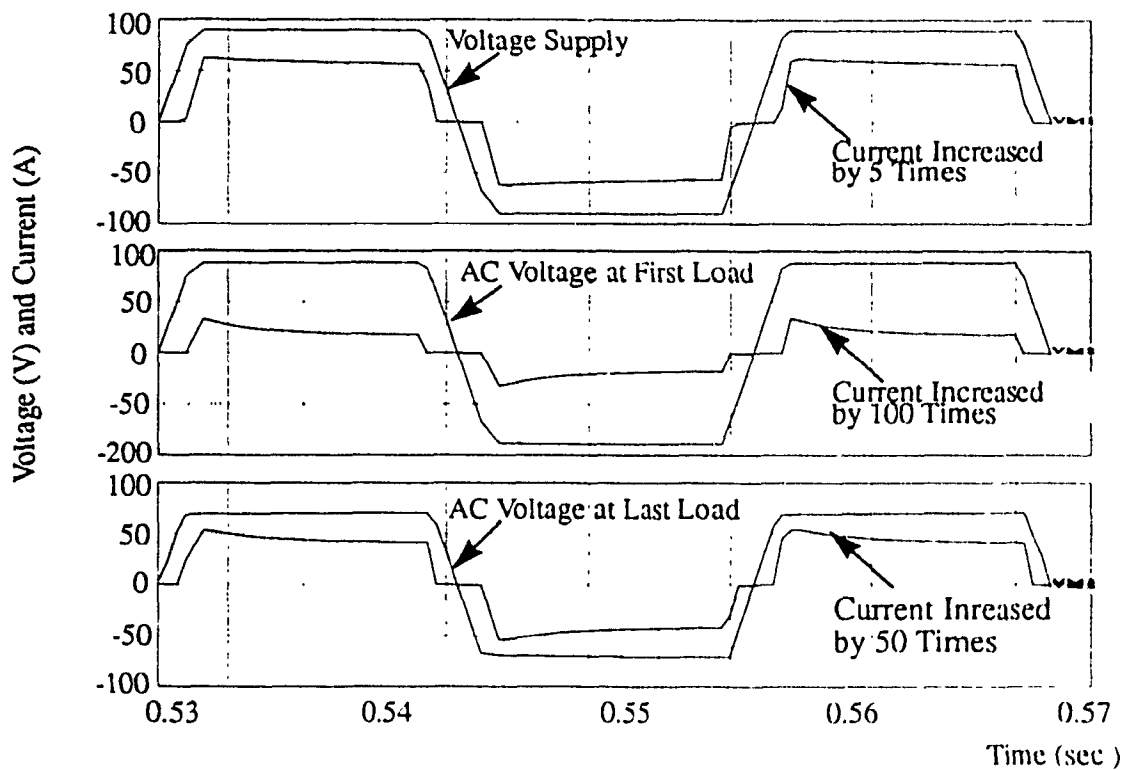
Fig. 2.6 (b): Generated by the ideal trapezoidal source

- 22 -
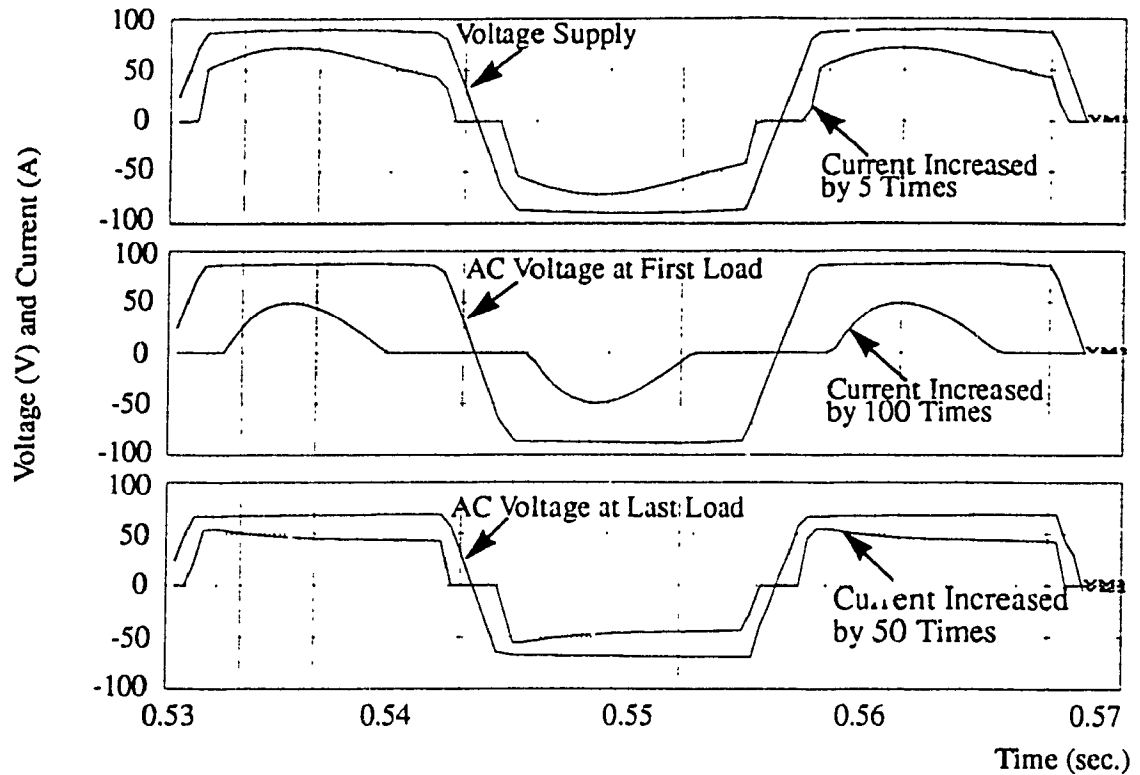
Fig. 2.6 (c): Generated by the non-ideal trapezoidal source

Fig. 2.6: Distorted waveforms at the supply point, first load and last load respectively

The phase shift (θ) between the voltage and current is often due to the energy-storage components in the system, and the waveform distortion is due to the ronlinearity of the loads.

One measure of distortion in the waveform is known as the total harmonic distortion (THD) which is defined as [12]:

$$THD = \sqrt{\frac{X_{rms}^2 - X_{1rms}^2}{X_{1rms}^2}} \qquad (2\text{-}3)$$

Where X_{1rms} is the rms value of the fundamental component of X.

Since the sinusoidal source and the trapeziodal s *urce have the different wave-forms at the supply point, to relect the distortion of the ac current and the voltage at the remote distance, a new definition of distortion factor is made as:

$$DF = \frac{|THD_n - THD_s|}{THD_s}$$ (2-4)

Where THD_s and THD_n are the THD of supply voltage and a certain component respectively.

The THDs, DFs and the phase shift angles (θ) for the waveforms in Fig. 2.6 are shown in Table 2.2 (The harmonic spectrum data for the waveforms in Fig. 2.6 are shown in Appendix C).

Table 2.2: THD and phase shift angle

	Position	Sinusoidal Source		Ideal Trapezoidal Source		Non-Ideal Trapezoidal Source	
		Voltage	Current	Voltage	Current	Voltage	Current
THD	Supply	0.100	0.689	0.355	0.308	0.306	0.183
	First Load	0.122	1.637	0.337	0.401	0.313	0.557
	Last Load	0.199	0.440	0.367	0.340	0.351	0.331
DF	Supply	0	5.89	0	0.13	0	0.4
	First Load	0.22	15.4	0.03	0.13	0.02	0.82
	Last Load	0.99	3.4	0.05	0.04	0.15	0.08
$\cos\theta$	Supply	0.769		0.976		0.975	
	First Load	0.307		0.969		0.875	
	Last Load	0.769		0.976		0.975	

From Table 2.2, the following points are observed:

(i) The current drawn by the first load is more distorted than that drawn by the last load since the discharge time of the capacitor is proportional to the impedance of the constant-power load, which is defined as:

$$R = \frac{V}{I} = \frac{V^2}{P}$$

(ii) The voltage at some distance from the generation point is distorted due to the system impedance.

(iii) The waveforms generated by the sinusoidal source are more distorted than those generated by the trapezoidal source. The current waveform at the trapezoidal supply point and the waveform of ac voltage at the last load are very similar to the waveform of the voltage sup.'ly.

2.3.3 Effects of the supply waveshape on the loading capability

To power the same load by a different source, the maximum current required from the supply and the voltage distributed at the last load are shown in Table 2.3. The more current required from the supply results in more voltage drops for the cable impedance. Therefore, the sinusoidal system has lower voltage (rms) at the ac side of the last load. However, the capacitor at the output of HTU converter is charged at the peak of ac waveform. The sinusoidal system has a little higher dc voltage at the last load.

Table 2.3: The maximum supply current and dc voltage at the last load

	Sinusoidal Source	Ideal Trapezoidal Source	Non-Ideal Trapezoidal Source
V_{rms}	83.9 V	83.5 V	82.3 V
$I_s (max)$	30.5 A	12.5 A	14.4 A
$V_{last} (ac)$	58.5 V	64.5 V	61.4 V
$V_{last} (dc)$	78.1 V	70.2 V	68.3 V

For the three types cf supplies, the voltages at the last load are above the limit (40V) with a large of margin. However, the supply current required from the sinusoidal source is higher than twice of that from the trapezoidal source. If the current limit of 15A is imposed to the source, the output voltage of the sinusoidal source will drop. Consequently, the distribution voltages across the loads will be very low resulting in collapse of system operation. Therefore, the trapezoidal source has higher loading capability. However, if the source is not ideal, the current requirement is increased, and this results in the system operation with little current margin.

2.4 Description of the system steady state performance

As seen from the above sections, the 90V 60Hz trapezoidal voltage supply can be chosen for powering the networks. The non-linear steady state performance of the distribution system is described in Fig. 2.7.

I II I II

100

(a) Input Voltage

0

Vac2

Voltage (V)

-100

82

(b) Output Voltage

78

V3_1C

74

2

(c) Input Current

0

I(RLS)

-2

Current (A)

0.72

(d) Output Current

0.68

I(Idc2)

0.64

0.50   0.51   0.52   0.53

Time (sec.)
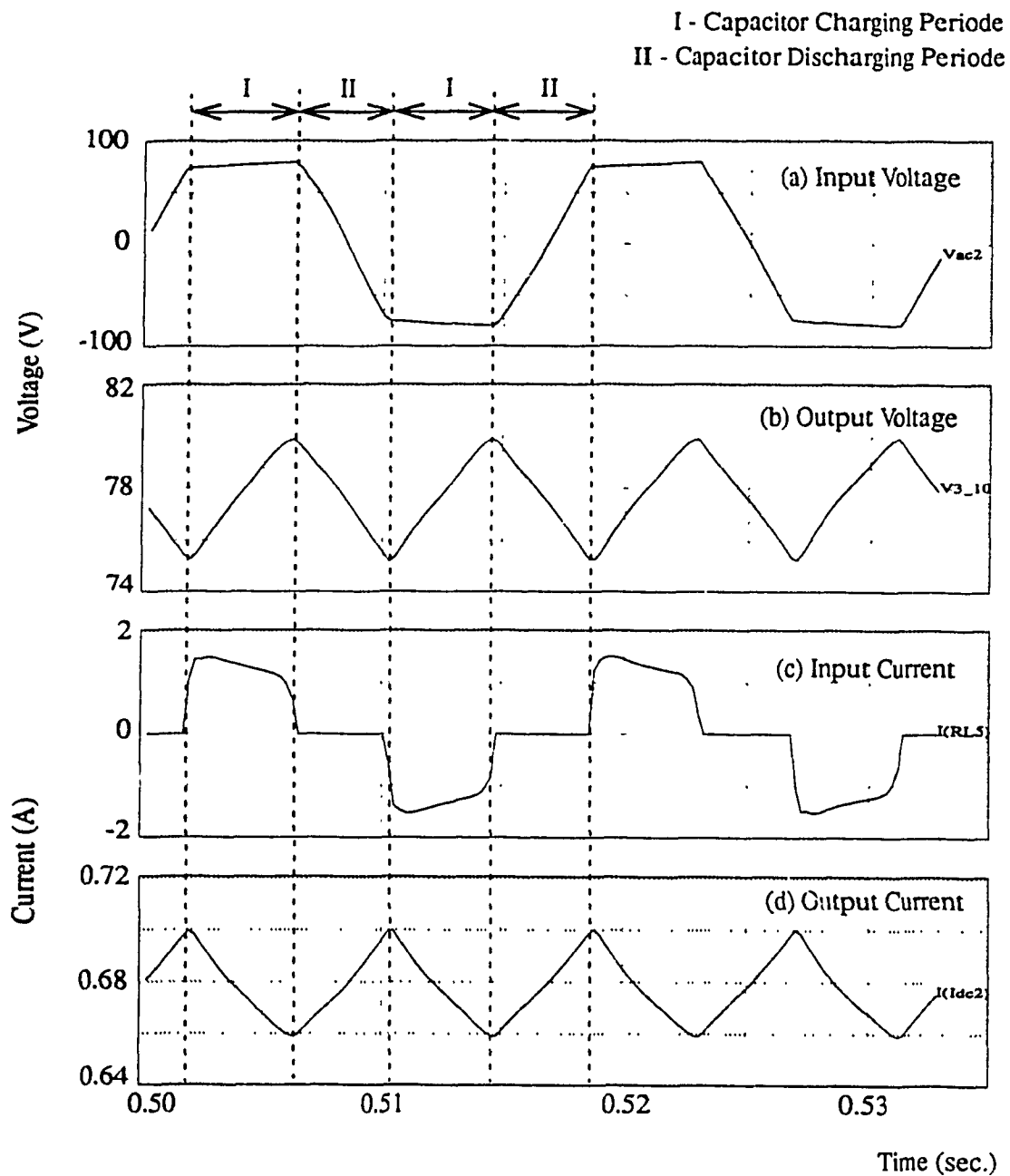
Fig. 2.7: Input/output voltage/current of the constant-power rectifier

Fig. 2.7(a) & (b) illustrate the waveforms of the voltage distributed over the drop cable and the dc voltage to power the load. Fig. 2.7(c) & (d) show the waveforms of the current through the drop cable and the load respectively. When the input voltage of the

rectifier is higher than the voltage across the capacitor, the diodes turn on, the capacitor is charged and the load draws current from the supply line. When the ac voltage drops below the capacitor voltage, the diodes turn off and the capacitor is discharged by the load. The load current is the discharging current, and no current is drawn from the ac line. It is shown that, for the chosen trapezoidal input waveform, the line current drawn by the load is flattened at the peak. This results in less distortion of line current and consequently of voltage at some distance from the generation point and thus high powering efficiency as discussed above.

2.5 Conclusions

In this chapter, the following conclusions are obtained:

(1) A 90V, 60Hz trapezoidal waveform voltage distribution over both the distribution and the drop cables provides a good comprise between safety, corrosion and distribution losses.

(2) The non-ideal trapezoidal source has little effect on the power factor and waveform distortion. However, it increases the supply current and reduces the loading capability of the network.

Chapter 3

Modeling of Power Distribution System for Hybrid Fiber/Coax Networks

3.1 Introduction

The power system for the HFC network is a very complex system. Studying the system performance by using basic theory and mathematical models is a time consuming process. By the aid of computer simulation, the behavior of the system can be studied in detail quickly and the results provide remarkable accuracy based on certain assumptions.

This chapter describes the considerations, constraints and procedures being used to develop the simulation model of the power system using PECAN [13]. Power circuit models of power node (PN), coax node (CN), cables and home terminal units in each possible state are presented.

3.2 System description

To study the behavior of the system in detail, various simulation models are developed in this section. Items of concern to the power distribution system for a model consist of:

- Power node (PN): 60Hz trapezoidal power source.

- Coax node (CN).

- Distribution and drop cables.

- Home termination: constant-power ac/dc converters.

A typical HFC power system, which is a basic configuration for modeling, is shown in Fig. 3.1:
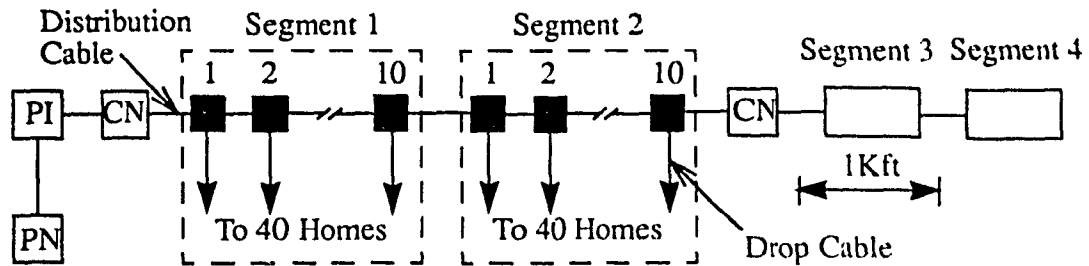
Fig. 3.1: Typical HFC power system layout

The power node is inserted to power 160 homes which are subdivided into four segments. Each segment has a typical length of 1000ft and contains 10 drop boxes over a span of 100ft. Each drop box serves four homes. The typical distance between a drop box and the home is about 100ft. A coax node is required between every two segments.

3.3 Reference segment and modeling constraints [14]

3.3.1 Reference segment

Designing the system to enable all homes to be able to simultaneously draw their peak power is clearly not cost-effective. Therefore, a "reference segment" is defined for system design purposes. In a reference segment, the states of 40 homes are:

- 28 Homes: On-Hook;

- 6 Homes: Off-Hook;

- 4 Homes: Ringing;

- 2 Homes: Ring Trip.

- 30 -

Assuming that the maximum traffic rate is 9ccs, the best estimates available from Nortel for the home power demand are shown in Table 3.1:

Table 3.1: Home power demand in various operating states

Home State	On-hook	Off-hook	Ring	Ringtrip
Power 1-line home	3.00W	4.06W	7.07W	14.00W
Power 2-line home	3.12W	4.91W	10.94W	14.86W
Ref. seg. power	84.48W	31.46W	28.28W	28.00W
Average power demand / Home = 4.3 W				

For the point of view of system stability, the power allocation in the reference segment should be considered very carefully since each home demands different power depending on the state it is in. Voltages at each home will fall if, for example, the last home changes from on-hook to ringing state. Since all homes act as constant power load, each will demand more current than before. This in turn reduces the voltage at homes even further, and may eventually result in the system operation failure if the voltage distribution is too low.

Therefore, for system design purposes, it is usually assumed that the higher power demands are located at the end of each segment, as shown in Fig. 3.2, even though the probability of all the last 12 homes being in the off-hook, ring or ring trip states at the same time is very low. Designing the powering layout in this way can maintain the system stability under large load transients.

2ON1 2ON1 2ON1 2ON1 2ON1 2ON1 2ON2 2OF2 2RG1 2RT2

↕   ↕   ↕   ↕   ↕   ↕   ↕   ↕   ↕   ↕

2ON1 2ON1 2ON1 2ON1 2ON1 2ON1 2ON2 2OF2 2OF2 2RG2
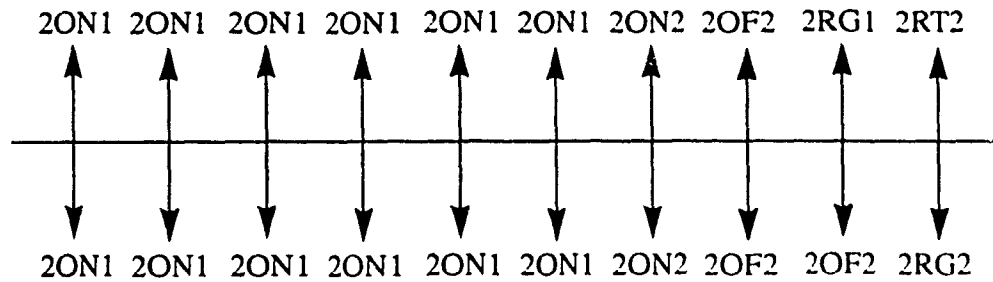
```
Note: 2ON1 = 2 Homes, On-hook, 1 line
      2ON2 = 2 Homes, On-hook, 2 lines
      2OF2 = 2 Homes, Off state, 2 lines
      2RG1 = 2 Homes, Ringing, 1 line
      2RG2 = 2 Homes, Ringing, 2 lines
      2RT2 = 2 Homes, Ring trip, 1 line
```

Fig. 3.2: Home states allocation

According to Table 3.1 and Fig. 3.2, the power allocation in the reference segment is shown in Fig. 3.3:

6.00   6.00   6.00   6.00   6.00   6.00   6.24   9.82   14.14   28.00 (W)

↕   ↕   ↕   ↕   ↕   ↕   ↕   ↕   ↕   ↕

6.00   6.00   6.00   6.00   6.00   6.00   6.24   9.82   9.82   28.00 (W)
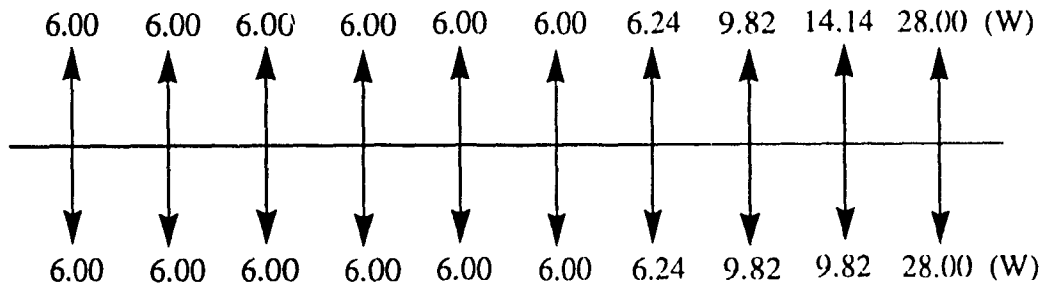
Fig. 3.3: Home power demands allocation

3.3.2 Modeling constraints

Efficiency and economy require that each PN be able to provide power at adequate voltage levels to all active devices over as long a distance as possible. However, the

system operation must meet the following constraints of current and voltage:

(i) Current limit: The maximum current which can be supplied by the PN, or delivered by each cable is limited to 15A;

(ii) Voltage limit: All devices (CN and homes) are being designed to operate at terminal voltages between 40 to 90V. At voltages below the minimum of 40V, all devices switch to a high resistance (>10 kΩ).

If these constraints are not met, the power demand (powering distance) should be reduced.

3.4 Modeling of Distribution System

The power distribution system layout in Fig. 3.1 can be represented by an equivalent circuit in PECAN as shown in Fig. 3.4.
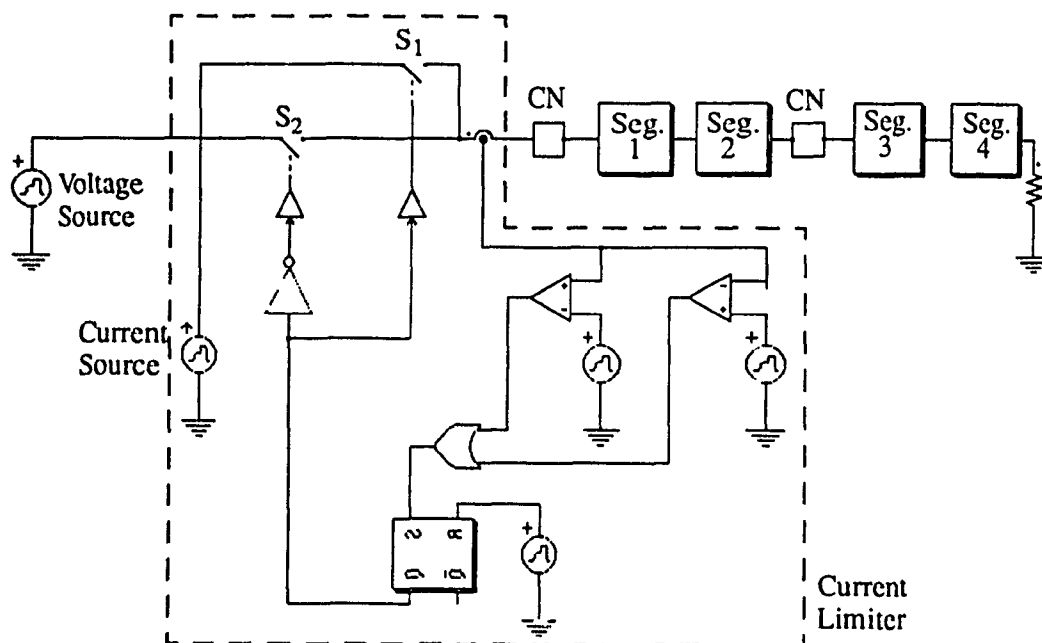
Fig. 3.4: Model of power distribution systems for HFC network

- 33 -

The power node is modeled as a voltage source with current limiter. Four segments are modeled according to the reference segment. Every two segments need one coax node, which has the constant power demand of 45W.

3.4.1 Power node with current limiter

In Fig. 3.4, the power node is a voltage source with a trapezoidal waveform, whose transition time from the positive peak to the negative is 1.8 ms, as shown in Fig. 3.5. Two different voltage levels, 60V and 90V, will be used in studying the system performance.
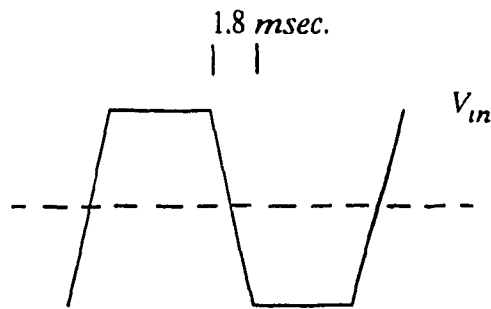
Fig. 3.5: Waveform of the coax node input voltage

In Fig. 3.4, switches S_1 and S_2 are used to implement the "constant-current" protection [15], as shown in Fig. 3.6. When the current is within $\pm 15A$, S_1 is ON and S_2 is OFF. The power supply provides a voltage with constant rms. Once the current exceeds the limit of 15A, S_1 turns OFF and S_2 turns ON. The peak value of output current will be limited at $\pm 15A$, and the power supply now acts as a current source, and the output voltage drops.
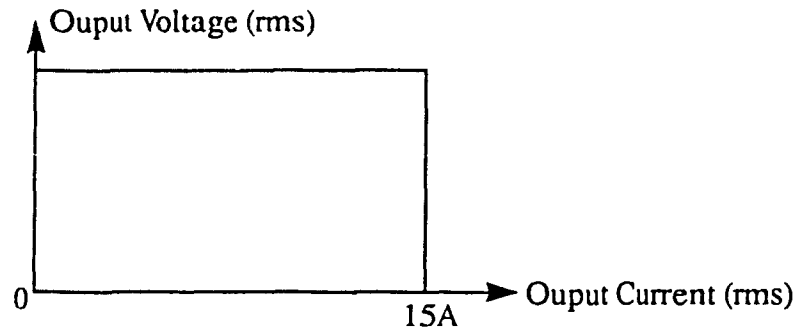
Fig. 3.6: "Constant-current" protection

The states of S_1 & S_2 are controlled by some comparators, logic gates and set-reset flip-flop, as shown in Table 3.2. At the beginning, the initial states of S_1 & S_2 are set by "S=0, R=1". After that, the switches states will not change by "S=0, R=0" if $-15A \leq I_s \leq 15A$. When the current exceeds the limit, S_1 turns off and S_2 turns on by "S=1, R=0", and these states will be locked by "S=0, R=0".

Table 3.2: The states of the switches at certain time

Time (sec)	Current (A)	S	R	Q	S_1	S_2
t=0.0 ~ 0.4	$-15 \leq I_s \leq 15$	0	1	0	0	1
t=0.4 ~ 0.6	$-15 \leq I_s \leq 15$	0	0	0	0	1
	$I_s < -15$ or $I_s > 15$	1	0	1	1	0
	$-15 \leq I_s \leq 15$	0	0	1	1	0

The operation of the current limiter is shown in Fig. 3.7. During the start up transient of the simulation, a high reference value is set so that the limiter is designed to respond to only the over current in the normal operating state. In Fig. 3.7(a), the system

operation does not exceed the limits of current and voltage. However, in Fig. 3.7(b), the current required from the source is 19.2A exceeding the limit. The source operates in a current limit mode, and load voltages drop greatly. The load voltage is represented as V_{i_j}, which means, the voltage is measured from the load connected to the jth drop box in the ith segment.

.
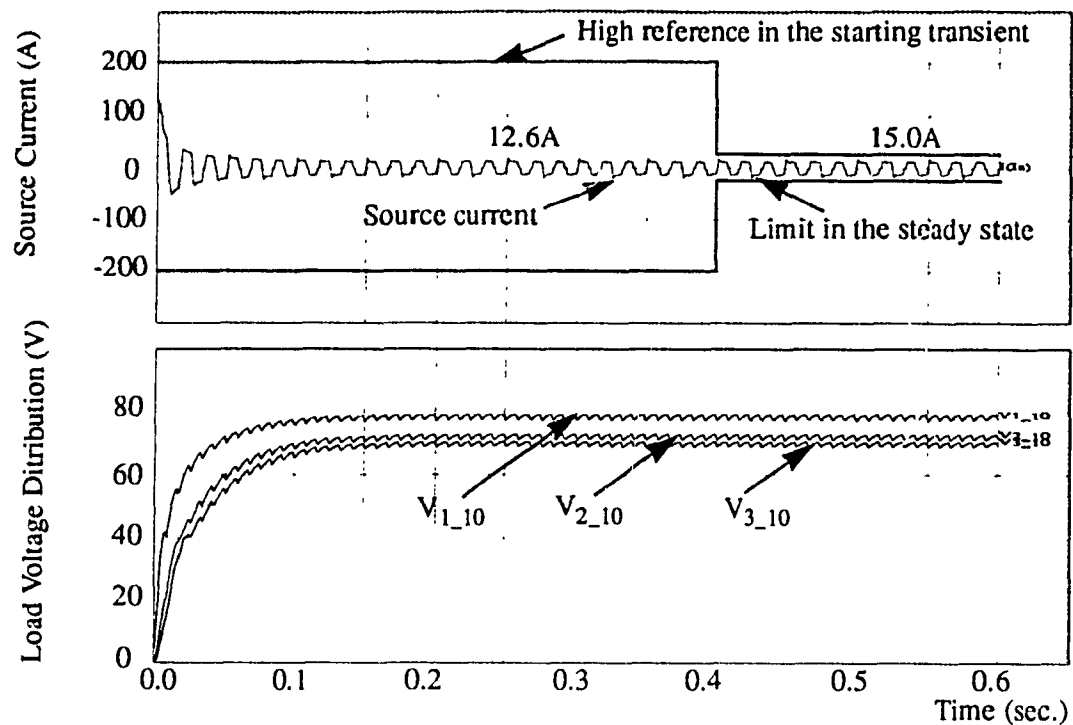
(a) $-15A \leq I_s \leq 15A$
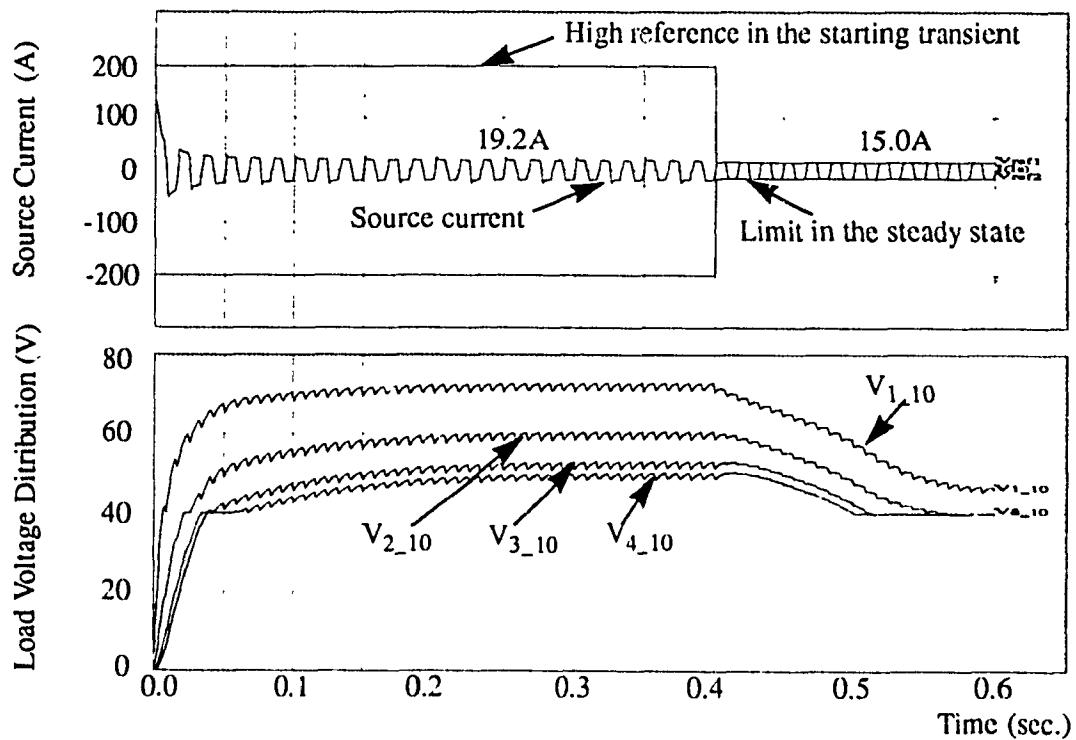
(b) $I_s > 15A$ or $I_s < -15A$

Fig. 3.7: Operation of the current limiter

3.4.2 Coax node and HTUs - constant power load model [16, 17]

The coax node and HTUs are modeled as constant power ac/dc converters, as shown in Fig. 3.8.
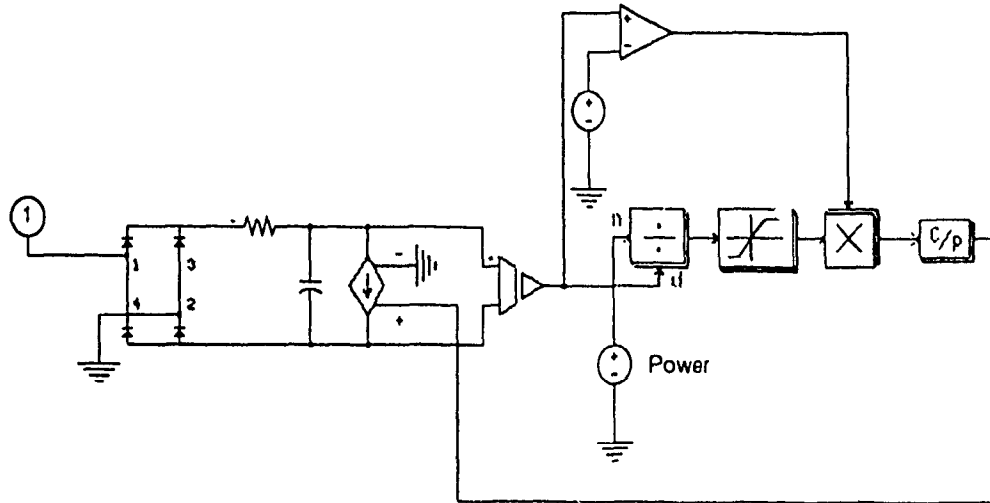
Fig. 3.8: The model of the constant-power load

A voltage controlled current source is connected to the output of the converter to ensure constant power demand. The amplitude of the source is determined by:

$$I_l = \frac{P_l}{V_o}$$

Where V_o is the voltage across the converter output filter, and P_l is the given load power, which depends on the CN power demand and the operating state of the home load.

Considering the constraint of operating voltage, a voltage limit of 40V is imposed. Below 40V, the load can not function properly and will be disconnected. In order to simulate the effect of the current clamping in the actual circuit, the load current is limited to 1 A through a limiter. This limiter is essential in the simulation since the load tends to draw excessive amount of current when the load voltage is low during the starting transient.

3.4.3 Distribution and drop cables

The structure and representation of the coax cable are shown in Fig. 3.9.
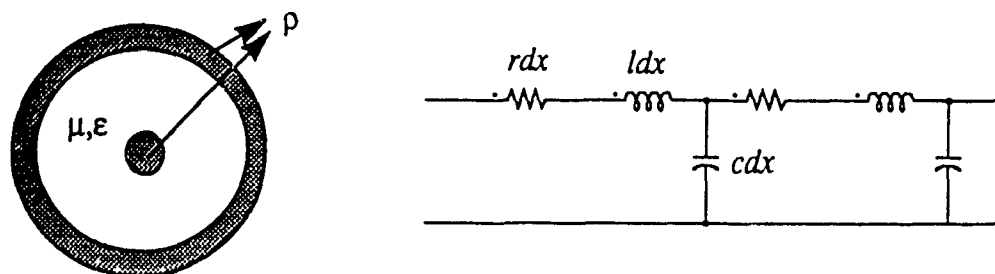
Fig. 3.9: Structure and representation of the coax cable

Current is carried by the inner conductor, and an equal and opposite current is carried by the outer tubular conductor. The resistance, inductance and capacitance of unit length (distributed elements) of the coax cable are:

$$r = \frac{\rho}{A}, \quad l = \frac{\mu}{2\pi}\ln\frac{b}{a} + \frac{\mu}{8\pi}, \quad c = \frac{\pi\varepsilon}{\ln\frac{b}{a}} \quad (3-1)$$

The orders of r, l and c per feet are $10^{-2}\Omega$, $10^{-8}H$ and $10^{-8}F$ respectively [18].

The impedance of a cable of 10.16m (100ft) length can be represented by the lumped elements R, L, C:

$$Z = \frac{R + j\omega L}{1 - \omega^2 LC + j\omega RC} \quad (3-2)$$

A.. ``he operating frequency of 60Hz, with $\omega^2 LC \ll 1$ and $\omega RC \ll 1$, Equation (3-2) becomes:

$$Z = R + j\omega L \quad (3-3)$$

Therefore, the capacitance can be neg.·cted and the cable of 100ft is modeled by a lumped resistance and inductance, as shown in Fig. 3.10.
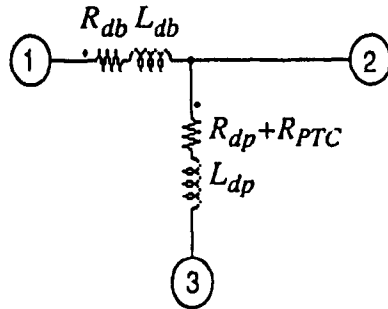
Fig. 3.10: The model of distribution & drop cables

Three types of distribution cable are considered:

(i) Cable A (0.5" dia.): $L_{db}=83$ µH/100m, $R_{db}=1.69$ Ω/100m;

$$(L_{db}=8.4 \text{ µ}H/100ft, R_{db}=0.172 \text{ Ω}/100ft)$$

(ii) Cable B (0.625" dia.): $L_{db}=83$ µH/100m, $R_{db}=1.05$ Ω/100m;

$$(L_{db}=8.4 \text{ µ}H/100ft, R_{db}=0.107 \text{ Ω}/100ft)$$

(iii) Cable C (0.75" dia.): $L_{db}=83$ µH/100m, $R_{db}=0.748$ Ω/100m.

$$(L_{db}=8.4 \text{ µ}H/100ft, R_{db}=0.076 \text{ Ω}/100ft)$$

The drop cable inductance and resistance are: $L_{dp}=0.83$ µH/m, $R_{dp}=0.59$ Ω/m $(L_{dp}=8.4 \text{ µ}H/100ft, R_{dp}=6 \text{ Ω}/100ft)$.

Considering the positive temperature coefficient (PTC) device used to limit the current during the fault, there is an extra resistance, R_{PTC}, added in series with the drop cable: $R_{dp}+R_{PTC}$.

3.4.4 Segment model

In Fig. 3.4, the power supply is powering 4 segments, which are represented by 4

identical subcircuit blocks. The circuit in each segment is shown in Fig. 3.11. Identical subcircuit blocks 1 to 10 represent the distribution and drop cables as modeled in Fig. 3.10. Subcircuits A to J are the homes modeled as the constant power loads in Fig. 3.8.
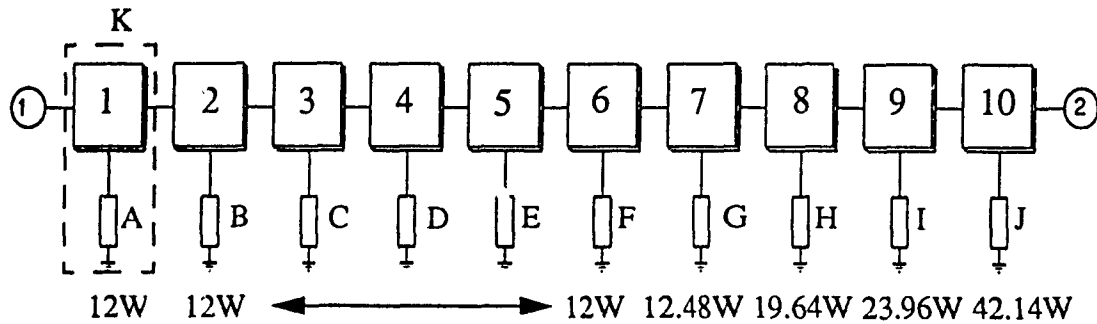
Fig. 3.11: The circuit in each segment in Fig. 3.2

In Fig. 3.11, there are 4 homes connected to each drop box. The detailed circuit in the block K is illustrated in Fig. 3.12(a). In order to reduce the dimension of the system and the simulation time, 4 homes are combined into one equivalent home, as shown in Fig. 3.12(b). The home power demand and allocation in Fig. 3.11 are defined according to the reference segment.

(a) Detailed circuit

(b) Combined circuit
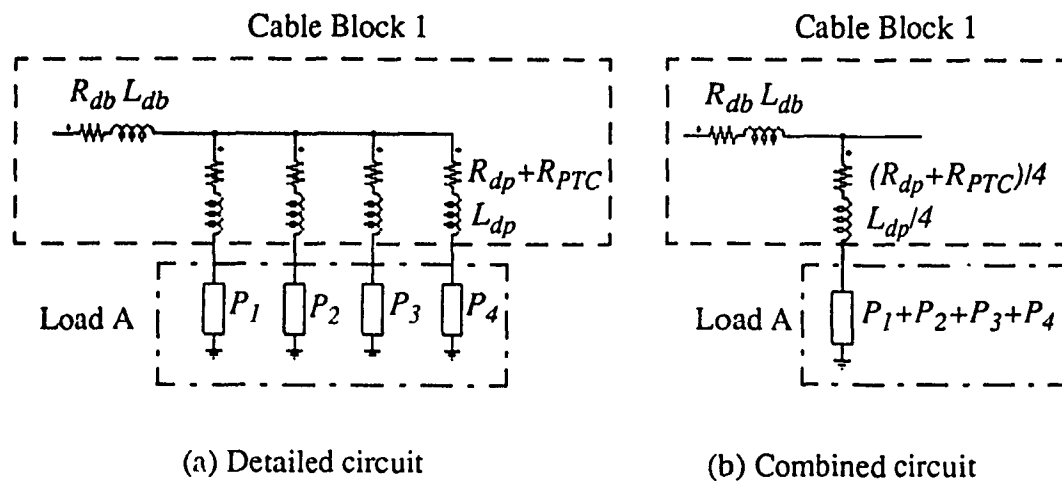
Fig. 3.12: The circuit in block K in Fig. 3.11

3.5 Conclusions

Taking into account the constraints of stability, current and voltage, the simulation model of the power system for HFC networks has been developed in PECAN. The model includes:

(i) PN - A trapezoidal voltage source with current limiter;

(ii) CN - Constant power load, which consists of single-phase diode bridge, capacitor filter and voltage controlled current source.

(iii) Distribution and drop cables - Lumped series RL.

(iv) 160 HTUs - Constant power loads.

Cables and HTUs are subdivided into 4 segments. The power demand and allocation are defined in the reference segment.

In the following chapters this model will be used to study the system performance.

Chapter 4

Loading Capability of the HFC Power System

4.1 Introduction

The study in this chapter focuses on the loading capability of the HFC network. The maximum loading capability will vary under different powering and operating conditions. These effects will be studied by the following work:

(i) Different distribution cables and different power node output voltages, 60V system and 90V system, are compared.

(ii) Different operating conditions are considered to ensure that the constraints of stability, voltage and current are met under all reasonable conditions.

(iii) Inserting multiple power nodes at certain places is tried to enhance the system loading capability greatly.

From the simulation results, the maximum loading capability of the system can be determined.

4.2 Effects of the input voltage levels and cable types

The system performance is studied with the input voltage levels of 60V and 90V. Three types of distribution cables are considered. The loading capability is shown in Table 4.1 and the load voltage distribution and the required source current are illustrated in Figs. 4.1 and 4.2 respectively.

<u>*Table 4.1*</u>: The loading capability under the normal operating condition

	60V	90V
Cable A	1.5 segment	3 segments
Cable B	2 segments	4 segments
Cable C	2 segments	4 segments
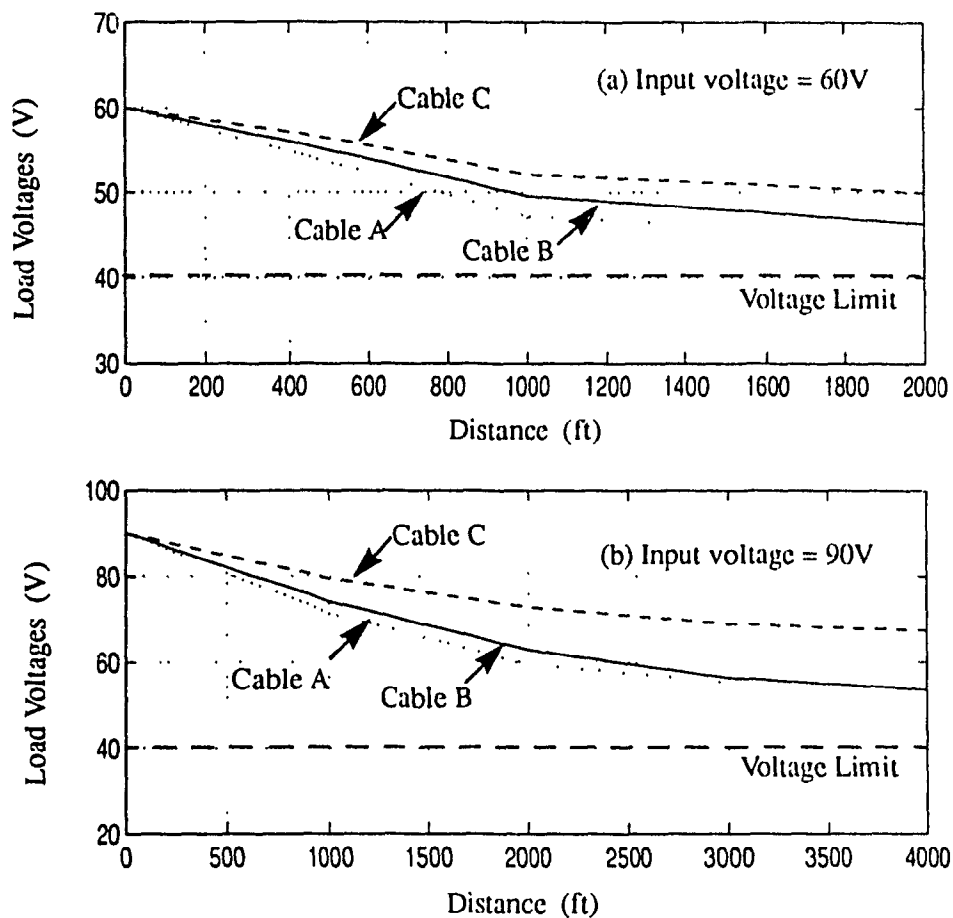
Fig. 4.1: Load voltage distributions under the normal operating condition

- 44 -

$\boxed{\diagup\diagup\diagup}$ - Cable A; $\boxed{\bowtie\bowtie}$ - Cable B; $\boxed{\diagdown\diagdown}$ - Cable C.

(a) Input Voltage = 60V   (b) Input Voltage = 90V
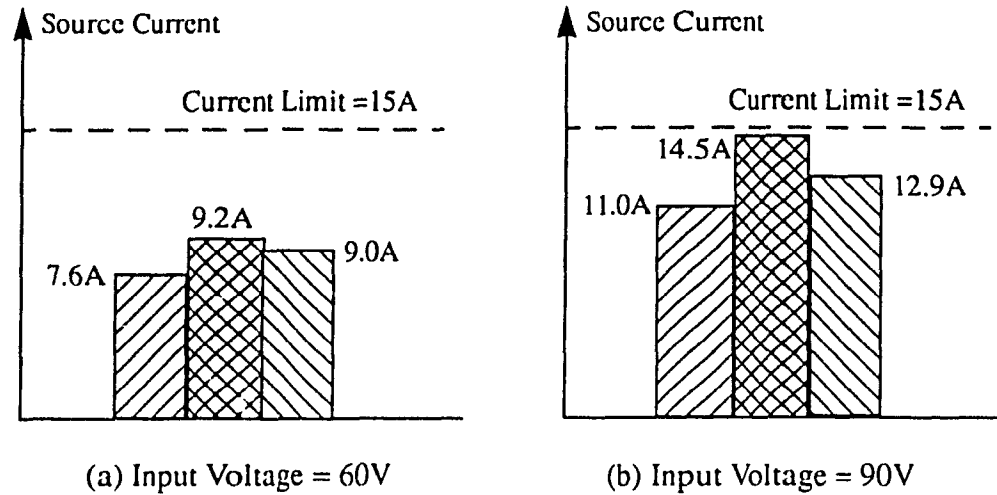
Fig. 4.2: Required source current under the normal operating condition

When the input voltage is 60V, all three types of cables fail to provide power to four segments. Specifically, by using cable A, the system can only provide power for 1.5 segments. By using cable B or C, the loading range can be extended to the second segment. Seen from Figs. 4.1 and 4.2, the 60V system is voltage limited rather than current limited, and has low power delivery efficiency.

When the input voltage is increased to 90V, the system with cable A can handle the loads up to segment 3. And with cable B and C the system can provide power for the complete 4-segment system. Compared with the 60V system, the 90V system is current limited rather than voltage limited. As can be noted from the system operation with cable B, even though the voltage at the last load is much higher than 40V, the current supplied by the voltage source is marginal. Any variations in the system may result in voltage collapse. For the system with cable C, the voltage at the last load is 67.3V and the source

current is 12.9A, which are acceptable from both voltage and current points of view. The power delivery efficiency is high.

The above results show that the choice of 60V input voltage is not feasible to provide power to all four segments of the load. In the following sections, only the input voltage of 90V will be considered, and the system performance with different distribution cables will be compared.

4.3 Effect of cable and load parameters variations

The resistance of the distribution cables will vary with temperature, increasing by about 0.4%/°C. Cable temperatures are expected to reach up to 75 °C so the resistance may be expected to increase by 20% from 20 °C to 75 °C.

The best available estimates of power demands of CN and loads are given in Chapter 3. However, there is little firm information available as to what power demand the various devices are actually going to achieve. Therefore, the system design should be based on a reasonable worst case. Increasing the distribution cable resistance by 20% and the load power by 25% is considered as the worst operating condition.
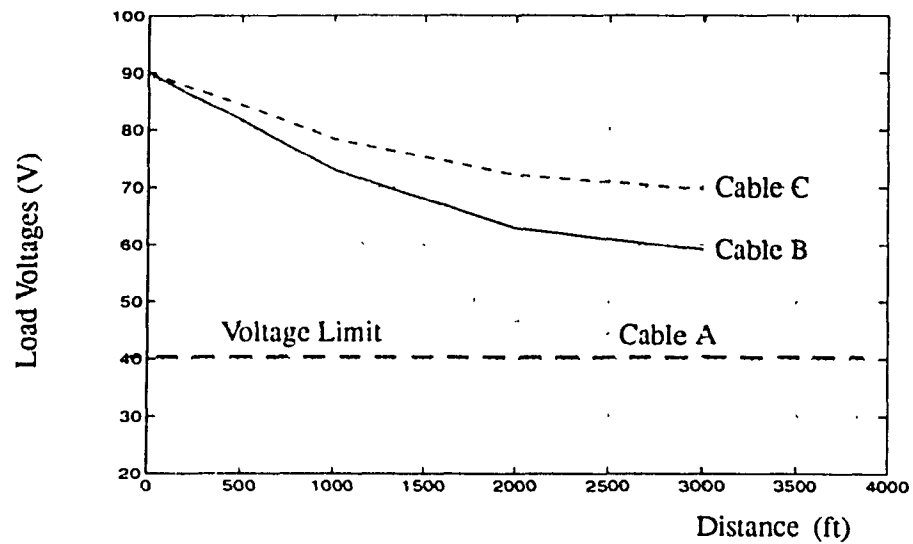
(a) Voltage distribution
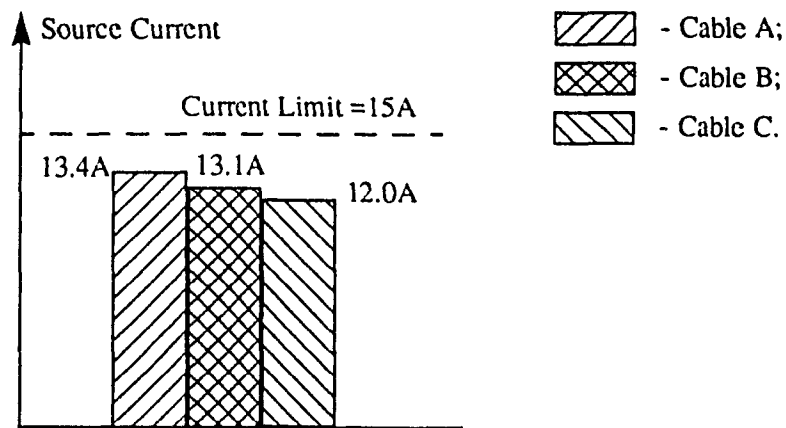
(b) Source Current

Fig. 4.3: System loading capability under the worst operating condition

As seen from Fig. 4.3, under the worst operating condition, the system with cable A can provide power for 2.5 segments. But the voltage at the last load (44.3V) and the source current (13.4A) are very close to the limits. The system with cable B or C can handle 3 segments. Specially for cable C, the system operation has more margin from the voltage and current points of view.

4.4 System with multiple sources

Previous studies show that a system with a single power supply can not provide power to the complete system with four segments under the worst operating condition. An additional power source is, therefore, required to power the network. By inserting additional sources, the system loading capability can be enhanced.

4.4.1 Synchronous sources

Another source, which is in phase with the first one, can be connected to a suitable place of the distribution network to increase the load voltage levels. The place of the power inserter has a great effect on the system loading capability. It is found that the best place of the second synchronous power node is after the 5th segment, as shown in Fig. 4.4. Under the worst operating condition, by using cable B or cable C, the system can handle a maximum of 8 segments. The voltage distributions and source currents are shown in Fig. 4.5 and Fig. 4.6 respectively. Compared with a single power node system, the system with multiple synchronous sources has higher loading capability, as well as a large voltage margin.
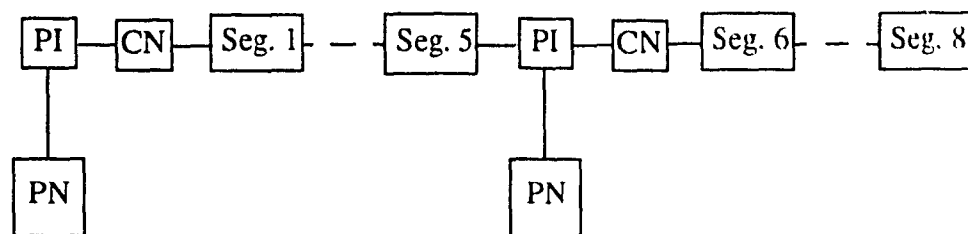
Fig. 4.4: Arrangement of synchronous sources
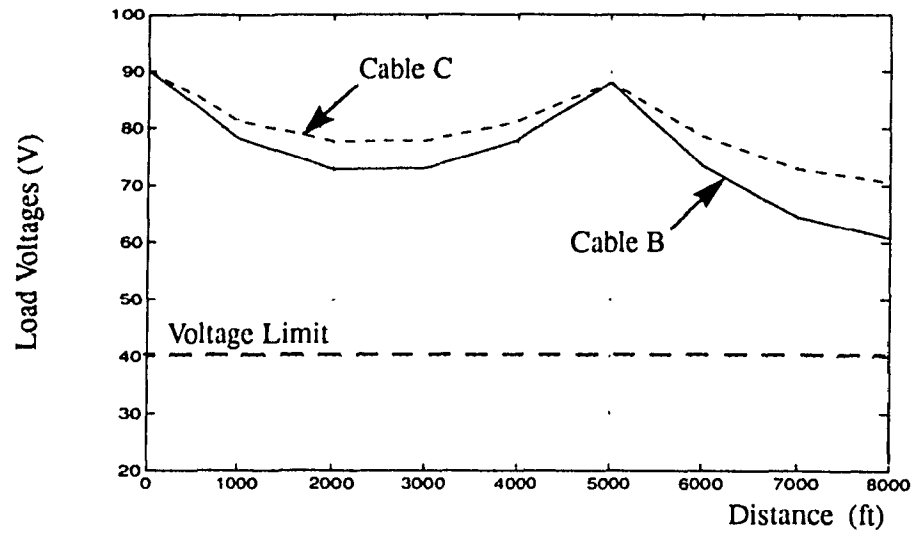
Fig. 4.5: Voltage distributions with synchronous sources
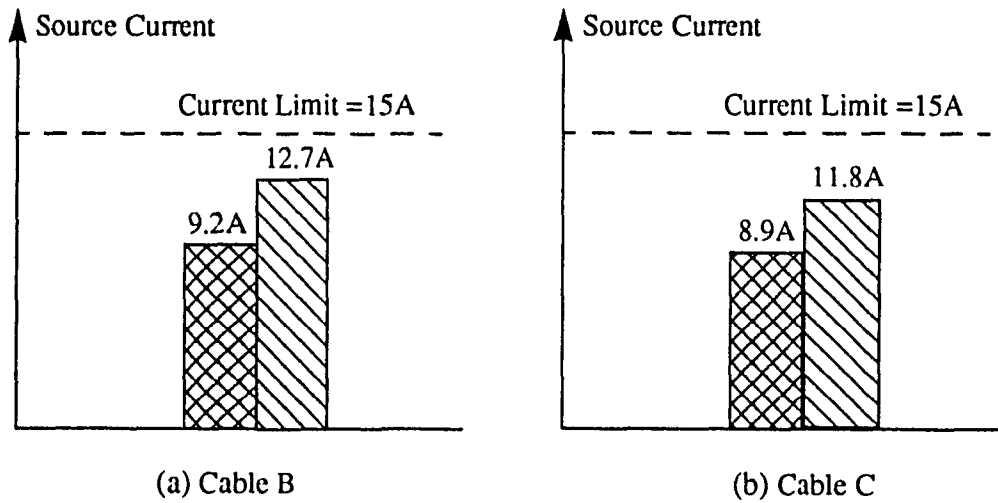
Fig. 4.6: Sources current with synchronous sources

4.4.2 Asynchronous sources

The operation described in the above section requires that the two power supply sources be synchron:zcd. Another option is to connect individual sources, which are not synchronized, into the network.

In this system, one powering section is separated from the other section by a capacitor. An advantage of this system is that there is no need for synchronization between different power supply sources. However, the loading capability of this system is the same as the summation of each single source system. For example, to power 8 segments of load, three power supplies would be required for cable B or cable C under the worst operating case, as shown in Fig. 4.7. The load voltage distributions are shown in Fig. 4.8. The current required from the power nodes is 13.1A and 12.0A for cables B and C respectively.
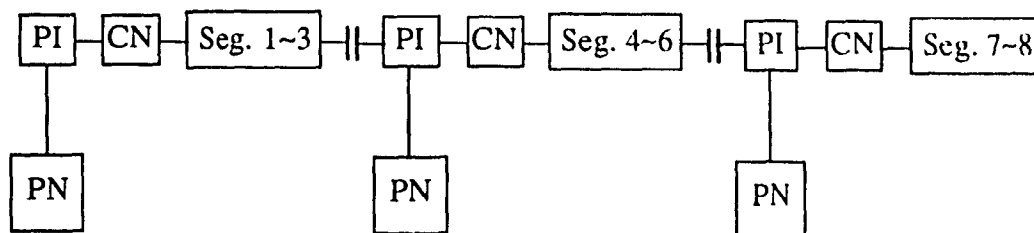
Fig. 4.7: Arrangement of asynchronous sources
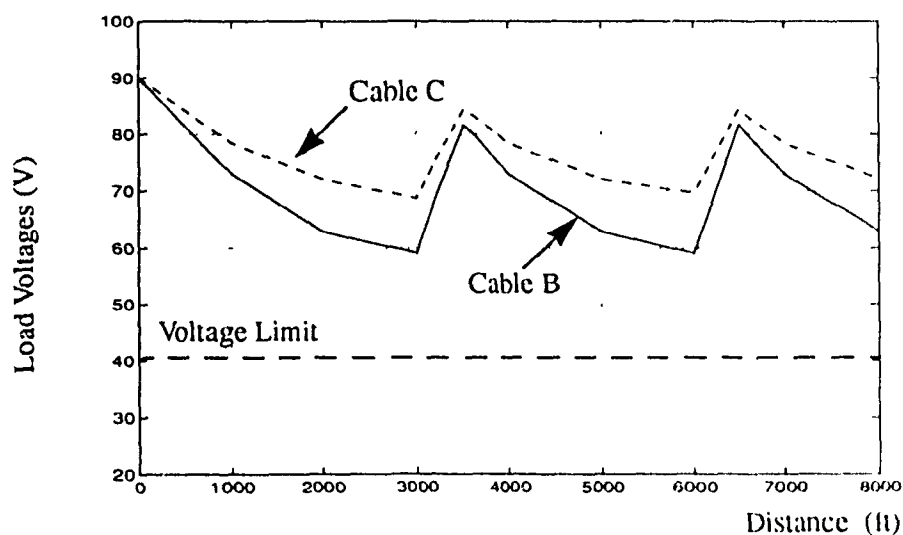
Fig. 4.8: Voltage distributions with asynchronous sources

4.5 Conclusions

In this chapter, some effects on the loading capability of the network have been studied. The following conclusions can be drawn.

(i) A 60V system has low power delivery capability. A 90V system is, therefore, selected to be the power node of the distribution system as it has greater power delivery capability.

(ii) It is not feasible to power a 4-segment system by Cable A under any conditions. Cable B and C have the same loading capability of 4 segments and 3 segments under the normal and the worst operating conditions, respectively. However, considering the limits on voltage and current, cable B has a narrow margin and cable C has a larger margin of safety.

(iii) By inserting an asynchronous source, the loading capability remains the same as that of the summation of each single source system.

(iv) The loading capability can be enhanced greatly by inserting synchronous sources. The best powering arrangement is shown in Fig. 4.9.
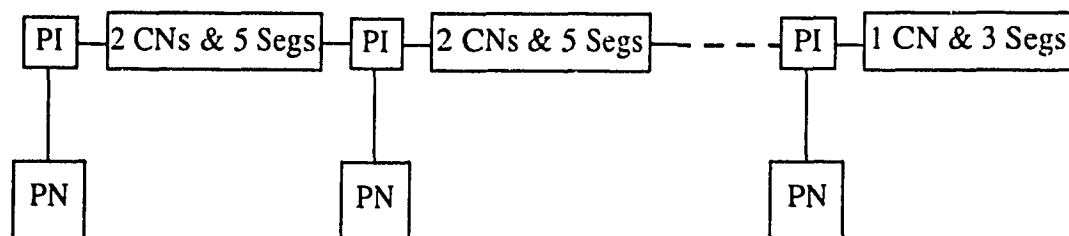
Fig. 4.9: Best arrangement of synchronous sources

Chapter 5: Fault Analysis

5.1 Introduction

If a short circuit occurs across a load in the home terminal unit, the network may become inoperational in whole or in part due to insufficient voltage levels across the other loads. For example, if the fault occurs at the HTU connected to the first drop box in segment 1 (worst fault location), the response of the power system is as shown in Fig. 5.1.

It can be seen from this figure that the current flowing through the drop cable with the fault increase from the normal value of 0.06A to the abnormally high value of 8.7A in the transient, and to 4.9A in the steady state. (Much more current would have been drawn from the source if it did not have a current limit at 15A). As a result, the distribution voltage after the fault location falls below the minimum voltage level and the system can not be operational even for 1 segment of the network as shown in Fig. 5.1(b).

In order to enhance the system operability, there is a positive temperature coefficient (PTC) resistor in series with each drop cable. The PTC resistor can provide overcurrent protection of individual components by tripping during fault conditions and resetting itself when the fault is removed.

In this chapter, the characteristics and the procedure for selection of the PTC device are introduced. The performance of the system under the fault conditions, especially during the trip time of the PTC device, is studied. The simulation results of the system against a single fault and two simultaneous faults are presented.
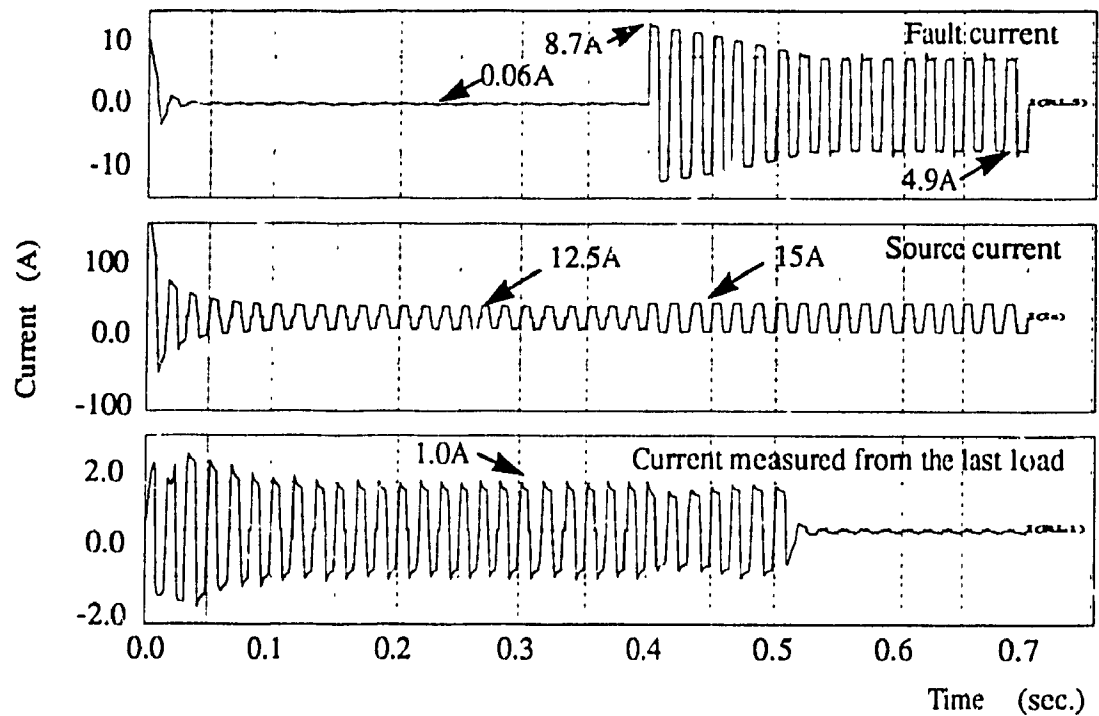
(a) Currents through the source, the last load and the load with fault
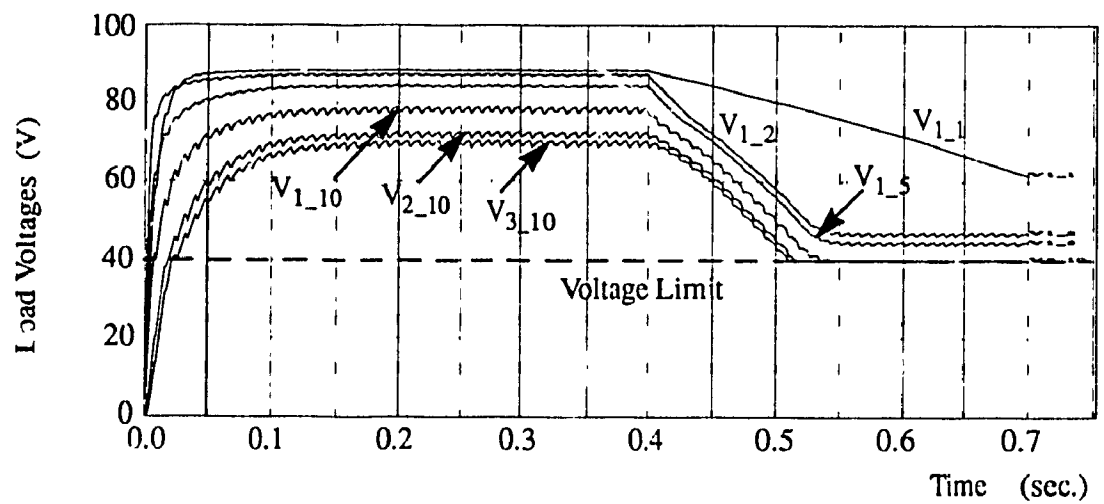
(b) Voltage distributions

Fig. 5.1: System response during a fault

5.2 Characteristics and Selection of PTC Resistor [19]

5.2.1 Characteristics of PTC devices

PTC devices are made from a conductive polymer blend of specially formulated plastics and various conductive materials. At normal operating temperatures these devices have very low resistance. During a fault, when abnormally high current is present, the temperature of the PTC device increases and the crystalline structure changes to an amorphous state and expands. The conductive paths within the polymer mass separate, causing a dramatic increase in the device's resistance. As the circuit resistance is increased, the current decreases until thermal equilibrium is achieved. As long as the fault is present, the PTC device will stay in the tripped state and protect the system without cycling.

When the fault is removed, the PTC device quickly cools and contracts. The conductive paths within the polymer mass come back together and normal operation can resume.

The applications of PTC devices in the telecommunications networks include:

(1) Resettable telecommunications protection.

PTC devices provide resettable overcurrent protection in telephone interface applications. When an overcurrent hazard occurs on a tip/ring interface, PTC devices effectively limit current, then return the circuit to normal operation once the fault subsides.

(2) Protection against failures.

A short circuit across telecommunication equipment or a back up battery's terminal can cause very dangerously high current to flow and start a fire. In order to reduce the

chance of a fire, PTC devices can trip quickly on short circuits to limit the fault current.

PTC devices have the following distinct advantages over other methods of circuit protection:

(1) Remotely resettable, they can automatically reset themselves thousands of times, thus eliminating unnecessary product downtime.

(2) Radial-leaded and surface-mount packaging make installation easy.

(3) Low resistance means low voltage drops in power circuits. Fig. 5.2 shows that the PTC devices do not have significant effect on the system loading capability since the inclusion of PTC devices does not cause substantial decrease of the load voltages.
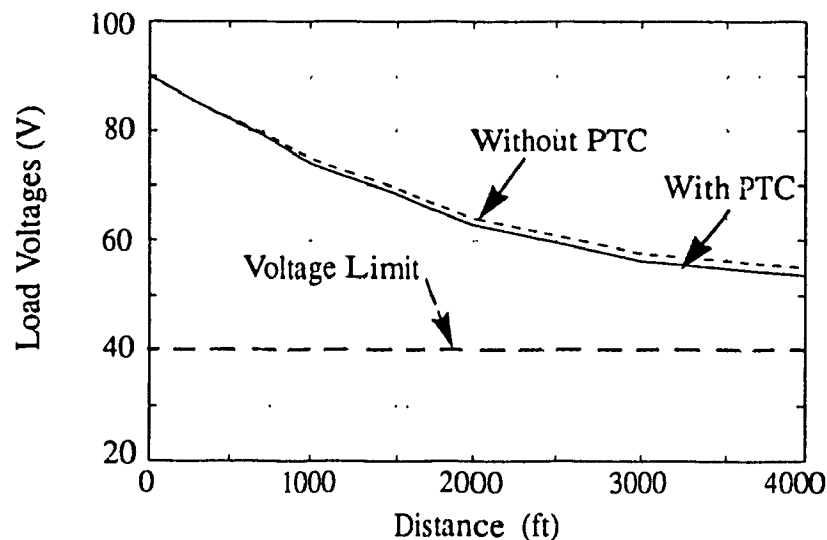
Fig. 5.2: Effect of PTC devices on the system voltage distribution

5...2 Selection of PTC resistors

When selecting a PTC device several factors must be considered: maximum voltage, maximum interrupt current, device resistance, hold current, trip current and trip time. The information from the PolySwitch products data sheets is shown in Table 5.1.

Table 5.1: Electrical characteristics of PTC devices

Part number	I_H (mA)	$V_{operating}$ (V)	V_{max} (Vrms)	I_{max} (A)	R_{min} (Ω)	R_{max} (Ω)
TC250-120	120	60	250	3	5.0	9.0
TR250-120	120	60	250	3	4.0	8.0
TR250-145	145	60	250	3	3.0	6.0
TC250-180	180	60	250	10	0.8	2.0
TR600-150	150	60	600	3	6.0	12.0
TR600-160	160	60	600	3	4.0	10.0

I_H = Hold current - maximum current device will pass without interruption in $20^{\circ}C$ still air environment.

V_{max} = Maximum voltage device can withstand without damage at rated current.

I_{max} = Maximum fault current device can withstand without damage at rated voltage.

R = As delivered resistance at $20^{\circ}C$.

The maximum time to trip vs. the fault current is shown in Fig. 5.3 and the hold current under certain temperature is shown in Fig. 5.4. Seen from these two figures and Table 5.1, the PTC which can hold a higher normal current and withstand a higher fault current needs a longer time to trip during a fault. TR600-160 is chosen for the drop segment since it provides a good compromise between the hold current, device resistance, trip current and trip time.

A = TR250-090
B = TC250-120
    TR250-120
C = TR250-145
D = TR600-150
    TR600-160
E = TC250-180
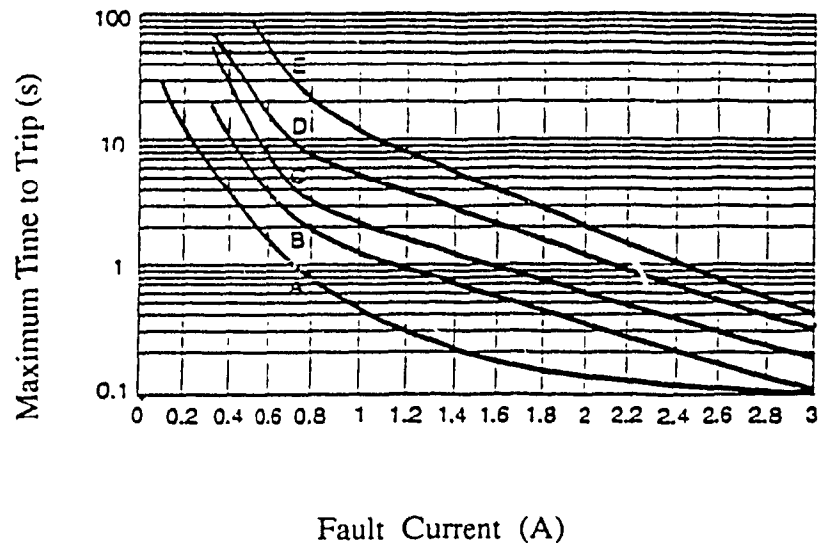
Fault Current (A)

Fig. 5.3: The maximum time to trip vs. the fault current

A = TR250-090
B = TC250-120
    TR250-120
C = TR250-145
D = TR600-150
    TR600-160
E = TC250-180
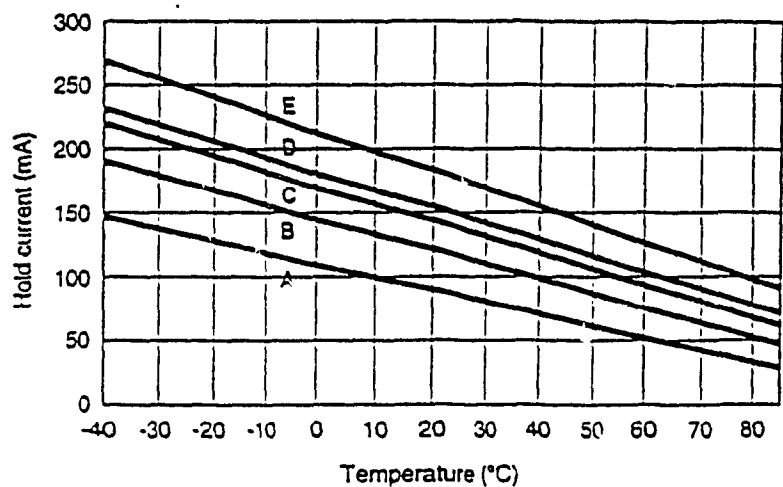
Fig. 5.4: The hold current under certain temperature

Fig. 5.5 illustrates how the PTC resistor TR600-160 trips with the current. In this figure the initial resistance of PTC is 6Ω. The current can pass through the PTC without interruption if it is less than 0.2A (the hold current of TR600-160), and the value of the PTC resistance is kept around 6Ω. However, when fault occurs, the current through PTC is increased, for example to 3A. The PTC resistance increases to 300Ω and trips quickly

(seen from Fig. 5.5(a)). Consequently the current is reduced to 0.09A (seen from Fig. 5.5(b)).

Figs. 5.4(d) and 5.5 indicate that the higher fault current results in faster trip time and higher resistance of PTC. The increased resistance reduces the fault current to a minimal level.

I - ON state of the PTC, current can pass without interruption

II - OFF (trip) state of the PTC, current is reduced by the increased PTC resistance
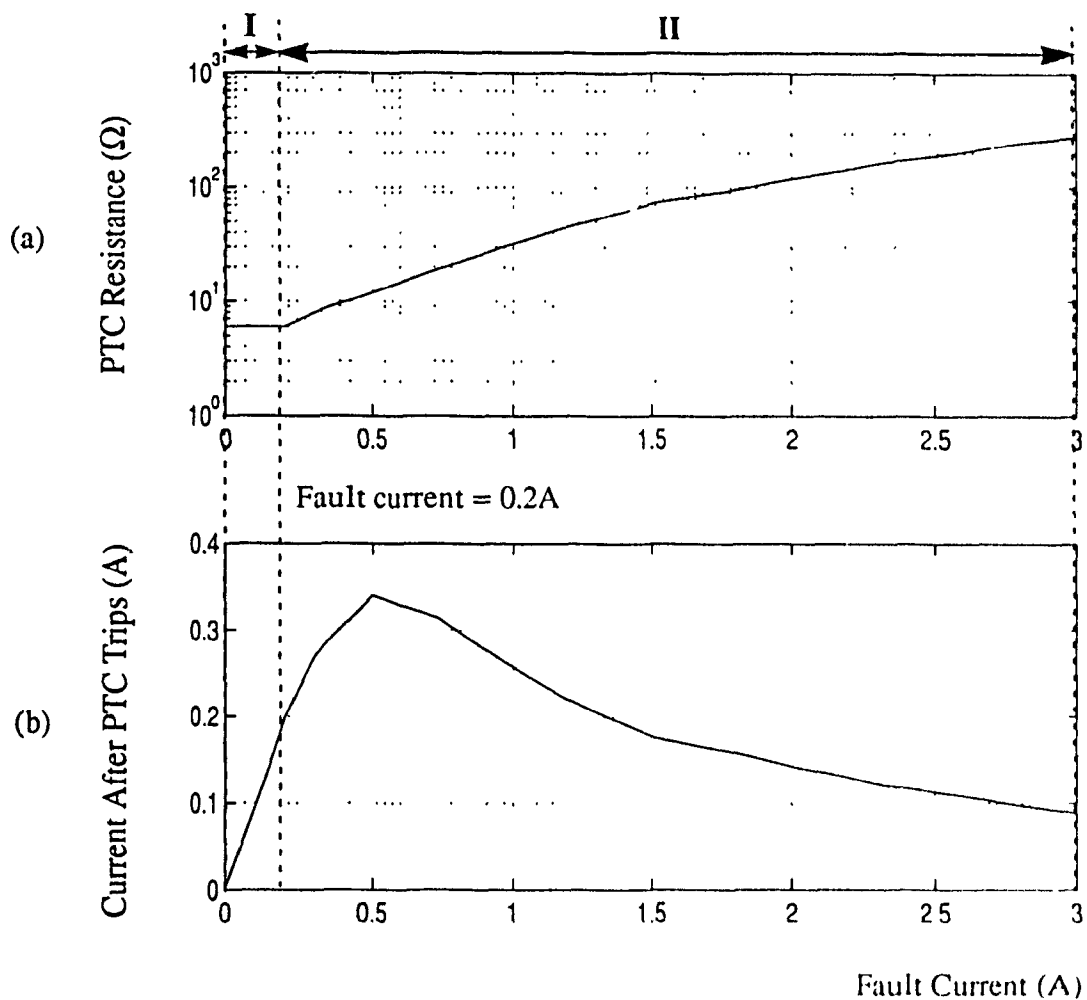
Fig. 5.5: Characteristics of TR600-160

5.3 System response under the fault conditions

5.3.1 The model of the system with fault
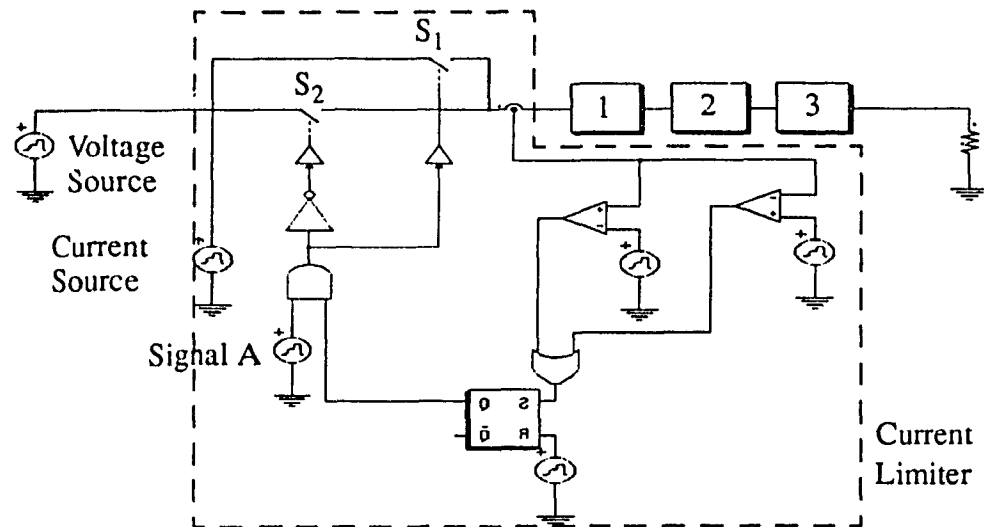
(a) System circuit
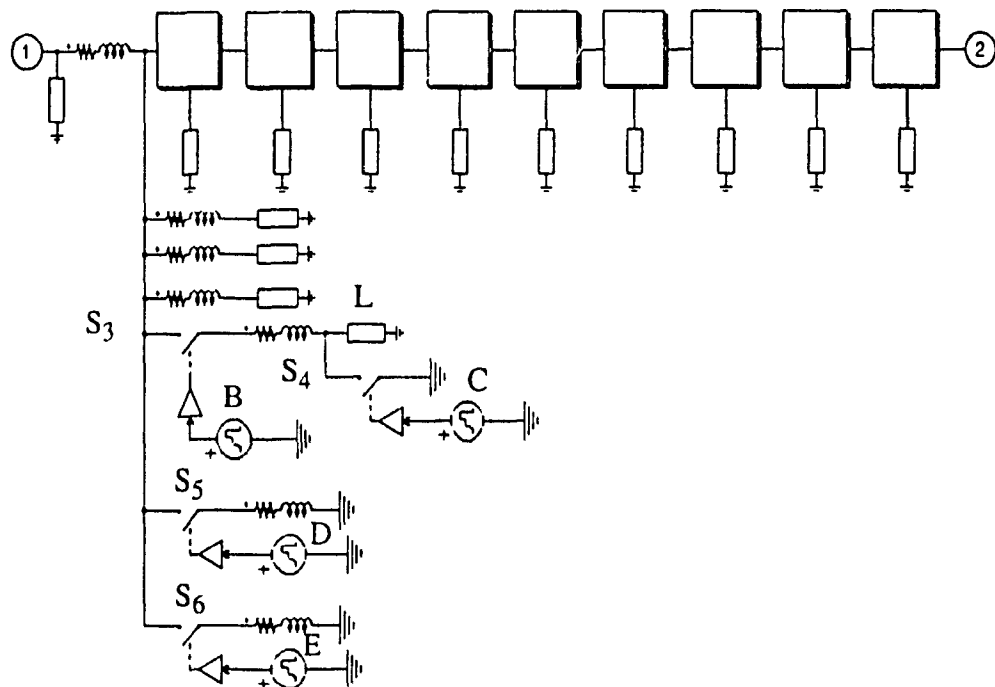
(b) Circuit in the segment 1

Fig. 5.6: System model during the fault

Fig. 5.6 shows the model of the system during the fault. The worst fault location which is at the load connected to the first drop box in the segment 1 is considered, as shown in Fig. 5.6(b). The load L is shorted to the ground for certain time by the switch S_4. The value of the PTC resistor (R_{PTC}) changes continuously during the fault as it goes from ON to OFF state. The simulation has approximated the value of R_{PTC} in the following five time intervals:

(1) Interval 1 (0<t<0.4s): the system is working normally and $R_{PTC} = 4\Omega$

(2) Interval 2 (0.4s<t<0.5s): Fault occurs at t=0.4s, the trip time for PTC resistor is 100ms and $R_{PTC} = 4\Omega$

(3) Interval 3 (0.5s<t<0.6s): The value of R_{PTC} has increased from 4Ω to 300Ω

(4) Interval 4 (0.6s<t<0.8s): The value of R_{PTC} has increased from 300Ω to 500Ω

(5) Interval 5 (t>0.8s): The fault has been removed and $R_{PTC}=4\Omega$

According to the above 5 intervals, the states of the switches S_3, S_4, S_5 & S_6 are controlled by signals B, C, D & E respectively as shown in Table 5.2.

Table 5.2: The states of the switches in Fig. 5.6(b) at certain time

Time (sec)	S_3 (B)	S_4 (C)	S_5 (D)	S_6 (E)
t=0.0	1	0	0	0
t=0.4	1	1	0	0
t=0.5	0	1	1	0
t=0.6	0	1	0	1
t=0.8	1	0	0	0
t=1.1	1	0	0	0

Several comparators, logic gates and set-reset flip-flop are used to control the states of S_1 & S_2 in Fig. 5.6(a), as shown in Table 5.3. Under the normal operating condi-

tion (0<t<0.4s), the current is within $\pm 15A$, S_1 is ON and S_2 is OFF. The power supply provides a constant voltage. Under the fault condition (0.4s<t<0.5s), if the current exceeds the limit of 15A, S_1 turns OFF and S_2 turns ON. The peak value of output current will be limited at $\pm 15A$. The power supply acts as a current source, and the output voltage drops. After PTC resistors trip (t>0.5s), S_1 and S_2 are reset to the initial states by the signal A.

Table 5.3: The states of the switches in Fig. 5.6(a) at certain time

Time (sec)	Current (A)	S	R	Q	A	S_1	S_2
t=0.0 ~ 0.4	$-15 \leq I_s \leq 15$	0	1	0	1	0	1
t=0.4 ~ 0.5	$-15 \leq I_s \leq 15$	0	0	0	1	0	1
	$I_s<-15$ or $I_s>15$	1	0	1	1	1	0
	$-15 \leq I_s \leq 15$	0	0	1	1	1	0
t=0.5 ~ 1.0	x	x	x	x	0	0	1

5.3.2 Simulation results

The following two operating conditions are considered:

Operating condition (i): Nominal cable resistance and load power demand;

Operating condition (ii): Distribution cable resistance is increased by 20% and load power demand is increased by 25%.

The simulation results of the system against a single fault are shown in Figs. 5.7 to 5.10.

Figs. 5.7 and 5.8 show the response of the system under the above two operating

conditions for the distribution cable B. When a fault occurs, the source current exceeds its rated value and the source inverter operates in a current limit mode. During this mode of operation the source voltage falls below the rated value of 90V. Since the fault current is high and the source voltage is low, the distribution voltage after the fault location drops dramatically bellow the minimum voltage limit of 40V.
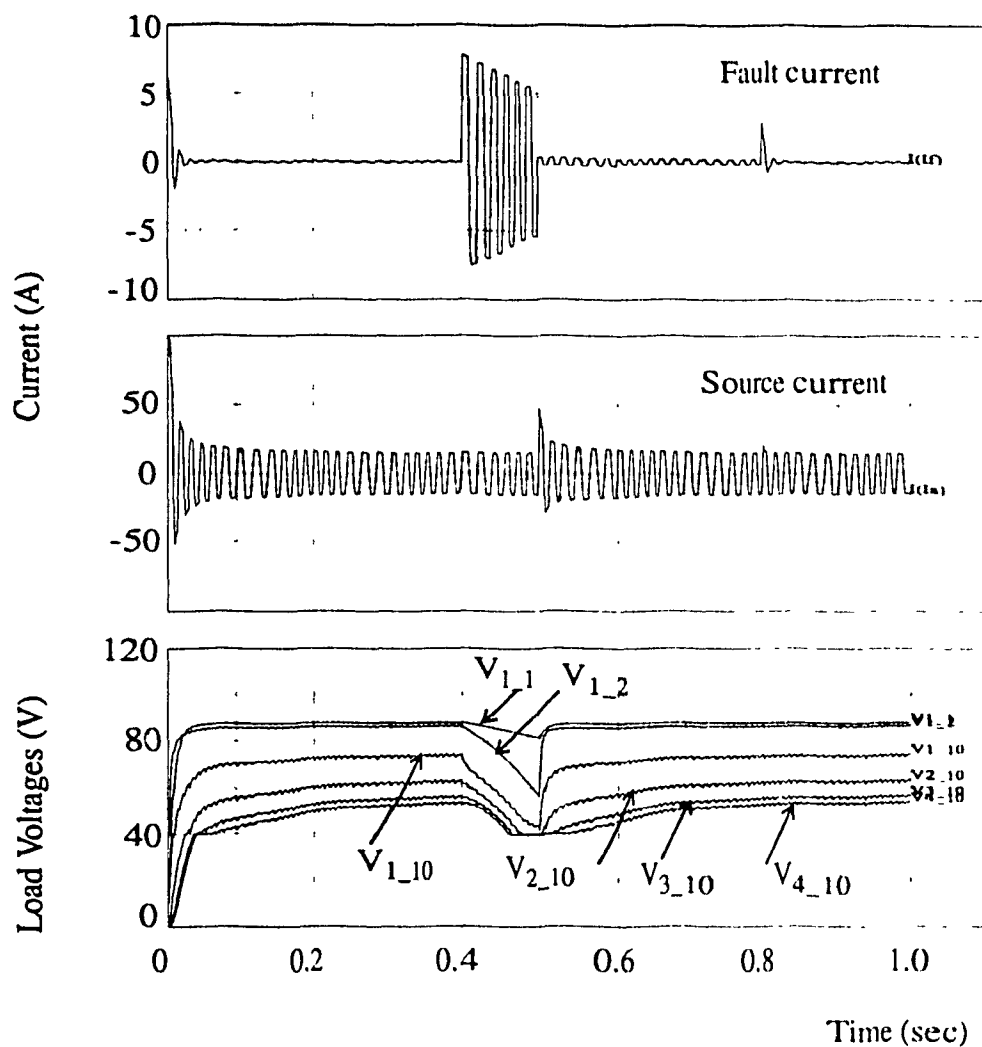
Fig. 5.7: The system with cable B under the normal loading condition against a single fault
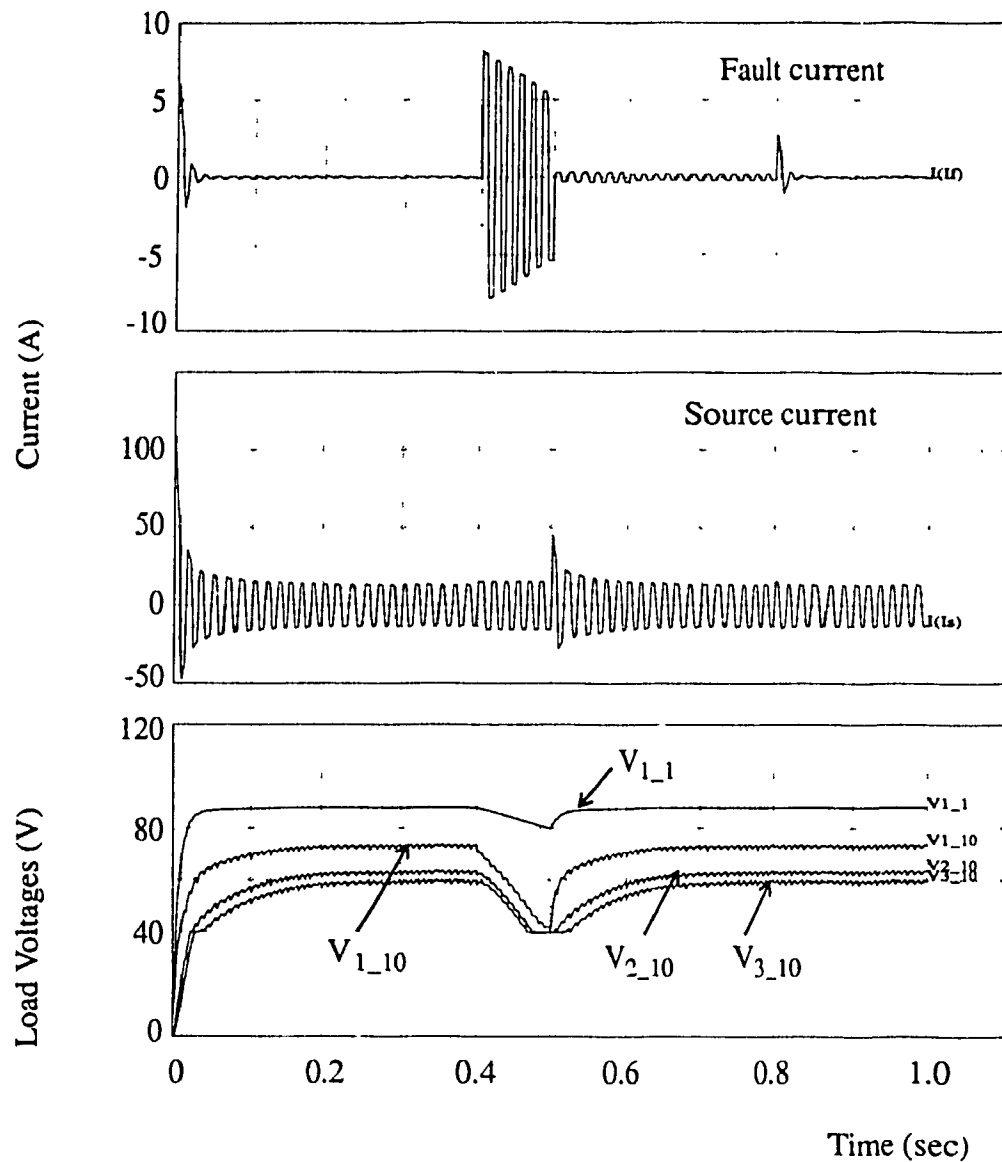
Fig. 5.8: The system with cable B under the worst loading condition

against a single fault

The following points are observed from Figs. 5.7 & 5.8:

(i) For a single fault under the operating conditions (i) and (ii), the distribution voltage across the last drop box of segment 1 drops to approximately 45V. This means

that segment 1 of the network can function properly as the distribution voltage is always above the minimum voltage limit of 40V.

(ii) For a single fault under both the operating conditions, the distribution voltage across the last drop boxes of segments 2 and 3 drops below 40V. This means that all segments of the distribution network, except segment 1, are inoperational as the power supplies used in home terminal units will shut down below the distribution voltage of 40V.

(iii) All the segments of the network will function properly once the fault has been cleared by tripping the PTC.

The above observations lead to the conclusion that the system becomes inoperational only during the trip time of PTC. This problem can be eliminated in one of the following two ways: (1) the distribution cable has lower resistance; (2) the power supplies have enough hold-up time capability. Since the typical trip time for the PTC is between 200-400ms, the size of hold-up capacitors in the power supplies become excessively large.

Figs. 5.9 and 5.10 show the response time of the system for the distribution cable C under the two operating conditions. These figures clearly show that the distribution voltage across the various segments of the network always stays above the minimum limit. Therefore, the system is fully operational during a single fault condition.
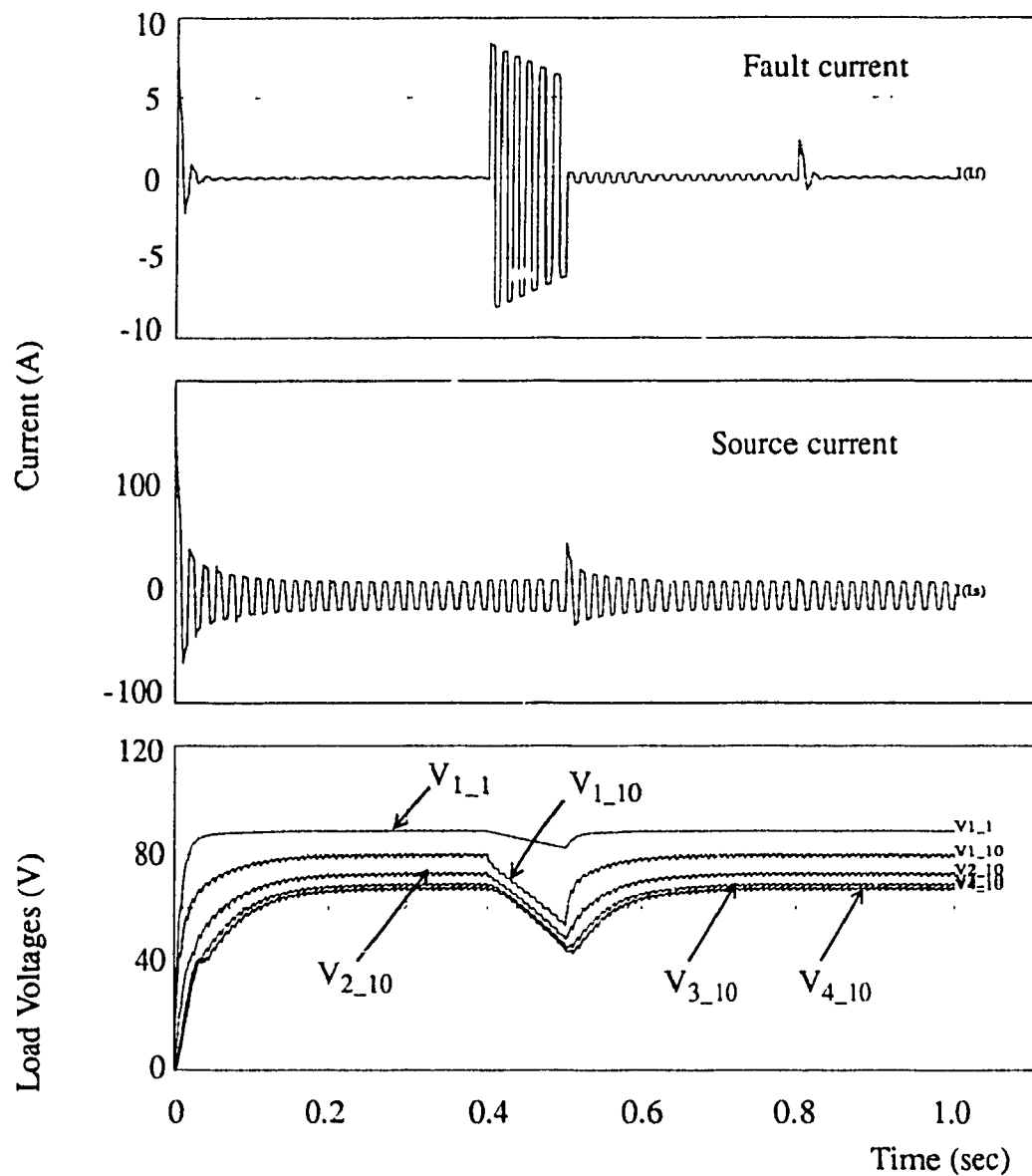
Fig. 5.9: The system with cable C under the normal loading condition

against a single fault
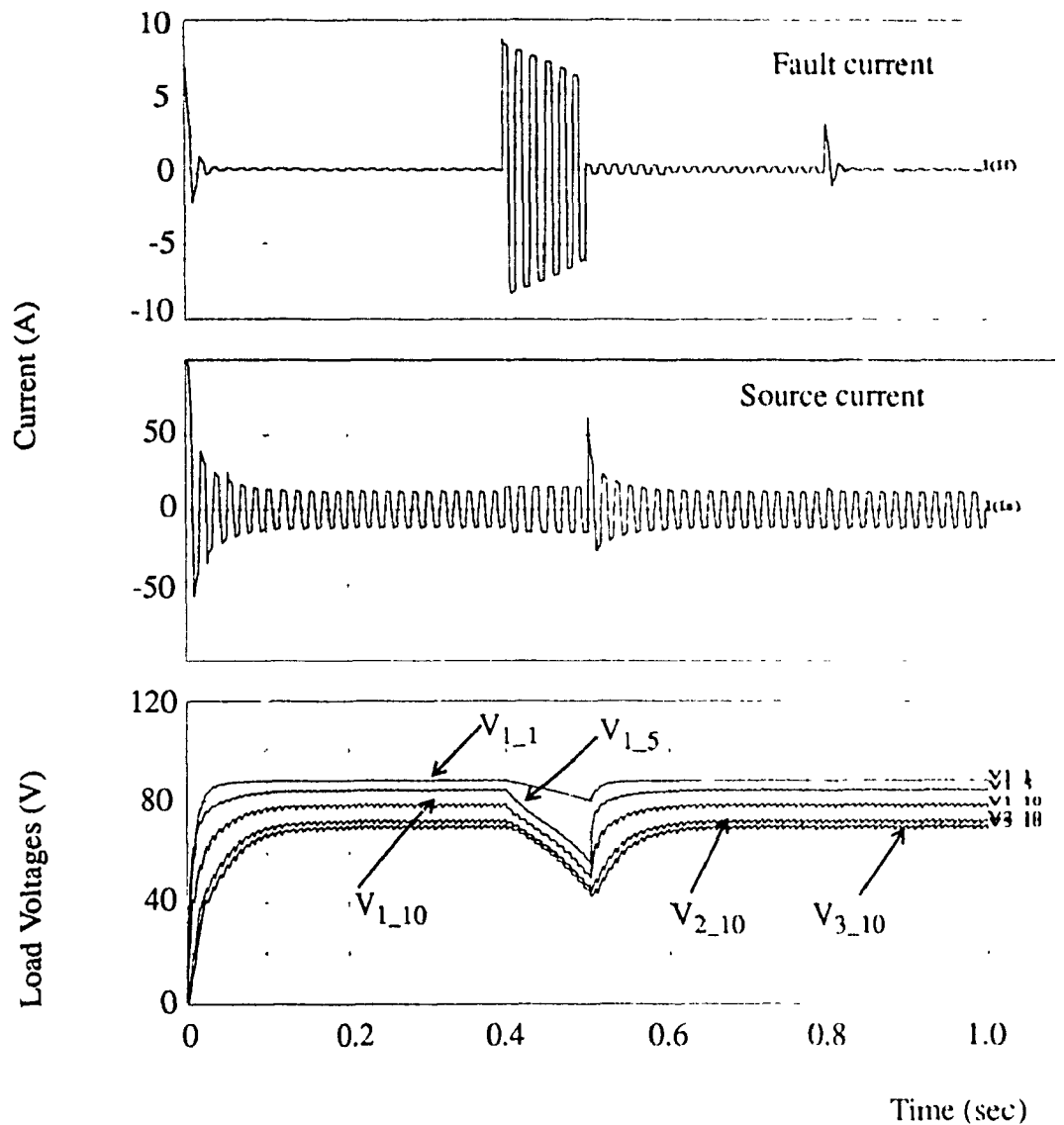
Fig. 5.10: The system with cable C under the worst loading condition

against a single fault

In the following section the performance of the system against two simultaneous short circuit faults in the network will be studied.

Fig. 5.11 shows the response of the system for operating condition (i) and with the distribution cable C when two faults occur at the same time. The two faults occur

across the HTUs which are located at the first and the second drop box respectively in segment 1. The distribution voltage drops below the minimum voltage limit for all segments of the network. Once the PTC trips, all HTUs without fault function normally as the voltage across them is greater than 40V. When the fault is removed, the operation of the system as a whole can resume by resetting PTC resistors.
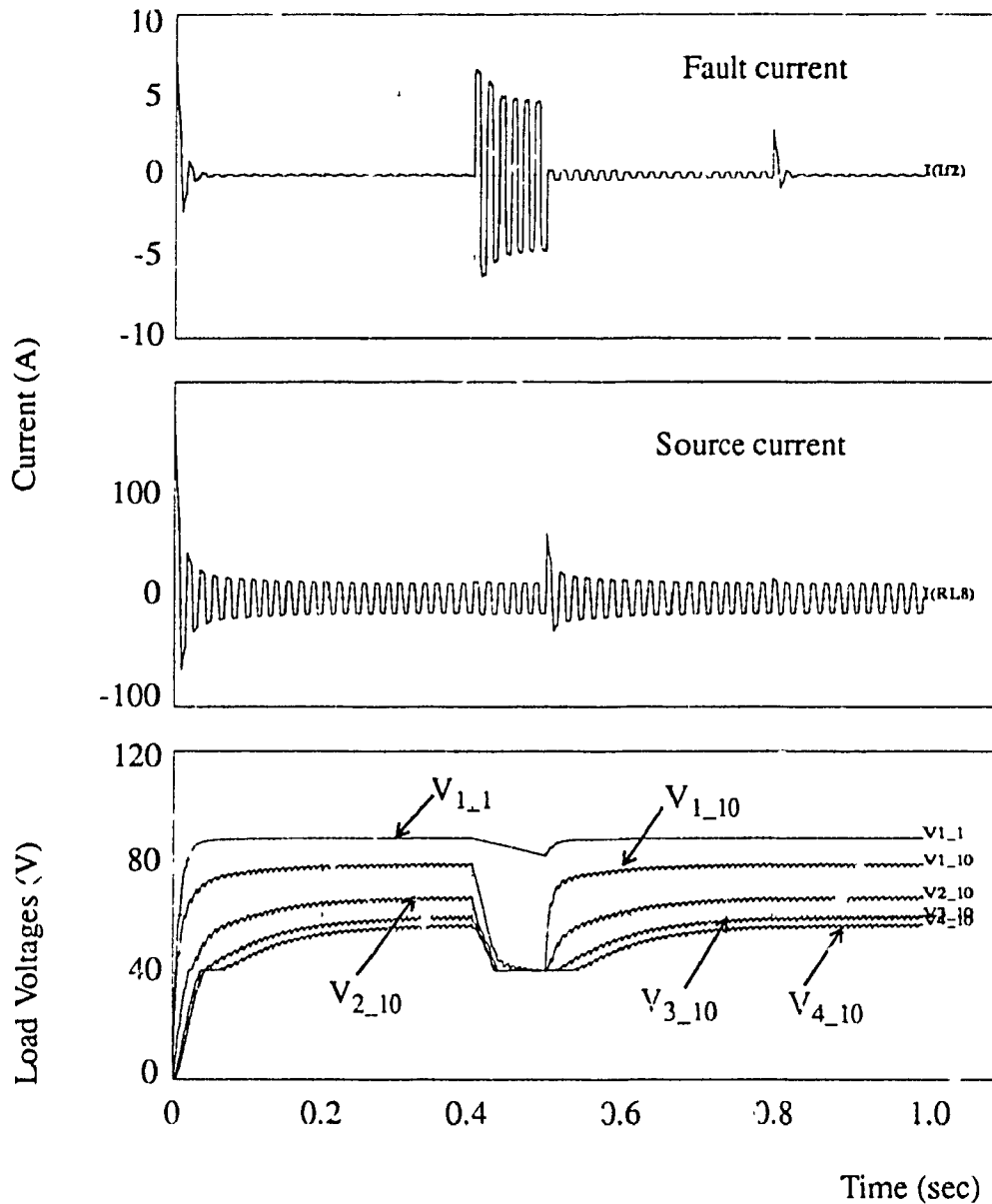
Fig. 5 11. The system with cable C under the normal loading condition

against two faults

5.4 Conclusions

From this chapter, the following conclusions can be drawn:

(i) TR600-160 is chosen as the protective device in series with each drop cable. It can provide good overcurrent protectio of individual components by tripping during fault conditions and resetting itself when the fault is removed;

(ii) Against the single fault, the system with cable B can handle only one segment during the PTC trip time;

(iii) The system with cable C can work normally during single fault. Even under the worst operating conditions, the system can still provide power for upto 3 segments. However, when two faults occur simultaneously, the system cannot handle even one segment during PTC trip time.

Chapter 6

Stability of System Operation

6.1 Introduction

In the hybrid fiber/coax system, the nominal operation of the power system involves a periodic steady state. However, the following disturbances can cause an instability in the power system:

(i) Large load transients;

(ii) Cyclic variations in load and circuit parameters.

Large load transients are caused by simultaneous ringing or ringtrip in many HTUs. Based on statistical data, the system is designed in such a way that the peak power demand is satisfied (see the definition of "reference segment" in the section 3.3). In this way the stability of the system is maintained under large load transients. Most of the stability issues are related to the cyclic variations in the supply voltage and load power. This chapter will present the detailed stability analysis for the later case.

Some definitions and theorems of stability of nonlinear systems are introduced. In general, the linear time invariant (LTI) system is stable if the poles of the transfer function of the system are strictly in the left half of the s-plane. Based on these basic concepts, the system with a single load is analyzed by calculating its eigenvalues. For the complete 4-segment system, the conditions of stability are found out by simulating the dynamic performance of the system during the switching transient.

6.2 Definition of stability in nonlinear systems [20]

The behavior of the nonlinear system can be defined as:

$$\dot{x} = f(t, x) \tag{6-1}$$

Where, the column vectors x and $f(.)$ represent the sets of state variables and sets of nonlinear, time varying, first-order differential equations respectively.

Definition 6-1 (Stability): Consider a solution curve $x^o(t)$, generated by an initial condition $x^o(a)=\xi$, and a neighboring solution curve $x(t)$. The solution, $x^o(t)$, is *stable* if for any $\varepsilon>0$, there exists a $\delta>0$ such that if

$$\left\| x(a) - x^o(a) \right\| < \delta \tag{6-2}$$

then

$$\left\| x(t) - x^o(t) \right\| < \varepsilon \qquad \text{for} \qquad \text{all } t \ge a \tag{6-3}$$

If $x^o(t)$ is not stable, it is said to be *unstable*.

Definition 6-2 (Asymptotic stability): Considering the solutions x^o and x as defined above, x^o is said to be *asymptotically stable* if it is stable, and if

$$\lim_{t \to \infty} \left\| x(t) - x^o(t) \right\| = 0 \tag{6-4}$$

The simple stability is actually a borderline condition between instability and asymptotic stability. It occurs only when there is no damping present.

Besides the definitions mentioned above, it is important to formalize the concept mathematically.

To determine the stability of a solution $x^o(t)$ of Eq. (6-1), the small deviation of the origin $\tilde{x} = x - x^o$ is given by:

$$\dot{\tilde{x}} = f(t, x^o + \tilde{x}) - \dot{x}^o(t) \tag{6-5}$$

The superscript $\sim$ denotes arbitrarily small perturbations of the original solution. It is so small that only the first term of a Taylor-series expansion about the solution $x^o(t)$ are to be considered. Therefore,

$$\dot{\tilde{x}} = \tilde{x} \cdot \frac{\partial}{\partial x}(f[t, x^o(t)]) + r(t, \tilde{x}) = A(t) \cdot \tilde{x} + r(t, \tilde{x}) \tag{6-6}$$

Where $r(t, \tilde{x}) = o(\|\tilde{x}\|)$

Assuming that:

(i) A and r are independent of t;

(ii) The nonlinear residue r is so small that it could be neglected in considering stability.

Eq. (6-6) is simplified to be linear with constant coefficients. Under these conditions the following extremely useful theorem applies:

Theorem 6-1: Given the equation

$$\dot{y} = Ay + r(y), \qquad r(y) = o(\|y\|) \tag{6-7}$$

If all the eigenvalues of the matrix A have negative real parts, then the origin is asymptotically stable. If at least one eigenvalue has positive real part, the origin is unstable.

In the theorem, it is mentioned that all eigenvalues have negative real parts, that is, none can lie on the imaginary axis. Intuitively one can see that if the hypothesis of the theorem is fulfilled, there is some finite damping present in the linearized system, which will be enough to overcome any destabilizing effects of the nonlinear residue, provided one is close enough to the origin. However, if some eigenvalues lie on the imaginary axis, the origin of the linearized system is effectively on the borderline between asymptotic stability and instability; hence the small nonlinear terms can be important in deciding the stability problems.

6.3 Stability evaluation for a single load

In the hybrid fiber/coax network the distribution & drop cables, power supplies and loads are basically considered as nonlinear RLC circuits.

The constant-power load exhibits the property of negative resistance, that is, an increase in terminal voltage causes a decrease in terminal current. The dynamic resistance of the constant-power load is defined as:

$$r = \frac{dv_o}{di_l} = \frac{dv_o}{d(P_l/v_o)} = -\frac{v_o^2}{P_l} \qquad (6\text{-}8)$$

Where v_o, i_l and P_l are instantaneous values of load voltage, current and power respectively.

Under certain conditions, the negative resistance load may act as an energy source which replaces the energy dissipated in its internal resistance and the circuit will oscillate. Therefore, the system with constant power ac/dc converters is inherently unstable [21] Since the cable parameters and loads are given, only the contribution of the filter capacitance to the conditions of the system stability is studied.

According to the definitions and theorem mentioned above, what is done is (i) linearize the system about the singular point x^o; (ii) find out the hypothesis of stability to satisfy that all the eigenvalues of the linearized system $\dot{y} = Ay + r(y)$ have negative real parts.

6.3.1 Linearization of the system

(1) AC/DC Converter
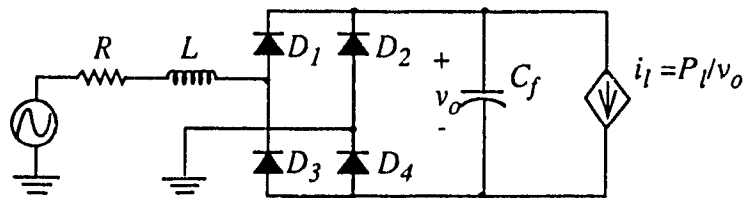
Fig. 6.1: The system with a single load

A circuit which contains an ac/dc constant-power converter is shown in Fig. 6.1. To simplify this circuit, the rectifier can be modeled as a multiple circuit (Fig. 6.2(a)) that contains only voltage-controlled voltage source and current-controlled current source connected at the input and output ports [22]. The signals controlling these sources are switching functions (Fig. 6.2(b)).

(a) Simplified circuit   (b) Switching function
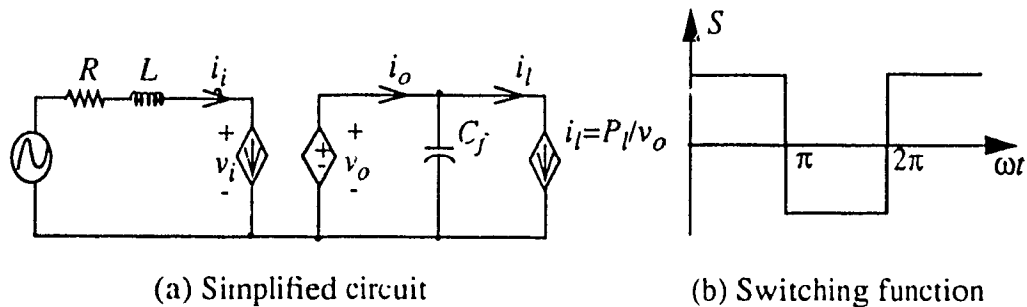
Fig. 6.2: Simplified circuit model

In Fig. 6.2, the behavior of the converter is given by:

Input (ac): $i_i = i_o \cdot S$

Output (dc): $v_o = v_i \cdot S$ (6-9)

Where S is a t. ⌐ level switching function, as shown in Fig. 6.2(b).

The waveforms of v_s, v_o, i_s, i_l are shown in Fig. 6.3.
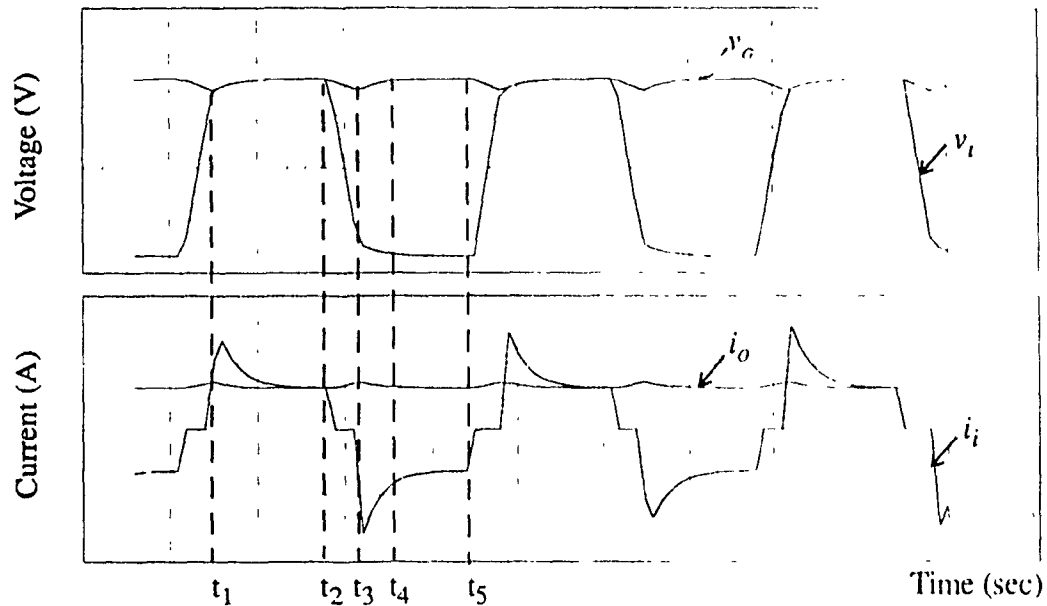
Fig. 6.3: Input/output waveforms of the ac/dc converter

During one cycle, the behavior of the power converter can be described as:

(i) $t_1 < t < t_2$: D_1 & D_4 are ON, D_2 & D_3 are OFF, $v_o = v_i$, $i_i = i_o$;

(ii) $t_2 \leq t < t_3$: v_i starts to drop at $t=t_2$ and D_1 & D_4 turn OFF. The capacitor is discharged, the load current is the discharge current and $i_i=0$;

(iii) $t_3 < t < t_4$: $v_o = -v_i$ at $t=t_2$ and D_2 & D_3 turn ON. The capacitor is charged

- 74 -

and $i_i = -i_o$;

(iv) $t_4 < t < t_5$: D_1 & D_4 are OFF, D_2 & D_3 are ON, $v_o = -v_i$, $i_i = -i_o$.

To study the stability problem during the switching transient, only the switching points are considered, where the circuit will be linearized. It can be seen that in the very small neighborhood of the switching points, the small deviations of v_s, v_o, i_s and i_l satisfy:

$$\tilde{v}_o = \pm \tilde{v}_i, \quad \tilde{i}_i = \pm \tilde{i}_o \qquad (6\text{-}10)$$

Where "+" and "-" refer to switch ON and switch OFF points respectively in one cycle. This equation is the small signal model of the ac/dc converter at switching points.

(2) Constant power load

At the nominal operating point, the characteristic of the constant power load is given by:

$$I_l = \frac{P_l}{V_o} = F(V_o, P_l) \qquad (6\text{-}11)$$

When the output voltage is perturbed from V_o to $v_o = V_o + \tilde{v}_o$, I_l becomes $i_l = I_l + \tilde{i}_l$. A linearized model of the constant-power load can be obtained by expanding all the nonlinear terms of the model into a Taylor series around the nominal values and retaining only first-order terms [12]:

$$i_l = I_l + \tilde{i}_l = F(V_o + \tilde{v}_o, P_l) = F(V_o, P_l) + \tilde{v}_o \cdot \left(-\frac{P_l}{v_o^2} \right) \qquad (6\text{-}12)$$

The linearized model of the constant-power load is:

$$\tilde{i}_l = -\tilde{v}_o \cdot \frac{P_l}{v_o^2} = \frac{-\tilde{v}_o}{r}$$

(6-13)

By replacing every voltage and current in the nonlinear circuit by their deviations from the nominal, and replacing every nonlinear component in the circuit with its linearized version (Eq. (6-10) & Eq. (6-13)), the linearized circuit is shown in Fig. 6.4.
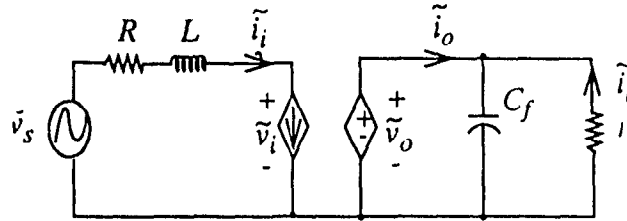
Fig. 6.4: Linearized circuit model

6.3.2 Hypothesis of the stability [23]

In Fig. 6.4, according to Kirchhoff's laws, the small signal behavior of the circuit is described as:

$$\tilde{v}_s = \tilde{i}_i \cdot (R + sL) + \tilde{v}_i$$

$$\tilde{i}_o = \tilde{v}_o \cdot sC_f - \frac{\tilde{v}_o}{r}$$

(6-14)

Considering that $\tilde{v}_o = \pm \tilde{v}_i$, $\tilde{i}_l = \pm \tilde{i}_o$, the transfer function of this circuit is:

$$\frac{\tilde{v}_o}{\tilde{v}_s} = \pm \frac{1}{LC_f} \cdot \frac{1}{s^2 + \dfrac{RrC_f - L}{LrC_f} s - \dfrac{r - R}{LrC_f}}$$

(6-15)

$$s^2 + \frac{RrC_f - L}{LrC_f}s - \frac{r - R}{LrC_f} = 0 \qquad \text{(6-16)}$$

The solutions of Eq. (6-16) (eigenvalues) are:

$$\begin{pmatrix} s_1 \\ s_2 \end{pmatrix} = \begin{bmatrix} -\dfrac{R}{2L} + \dfrac{1}{2rC_f} + \dfrac{1}{2}\dfrac{\sqrt{(RC_f r)^2 + 2C_f LRr + L^2 - 4LC_f r^2}}{LC_f r} \\[2em] -\dfrac{R}{2L} + \dfrac{1}{2rC_f} - \dfrac{1}{2}\dfrac{\sqrt{(RC_f r)^2 + 2C_f LRr + L^2 - 4LC_f r^2}}{LC_f r} \end{bmatrix} = \alpha \pm \sqrt{\alpha^2 - \omega_o^2}$$

$$\text{(6-17)}$$

$$\text{Where } \alpha = -\frac{R}{2L} + \frac{1}{2rC_f}, \quad \omega_o = \sqrt{-\frac{R}{LC_f r} + \frac{1}{LC_f}}$$

To assure asymptotic stability, the eigenvalues must be in the left ha.f-plane. Thus a sufficient condition for asymptotic stability becomes:

$$\alpha < 0, \quad \omega_o > 0 \qquad \text{(6-18)}$$

That is,

$$C_f > \frac{L}{Rr}, \quad \frac{R}{r} < 1 \qquad \text{(6-19)}$$

It is clear that the second condition is fulfilled automatically since the impedance of the constant-power load is much greater than the resistance of the distribution and drop cables. The necessary condition for stability of this circuit becomes:

$$C_f > \frac{L}{R \cdot r} \qquad \text{(6-20)}$$

When the eigenvalues are in the left hand of the s-plane, according to the relation-

ship between α and ω_0, three forms of response could occur:

(i) $\alpha > \omega_0$, that is $C_f > C_f*$, Overdamped response;

(ii) $\alpha = \omega_0$, that is $C_f = C_f*$, Critical damping;

(iii) $\alpha < \omega_0$, that is $C_f < C_f*$, Oscillatory response.

Where

$$C_f* = \frac{1}{R^2 r^2}[-RrL + 2Lr^2 + 2r^{3/2}L\sqrt{-R+r}] \qquad (6\text{-}21)$$

A simple system with the distribution & drop cable and a single constant power converter load is considered as an example. In this system (with reference to Fig. 6.1), $v_s = 90V(peak,$ trapezoidal), $R = 2.6\Omega$ (the sum resistance of the distribution and drop cables), $L = 10.5\mu H$ (the sum inductance of the distribution & drop cables), $p = 20W$ (the average power demand of the constant-power loads), and $r = 405\Omega$. Therefore, according to Eq. (6-20), the condition for stability of this system is $C_f > 10nF$. According to Eq. (6-21), to avoid oscillation in the system response, the capacitance should be greater than $6\mu F$. The calculations are proved by simulating the circuit of Fig. 6.1. The results are shown in Figs. 6.5 ~ 6.8.
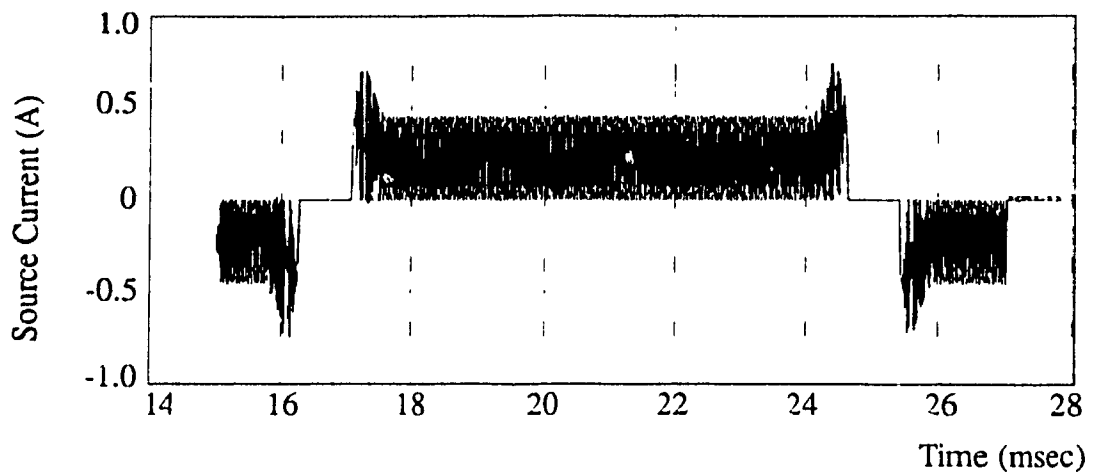
Fig. 6.5: Transient response of the system with single load (C_f=8nF)
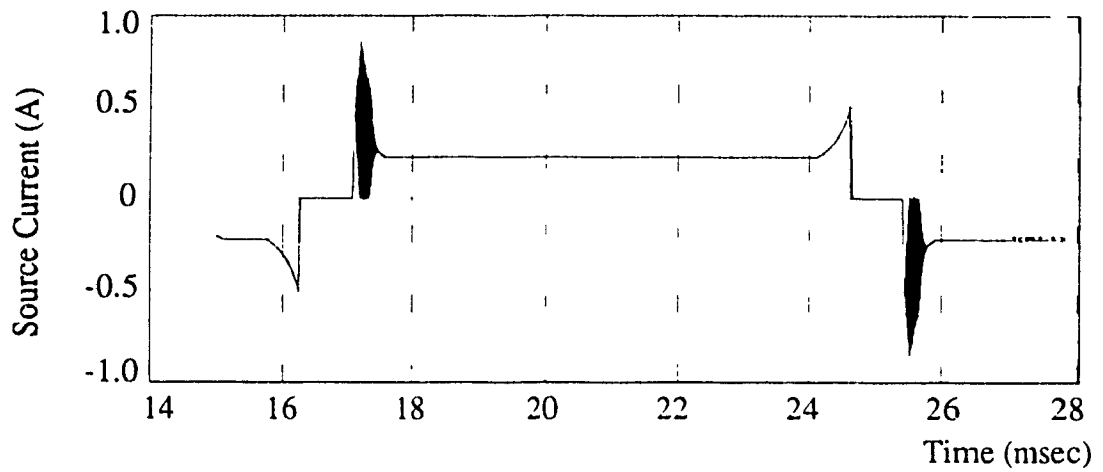
Fig. 6.6: Transient response of the system with single load (C_f=15nF)
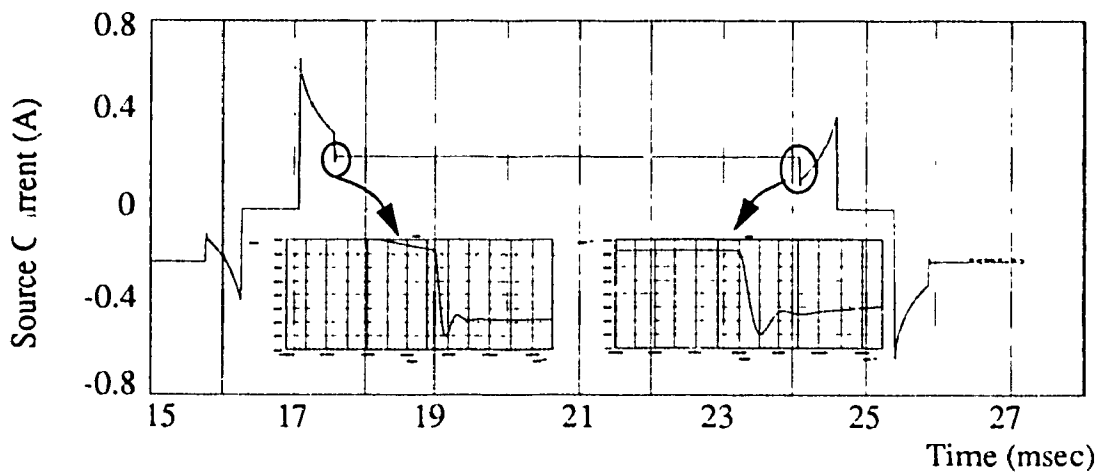
Fig. 6.7: Transient response of the system with single load (C_f=1μF)
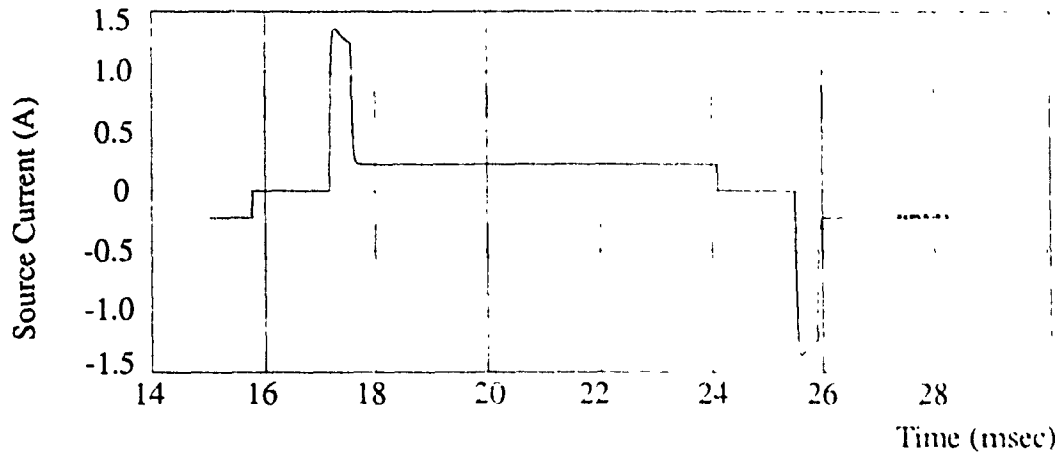
Fig. 6.8: Transient response of the system with single load ($C_f = 10\mu F$)

With references to Figs. 6.5-6.8, the transient responses of the input current for the different filter capacitances are shown in Table 6.1. It can be seen that the simulation results are very close to the stability evaluation based on the theorem 6-1.

Table 6.1: The transient response of the input current of the system with a single load

Capacitance	Switching Period	Steady State
$C_f = 5nF$ (Fig. 6.5)	Increased oscillation	Oscillation
$C_f = 20nF$ (Fig. 6.6)	Damped oscillation	No oscillation
$C_f = 1\mu F$ (Fig. 6.7)	Fast underdamped	No oscillation
$C_f = 10\mu F$ (Fig. 6.8)	No oscillation	No oscillation

6.4 Simulation results of system stability

When hundreds of converter-loads of HTUs are connected together through distribution & drop cables in the power system and fed by the same power source, it is difficult to determine conditions for the system stability using analytical methods. Computer simulation is a convenient tool for obtaining the required details related to the stability of the power system. This section studies the stability of the system using such simulation tools.

The system under study provides power for 3 segments and uses cable B. Figs. 6.9~6.16 illustrate the waveforms of the source current and the voltage at the last HTU load for the different filter capacitances of *300nF, 304nF, 310nF, 400nF, 6μF, 10μF, 50μF* and *400μF* respectively.
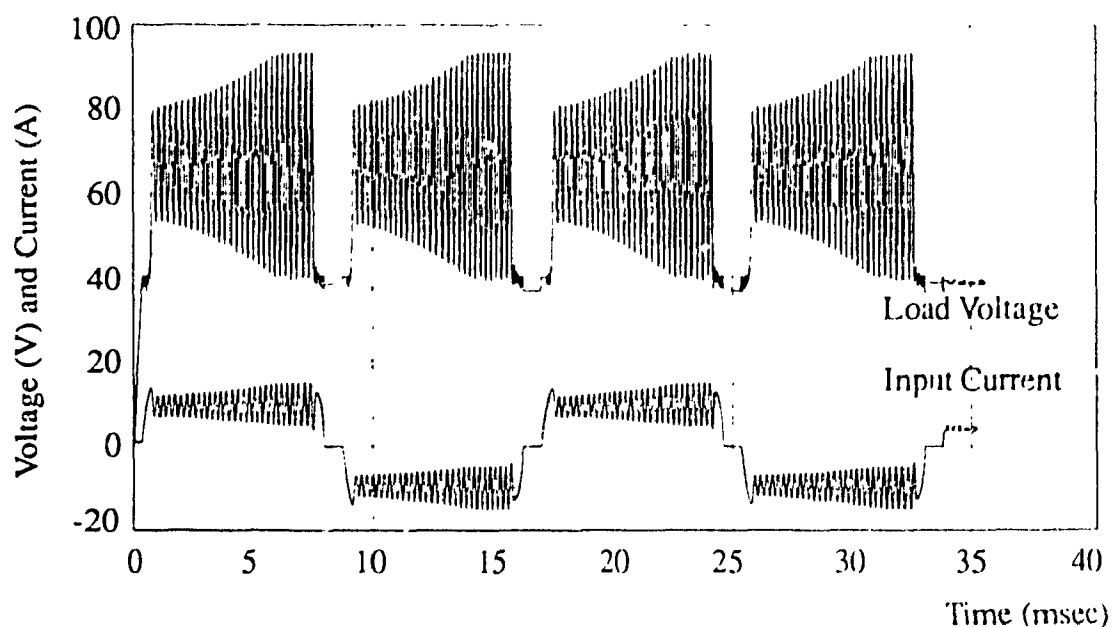
Fig. 6.9: Transient response of the complete system (C_f =300nF)
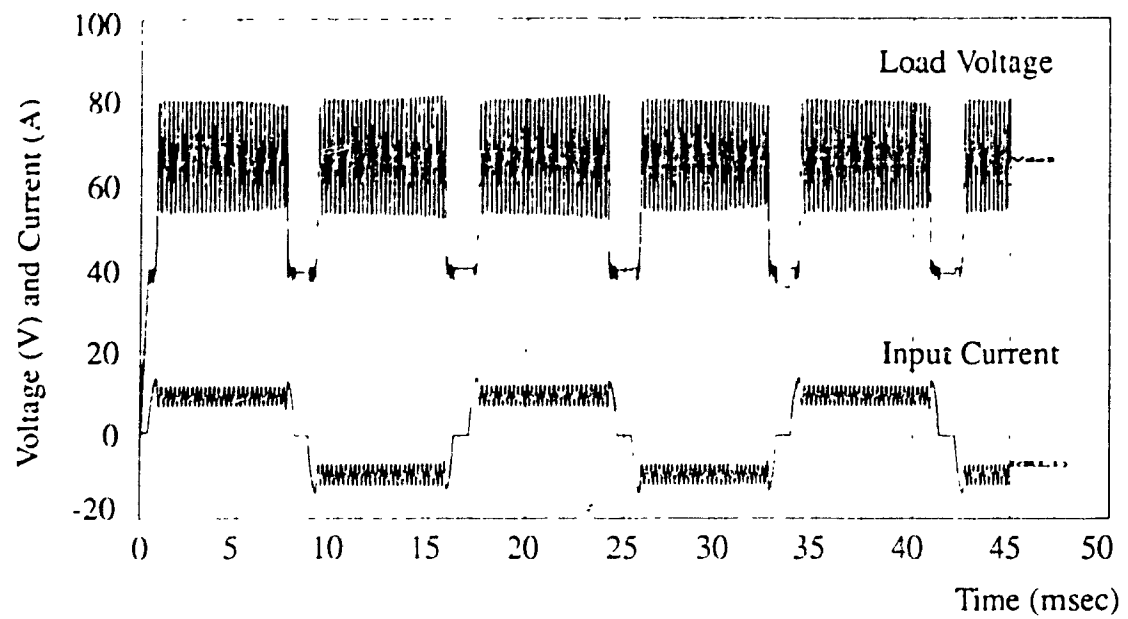
Fig. 6.10: Transient response of the complete system (C_f=304nF)
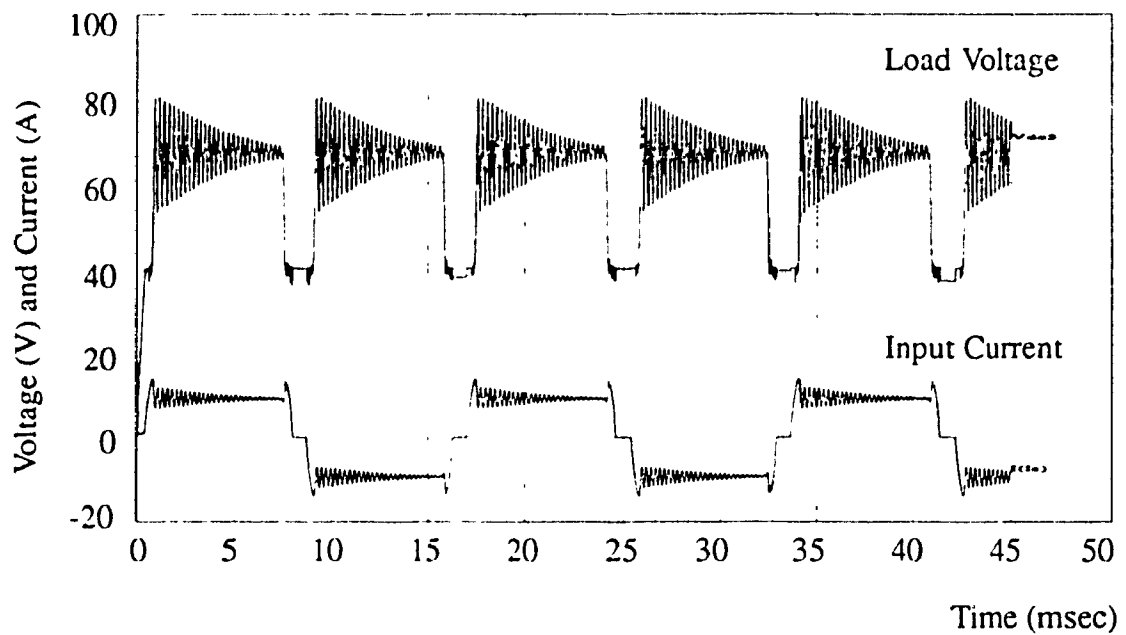
Fig. 6.11: Transient response of tne complete system (C_f=310nF)
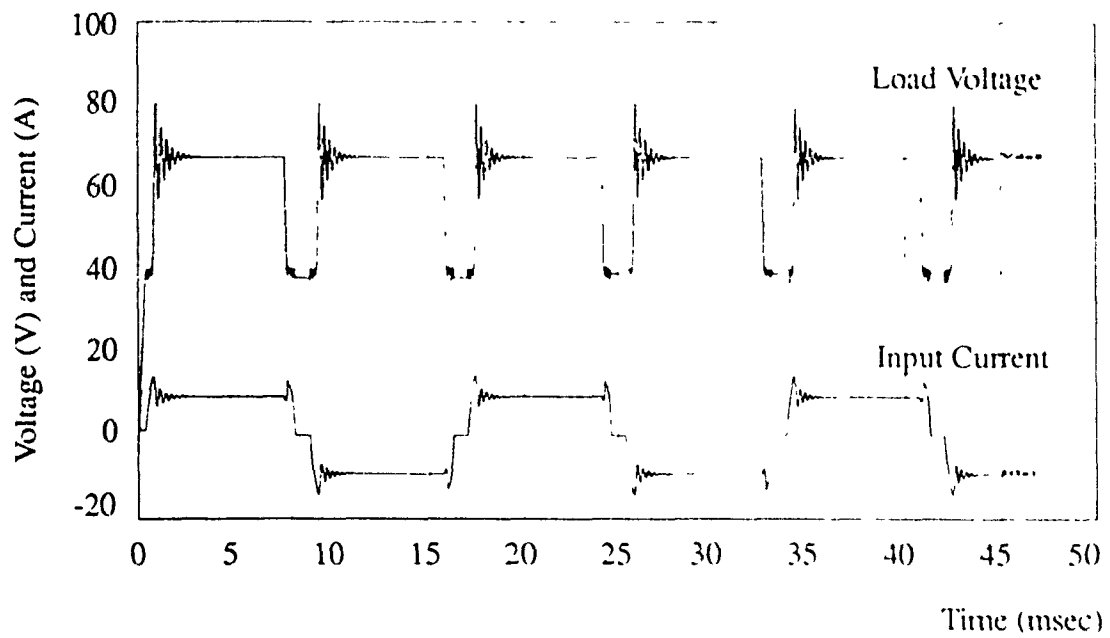
Fig. 6.12: Transient response of the complete system (C_f =400nF)
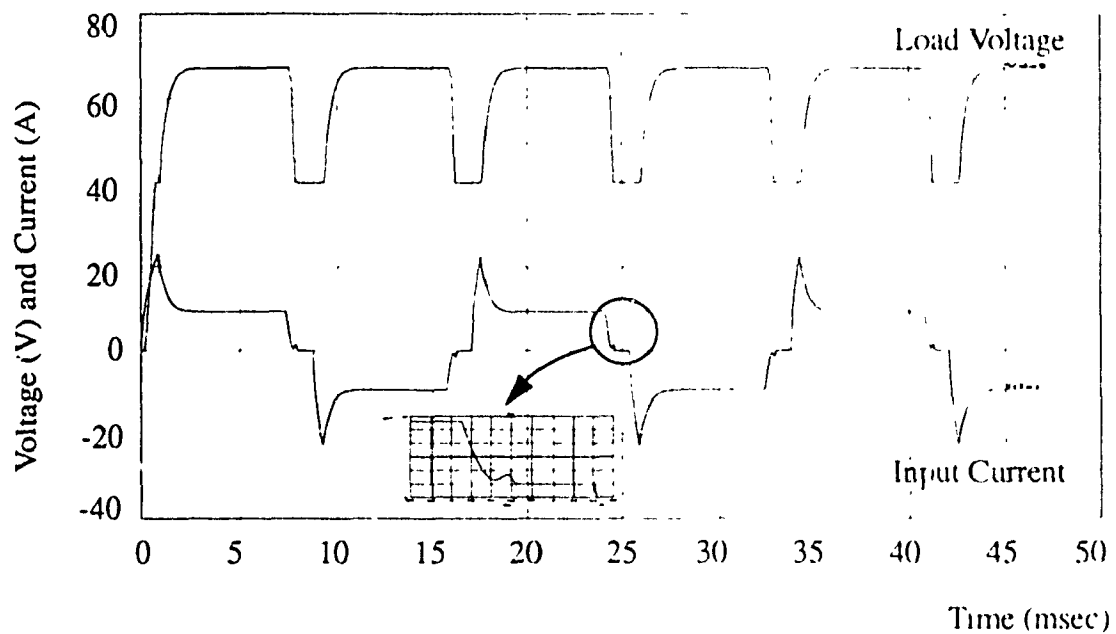
Fig. 6.13: Transient response of the complete system (C_f =6μF)
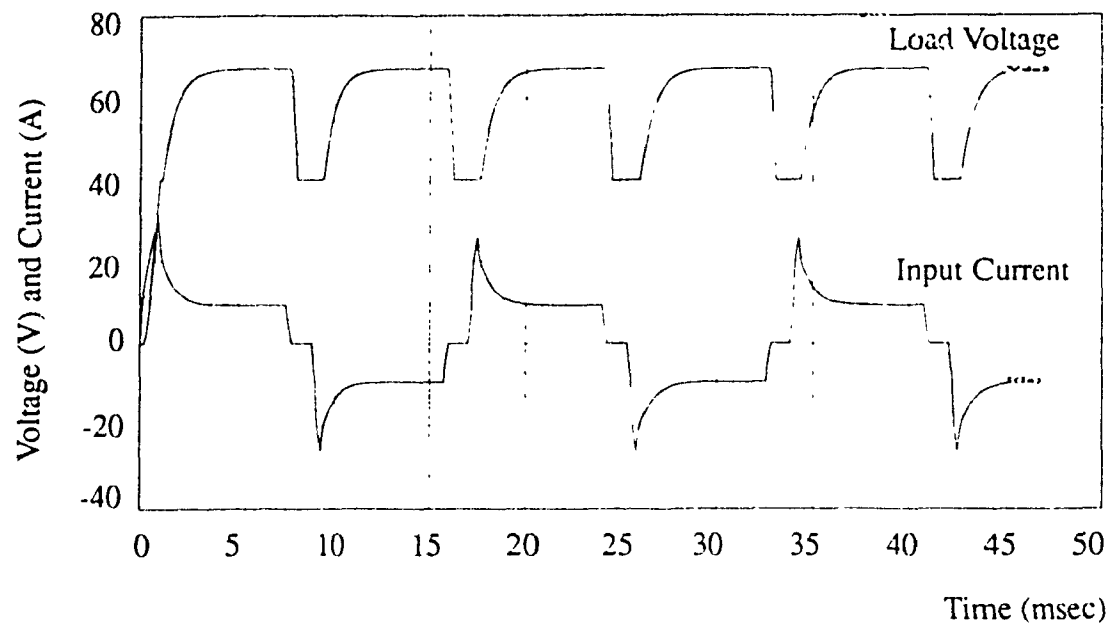
Fig. 6.14: Transient response of the complete system ($C_f = 10\mu F$)
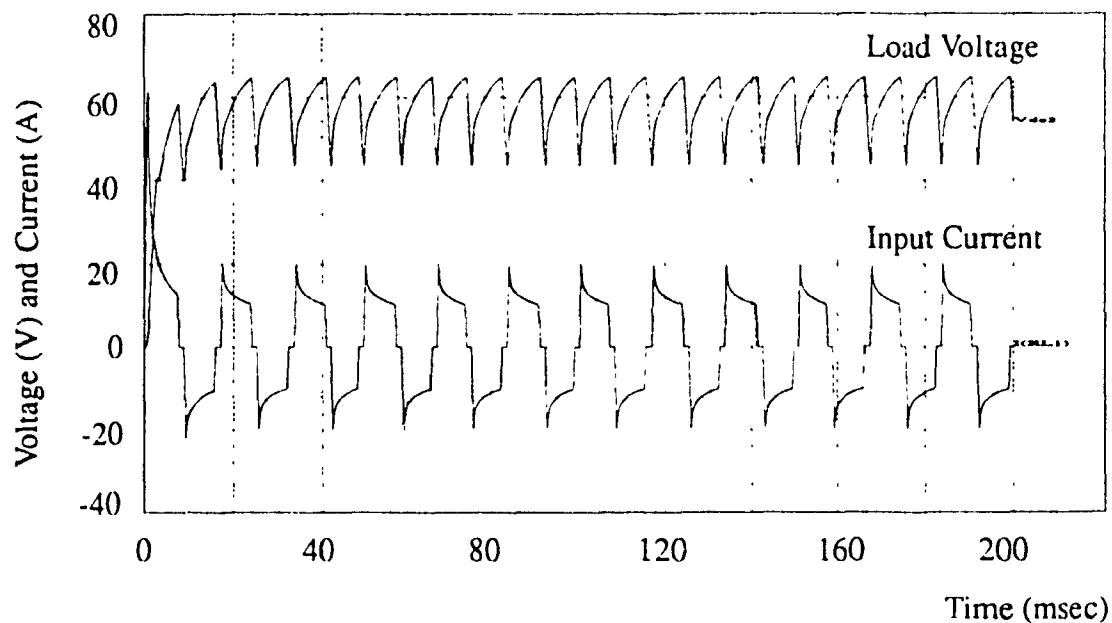
Fig. 6.15: Transient response of the complete system ($C_f = 50\mu F$)
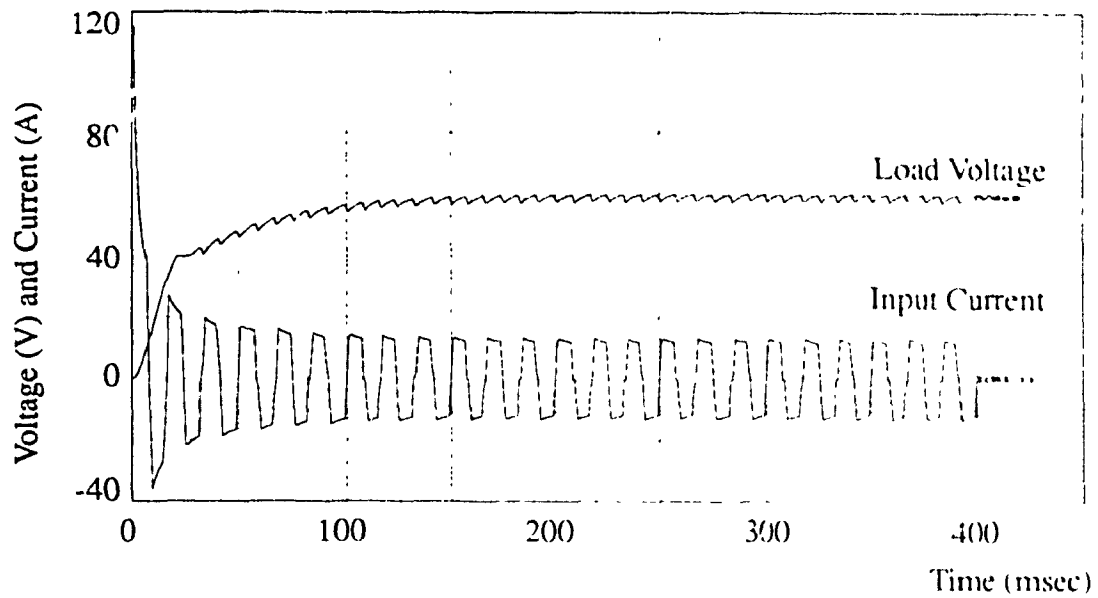
Fig. 6.16: Transient response of the complete system (C_f =400µF)

It can be seen from Fig. 6.9 that the system is unstable for a filter capacitance of *300nF*. The capacitance of *304nF* is a borderline condition between instability and asymptotic stability and the system oscillates without damping (Fig. 6 10). Under the condition of $304nF \le C_f < 10\mu F$, the transient response of the system has damped oscillations (Figs. 6.11~6.14). In Figs. 6.15~6.16, C_f >10µF, the system has the overdamped response. The current rises to a maximum and then decays exponentially to the steady state. A higher capacitance results in a lower maximum transient current.

The values of the filter capacitor and the corresponding system switching transient responses are shown in Fig. 6.17.
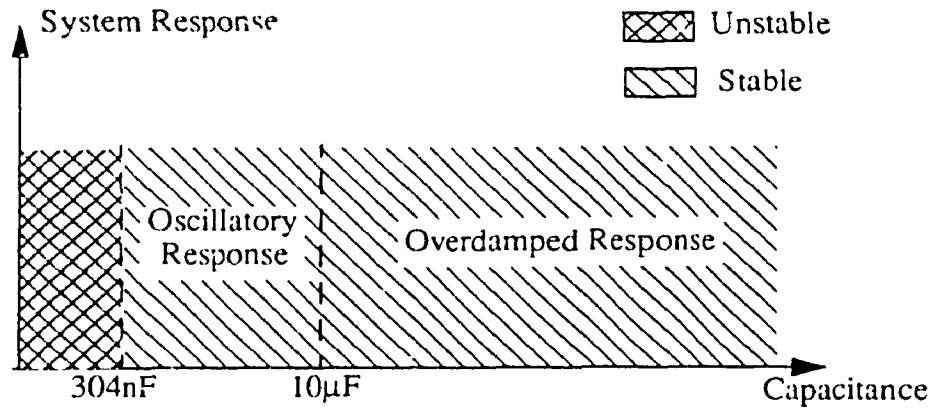
Fig. 6.17: Effects of filter capacitance on system transient response

The persistence of the oscillations is measured by the numerical decrement ND:

$$ND_{ON} = \frac{i_{ON} - i_{ON+1}}{i_{ON}}$$

$$ND_{OFF} = \frac{i_{OFF} - i_{OFF+1}}{i_{OFF}} \qquad (6\text{-}22)$$

Where, ND_{ON} and ND_{OFF} are ND measured at switch-ON and switch-OFF respectively. The definitions of i_{ON}, i_{ON+1}, i_{OFF} and i_{OFF+1} are shown in Fig. 6.18. Specially, in the case of no oscillation, $i_{ON+1}=i_{OFF+1}=0$, and thus $ND_{ON}=ND_{OFF}=1$.
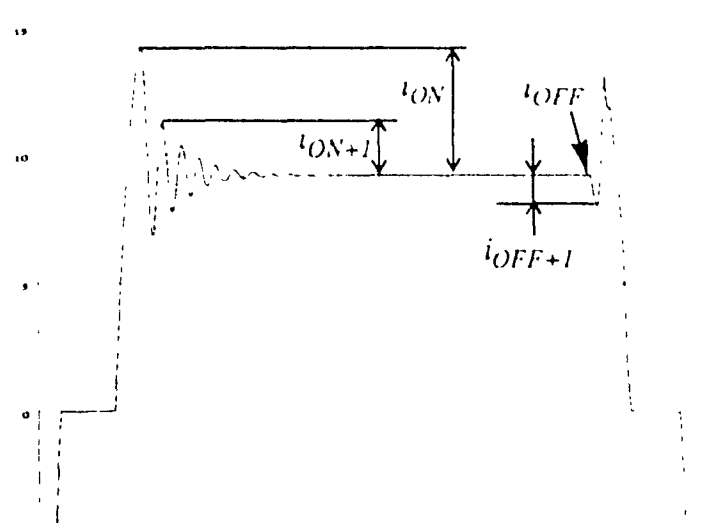
Fig. 6.18: Definitions of i_{ON}, i_{ON+1}, i_{OFF} and i_{OFF+1}

In terms of ND_{ON} and ND_{OFF}, the effect of the filter capacitance on the degree of damped oscillation is shown in Fig. 6.19. It is clear that increasing the filter capacitance can provide an effective way in reducing the oscillation.
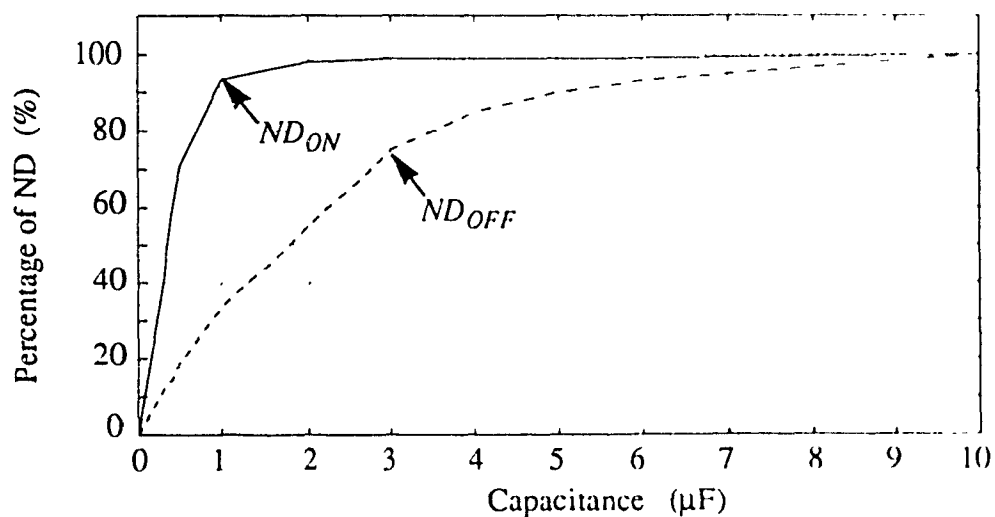
Fig. 6.19: Effect of filter capacitance on the degree of damped oscillation

The effects of the filter capacitor on the maximum input current and the load voltage ripple are shown in Fig. 6.20. In the region of oscillatory response $(C_f < 10\mu F)$, higher capacitance results in faster response with larger overshoot. However, in the region of overdamped response $(C_f > 10\mu F)$, the peak value decreases with increasing capacitance. When the value of the capacitor is increased to above 200μF, the peak value of the supply current is suppressed to less than 15A. It can also be seen that the value of the filter capacitor chosen should be greater than 500μF to obtain a low voltage ripple (around 1V) at the output of the HTU power supply. This value is much greater than 10μF, which is required to prevent oscillations in the system. Therefore, the power distribution system is inherently stable.
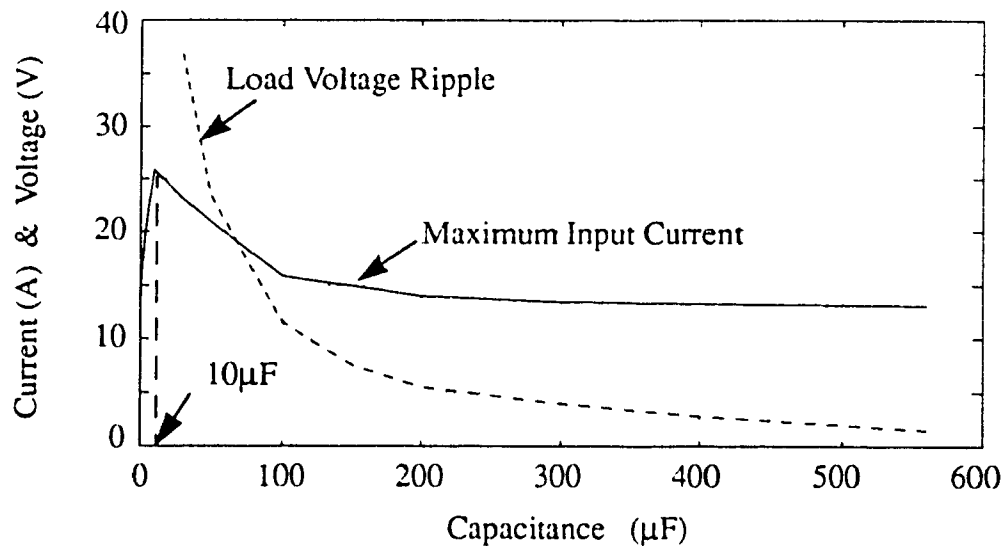
Fig. 6.20: Effects of capacitance on the maximum input current and load voltage ripple

6.5 Conclusions

The dynamic performance of the power system during the switching period has been studied. The following conclusions have been drawn:

(i) By analytical method and simulation, it is found that for the system with a single constant-power converter, the circuit is stable if the output filter capacitance is greater than $6\mu F$;

(ii) For the complete 4-segment system, by the aid of simulation, it is found that to avoid oscillations in the switching transient, the output filter capacitance of the HTU power supply should be greater than $10\mu F$. In most of the converters this is normally the case to meet the constraints of peak supply current and low voltage ripple at the output of the HTU power supply. The power system, therefore, is inherently stable.

Chapter 7

Conclusions

7.1 Conclusions

In this thesis, a power distribution system for the hybrid fiber/coax networks has been presented. A steady state analysis of the system is given. This analysis describes the nonlinear operation and the loading capability of the system. A transient analysis of the system is developed which includes the fault and stability analyses. The major contributions of this thesis are:

(1) Selection of a power scheme for the distribution system. It is found that a 90V 60Hz trapeziodal voltage distribution provides a good compromise between the safety, corrosion and distribution losses.

(2) Development of the model to simulate the performance of the distribution system. In the model, the PN, CN, distribution & drop cables and HTUs are described by the power circuits under the consideration of some constraints of the system operation.

(3) Study of the loading capability under all the possible operating conditions. It is found that the loading capability can be enhanced greatly by inserting multiple synchronous power nodes at certain suitable places.

(4) A presentation of the system performance under the fault conditions. It is shown that during the trip time of PTC, only the system with cable C can work normally against a single fault. However, when two faults occur simultaneously, the whole system fails to operate.

(5) An analysis of the stability of the system operation. It is concluded that the distribution system is inherently stable.

7.2 Further Work Required

The following works are proposed in the future research:

(1) The development of the power scheme of high frequency distribution for the drop segment. Further simulation based analysis should be carried out to study the performance of such advanced power distribution system.

(2) The development of the protective device which can trip faster under the fault conditions.

References

[1] Lorenzo Cividino, "Power system architecture's for the emerging information highway," Northern Telecom, Power Products Division, 1994.

[2] J. Terry, "Beyond switching? - Future visions of the telecommunications manufacturer," InfoVision ComForum'92, Paper No. 33-04.

[3] C.J. Brunet, "Hybridizing the loop," IEEE Spectrum, June 1994.

[4] David Large, "Creating a network for interactivity," IEEE Spectrum, pp. 58~63, April 1995.

[5] P. Jain, "Powering the information superhighway of the future," IEEE Industrial Electronic Conference, Orlando, USA, 1995.

[6] N. Dalarsson, "A recommendation for centralized powering of local network elements," in Proc. IEEE INTELEC'94, pp. 108~114, 1994.

[7] Stephen J. Bigelow, "Understanding telephone electronics (third edition)," SAMS, A Division of Prentice Hall Computer Publishing, 1991.

[8] A. Michael Noll, "Introduction to telephones and telephone systems," Artech House, Inc., pp. 112, 1986.

[9] P. Jain, D. Cooper and N. Tullius, "Alternatives for powering the hybrid fiber/coax networks," in Proc. IEEE INTELEC'94, pp. 83~89, 1994.

[10] K. Mistry and T. Taylor, "hybrid fiber/coaxial systems: powering issues," in Proc. IEEE INTELEC'94, pp. 75~82, 1994.

[11] David A. Weiner, "Lorain products power systems for coaxial cable," in Proc. IEEE INTELEC'94, pp. 98~100.

[12] John G. Kassakian, Martin F. Schlecht, George C. Verghese, "Principles of power

electronics," Addison-Wesley, 1991.

[13] H. Jin, "Computer simulation of power electronic circuits and systems using PSIM," 1995 International Conf. on Power Electronics, Oct 10-14, 1995, Seoul, South Korea.

[14] Alan Combellack, "Discussion paper: powering of the BSN," BNR outside plant integration, March 25, 1996.

[15] Irving M. Gottlieb, "Regulated power supplies," 4th Edition, TAB Books, pp 77-78, 1992.

[16] Y. S. Tzeng, R. N. Wu and N. Chen, "Unified AC/DC power flow for system simulation in DC electrified transit railways," IEE Proc. -Electr Power Appl , Vol 142, No. 6, November 1995.

[17] Robert L. Shrader, "Electronic communication," Gregg Division, McGraw Hill Book Company, pp. 193-199, 1980.

[18] Data from Times Fiber Communication Inc. and Extended Reach Inc

[19] "PolySwitch RUE and RXE resettable fuse devices"

[20] Thomas E. Stern, "Theory of nonlinear networks and systems," Addison-Wesley, Reading, Massachusetts, pp. 309-323, 1965.

[21] Dennis Roddy and John Coolen, "Electronic communications (third edition)," Reston Publishing Company, Inc., 1984.

[22] L. Salazar, "PSPICE simulation of three-phase inverters by means of switching functions," IEEE Trans. on Power Electronics, vol 9, No 1, pp. 35-42, January 1994.

[23] Sylvan Fich, "Transient analysis in Electrical engineering," Prentice-Hall, pp 76-85, 1951.

Published Papers Related to This Thesis

[1] P. Jain, H. Jin, M. Qiu, "Modeling and simulation of power distribution systems for hybrid fiber/coax network", IEEE INTELEC'95.

[2] M. Qiu, P. Jain, H. Jin, "Dynamic performance of power distribution systems for gybrid fiber/coax networks", IEEE INTELEC'96.

Appendix A - Existing CATV System

Fig. A-1 shows a typical CATV architecture currently in use to carry analog signals (50MHz - 330MHz) for cable TV services to the customer. The TV signals are received and converted into electrical signals at the headend station and fed into a large coaxial cable. Trunk amplifiers are inserted at appropriate distances to boost signal strength when it has reduced by approximately 20 dB due to cable impedance. At each trunk amplifier a portion of the signal is commonly tapped off and fed into a splitter or line extender amplifier. From there a distribution cable delivers the signal to neighbourhoods of 120 to 160 homes. The distribution cable has a number of taps that provide multiple feeds to drop cables which bring the signal to the home.
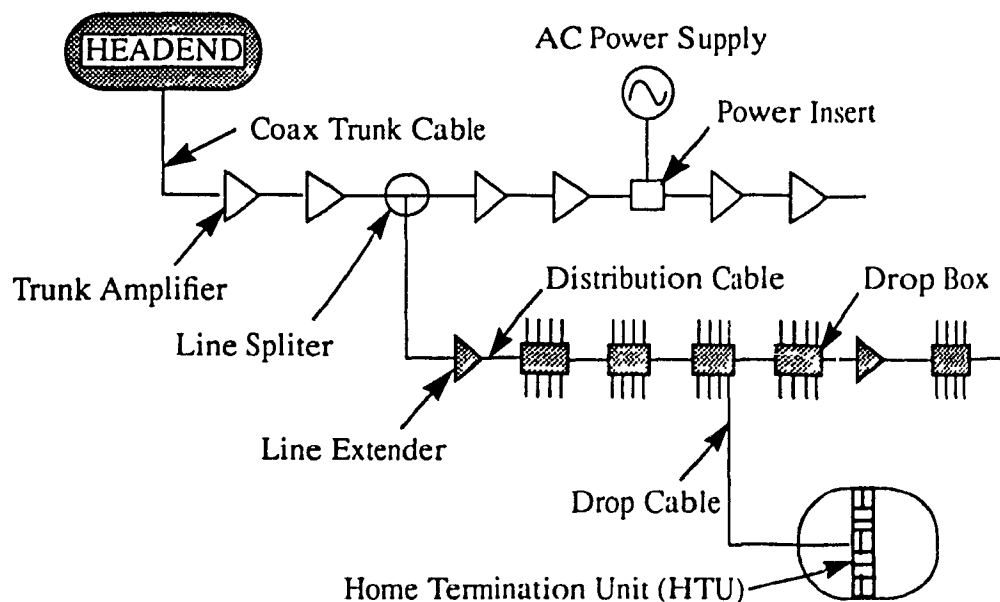
Fig. A-1: Existing CATV architecture

The distribution cables extend to approximately 2000 feet, limited in length by signal strength. The power required by the trunk and line extender amplifiers is derived from the local utility. Stepdown voltage regulating transformers are located along the cable route and provide 60V ac to the amplifiers via the coaxial cable. AC power is blocked at the drop box and only the signal is transmitted down the drop cable to the residence. There is no need to distribute power over the drop cable as the home equipments are locally powered.

This traditional CATV architecture is very costly and cannot meet the demands of the emerging network. Some improvements have been made to increase system reliability. Fiber cables have replaced many of the lengthy trunk cables thus eliminating many of the amplifiers and improving signal quality. Uninterruptible power supplies are used at critical system locations replacing the basic ac power supply in order to provide service during local power outages.

However, if some additional services such as video, telephony and audio are provided using the CATV networks, there is a need to power minimum essential services at the home termination unit by network power. Therefore, a hybrid power architecture called hybrid fiber/coax network is proposed.

Appendix B - Characteristics of Telephony Loads

In the HFC architecture (Fig. 1.1), the home services can be video, telephony, audio, interactive multimedia, etc. This thesis focuses on the telephony loads.

Fig. B-1 is a block diagram of a telephone set which shows its major functions. The ringer circuit is always connected across the line so it can signal an incoming call. The remainder of the telephone set is connected/disconnected to the line by the closed/open switchhook.

Fig. B-1: Telephone set block diagram

The load is variable and depends on the states of the phone, which are mainly described as following:

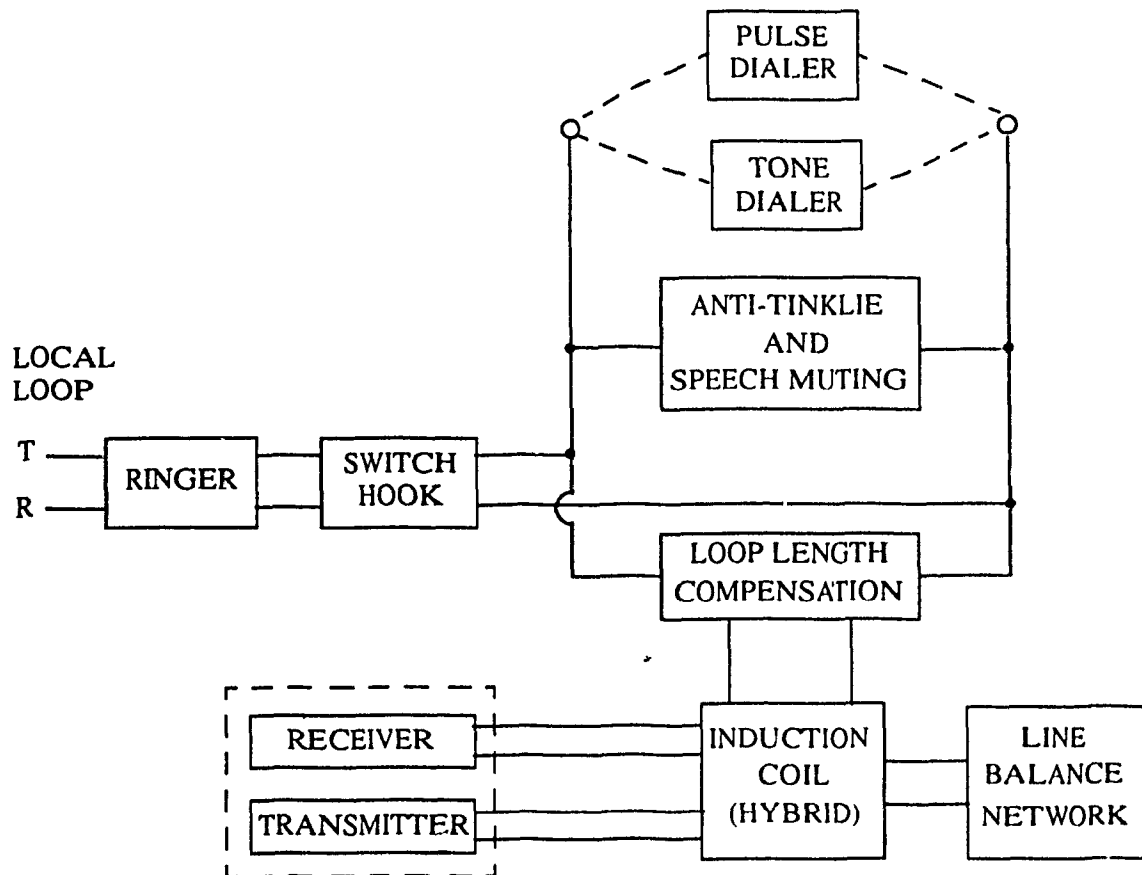(i) On-hook/off-hook: When service is desired, the user lifts the handset from its cradle, and a dc circuit is completed by the closed contacts of the switchhook, so that the telephone starts drawing dc from the line. This active state is called off-hook. The opposite condition is on-hook and no dc flows.

(ii) Ringing: When the voltage of 75 V at about 17 Hz appears across the ringer, the telephone starts ringing. The ac ringing signal is always generated by a solid-state inverter, which is powered by the 48V dc supply.

(iii) Ringtrip: If the call is answered while the bell is ringing, it is necessary for the exchange to detect that direct current has begun to flow at the same time that ringing current is flowing, so that the ringing can be removed before the receiver is applied to the called party's ear. This process is called ringtrip.

The power demand of the telephone in its various operating states is different. The highest power demand occurs when the telephone is in the ringtrip state.

To simulate the system operation, a suitable model has to be found for telephone set. As it is well known, loads can be represented by different models as constant current, constant power, constant impedance and any combination of the previous models. The characteristic of telecom power converter is one of a constant power type. When the operating state changes, the telephone set can automatically adjust for changes of the power demand. Hence the current required to power the load increases as the voltage decreases, and vice versa.

The power system must be designed to handle the expected traffic. The maximum traffic loading assumed is 9 ccs. (Traffic is measured in units of hundred-call-seconds, or

CCS. The product of the number of calls times their average duration in seconds gives the traffic in call-seconds. Dividing this figure by 100 gives the number of hundred-call-seconds (CCS)).

Appendix C - The Harmonic Spectrum Data

Considering the harmonic order up to the 15th component, the harmonic spectrum data of the waveforms in Figs. 2.6 (a), (b) and (c) are shown respectively in Tables C-1, C-2 and C-3. (In the Tables, v_s and i_s are the voltage and current at the supply point; v_{ac1} and i_{ac1} are the ac voltage and current at the first load; v_{ac2} and i_{ac2} are the ac voltage and current at the last load.)

Table C-1: The harmonic spectrum data of the waveforms in Fig. 2.6 (a)

n	v_s (peak, V)	i_s (peak, A)	v_{ac1} (peak, V)	i_{ac1} (peak, A)	v_{ac2} (peak, V)	i_{ac2} (peak, A)
0	0.103	0.036	0.100	0.002	0.122	0.002
1	118.04	15.592	116.04	0.261	91.44	1.222
2	0.207	0.074	0.211	0.006	0.211	0.003
3	0.207	9.996	1.603	0.248	14.029	0.395
4	0.208	0.066	0.219	0.009	0.190	0.008
5	0.208	3.704	0.688	0.225	1.092	0.249
6	0.209	0.064	0.185	0.010	0.199	0.001
7	0.209	0.981	0.722	0.192	2.095	0.147
8	0.211	0.073	0.236	0.009	0.204	0.009
9	0.212	0.777	0.216	0.154	0.311	0.129
10	0.214	0.078	0.201	0.007	0.212	0.001
11	0.215	0.589	0.518	0.114	1.103	0.065
12	0.217	0.087	0.215	0.004	0.242	0.010
13	0.219	0.446	0.227	0.075	0.302	0.090
14	0.221	0.089	0.235	0.006	0.241	0.003
15	0.223	0.592	0.230	0.039	0.493	0.031
rms	84.08	13.39	82.66	0.354	65.93	0.944

Table C-2: The harmonic spectrum data of the waveforms in Fig. 2.6 (b)

n	v_s	i_s (peak, A)	v_{ac1}	i_{ac1} (peak, A)	v_{ac2}	i_{ac2} (peak, A)
0	0.881	0.089	0.864	0.002	0.525	0.020
1	111.93	14.190	110.06	0.256	87.73	1.102
2	1.791	0.197	1.757	0.005	1.118	0.039
3	30.659	2.785	30.262	0.066	25.823	0.284
4	1.822	0.213	1.785	0.006	1.264	0.040
5	11.707	0.297	11.751	0.020	11.973	0.054
6	1.764	0.195	1.731	0.005	1.353	0.042
7	3.240	1.460	3.456	0.035	5.492	0.069
8	1.609	0.164	1.588	0.002	1.317	0.040
9	1.379	1.622	1.241	0.037	2.065	0.107
10	1.442	0.180	1.430	0.003	1.163	0.036
11	2.324	1.148	2.174	0.026	1.070	0.101
12	1.345	0.218	1.330	0.005	0.964	0.032
13	1.921	0.406	1.875	0.010	1.393	0.069
14	1.280	0.216	1.258	0.005	0.855	0.034
15	0.903	0.283	0.951	0.012	1.346	0.029
rms	83.48	10.50	82.12	0.195	66.08	0.823

Table C-3: The harmonic spectrum data of the waveforms in Fig. 2.6 (c)

n	v_s (peak, V)	i_s (peak, A)	v_{ac1} (peak, V)	i_{ac1} (peak, A)	v_{ac2} (peak, V)	i_{ac2} (peak, A)
0	0.141	0.041	0.146	0.001	0.082	0.004
1	111.24	15.303	109.13	0.320	85.69	1.144
2	0.312	0.045	0.320	0.001	0.280	0.004
3	30.375	1.744	30.586	0.171	26.043	0.301
4	0.377	0.040	0.376	0.001	0.393	0.008
5	12.980	0.395	13.033	0.027	12.976	0.065
6	0.430	0.037	0.424	0.000	0.479	0.013
7	4.902	1.077	4.964	0.031	6.813	0.066
8	0.445	0.051	0.438	0.001	0.510	0.014
9	0.756	1.227	0.847	0.008	3.222	0.109
10	0.425	0.068	0.423	0.000	0.475	0.012
11	1.080	0.971	1.003	0.013	1.032	0.110
12	0.414	0.066	0.420	0.001	0.384	0.008
13	1.461	0.508	1.411	0.004	0.253	0.083
14	0.462	0.038	0.462	0.001	0.269	0.002
15	1.062	0.063	1.053	0.007	0.872	0.043
rms	82.25	11.00	80.86	0.259	64.22	0.852